SC

PYROLYSES OF SOME ALKYL IODIDES

BY

GANGADHAR CHOUDHARY

A thesis submitted in partial fulfillment

of the requirements for the degree of

Doctor of Philosophy

in the

Department of Chemistry

University of Ottawa

Ottawa, Canada

J.L. Holmes
Associate Professor of
Chemistry; Research
Supervisor

G. Choudhary
Ph.D. Candidate

PREFACE

Kinetic studies are among the most powerful tools for the investigation of the mechanism of a chemical reaction. Ingold and co-workers achieved great success in interpreting reaction mechanisms in solutions. However, these studies have been observed to be simpler in the case of gas phase reactions, particularly in the case of pyrolytic decompositions where only one reactant is involved and complicating solvent effects are absent.

In general, gas phase decompositions of alkyl halides have been found to be kinetically simpler than other organic compounds. This is due to the fact that complications arising from chain reactions are less often found in these systems. One of the main difficulties often encountered in the case of alkyl halide pyrolyses, is a surface effect due to the polar nature of these compounds. Barton and co-workers, in the case of alkyl chlorides and Maccoll and co-workers in the case of alkyl bromides, have successfully studied and interpreted the pyrolyses of these compounds. These authors have concluded that alkyl chlorides and bromides can eliminate hydrogen halide in the gas phase either by a unimolecular mechanism or by a mixed unimolecular-free radical mechanism.

The thermal decompositions of alkyl iodides are more complex. Surface effects are more prominent in the pyrolysis than in the case of chlorides or bromides. Also, the very weak carbon-iodine bond becomes kinetically important

in these systems. However, previous workers such as Butler and Polanyi, Jones and Ogg, Maccoll, Holmes, Benson etc., have found that alkyl iodides show the same trends as alkyl chlorides or bromides, with respect to the effect of structure on the kinetics of the decompositions.

The present thesis deals with the pyrolysis of three alkyl iodides whose kinetic mechanisms were uncertain. The compounds under investigation are:

(1) t-butyl iodide

(2) n-propyl iodide

(3) ethyl iodide

These are dealt with in different sections of the thesis.

The kinetic investigation of a homogeneous pyrolysis of t-C_4H_9I was unsuccessful in the past because of a heterogeneous decomposition of this compound at the surface of the reaction vessel. In this thesis, an attempt has been made to find a homogeneous rate by using different conditions of surface of the reaction vessel. The other two compounds n-C_3H_7I and C_2H_5I pyrolyse homogeneously. The mechanisms proposed for these two compounds are different from those of previous workers.

A separate section of this thesis comprises a general discussion of alkyl iodide pyrolyses.

A C K N O W L E D G E M E N T S

The author is especially grateful to Professor J. L. Holmes for his kindness, witty guidance, constructive suggestions and timely encouragement during this work. He also gives his sincere thanks to Dr. D. Paskovitch, Dr. (Mrs.) M. Back, Dr. M. R. Bridge, Dr. M. C. Lin and Mr. B. M. Nayar for their assistance and valuable discussions at various stages of this work. Thanks are also due to all those of this department, who helped to make the author's stay a pleasant one. The author, however, cannot forget his wife's patience and understanding while this work was being undertaken and shows his deep appreciation and gratitude to her.

Finally, the author is also indebted to Patna University for granting leave of absence.

C O N T E N T S

	Page
Preface	i.
Acknowledgement	iii.
Table of Contents	iv.
List of Tables	vii.
List of Figures	ix.

Section 1.

Abstract and Introduction

1.1. Abstract	1.
1.2. Mechanism of homogeneous gas phase reactions	4.
1.3. Evidence for the molecular elimination reaction in the pyrolysis of alkyl halides	15.
1.4. Structural effects upon the unimolecular elimination mechanism in organic halide pyrolyses	17.
1.5. Surface effects in gas phase reactions	25.

Section 2.

A survey of the previous work on alkyl halides

2.1. Alkyl chlorides and bromides	28.
2.2. Alkyl Iodides	32.
2.3. Relative rates of pyrolysis of simple alkyl chlorides, bromides and iodides	37.

Section 3. Page

Description of the apparatus and experimental technique

3.1. General outline 39.

3.2. The thermostat and the reaction vessel 39.

3.3. The pressure measurement 43.

3.4. The vacuum system 46.

3.5. Chromatographic apparatus 50.

3.6. Procedure for a typical run 51.

3.7. Homogeneity tests 53.

3.8. Preparation, purification and storage of materials 54.

Section 4.

Pyrolysis of t-butyl iodide

4.1. Introduction 61.

4.2. Experimental 63.

4.3. Product analysis and Stoicheiometry 63.

4.4. Results 76.

4.5. Mechanism 94.

Section 5.

Pyrolysis of n-propyl iodide

5.1. Introduction 109.

5.2. Experimental 112.

5.3. Stoicheiometry and Principles of calculation 113.

5.4. Results 114.

5.5. Discussion of Results and mechanism 134.

Note:- A brief investigation of the pyrolysis of n-butyl iodide 137.

Section 6.

Pyrolysis of ethyl iodide

6.1. Introduction 140.

6.2. Experimental 143.

6.3. Stoicheiometry and Principles of calculation 143.

6.4. Results 144.

6.5. Discussion of Results and mechanism 158.

Note:- Cyclohexene inhibition study of C_2H_5I 168.

Section 7.

A general discussion of the alkyl iodide pyrolysis 172.

x

Claims to the original research 176.

References 177.

LIST OF TABLES

Tables		Page.
1.1.	Effect of method of initiation and termination on order of reaction	9.
1.2.	Comparison of the unimolecular activation energies E_{H-X} for the elimination of H-X, the homolytic bond dissociation energy D(R-X) and heterolytic bond dissociation energies $D(R^+X^-)$ of the carbon halogen bond	21.
1.3.	The same data as in table 1.2. for iodides	22.
2.1.	The decompositions of organic mono-chloro and mono-bromo alkanes	28.
2.2.	Activation energy for the thermal decomposition of alkyl iodides compared with the bond dissociation energy	35.
2.3.	Relative rates of pyrolysis of alkyl halides of β methylated series	38.
2.4.	Relative rates of halides having the same organic residue	38.
4.1.	Relation between i-butane and I_2 during the $t\text{-}C_4H_9I$ pyrolysis	65.
4.2.	Iodine production compared with pressure change during the pyrolysis of $t\text{-}C_4H_9I$	66.
4.3.	Indirect proof of i-butane and iodine equality	75.
4.4.	Kinetic results on allyl bromide carbon surface	76.
4.5.	Kinetic results on isobutene carbon surface	85.
4.6.	Effect of HI on $t\text{-}C_4H_9I$ pyrolysis	91.
4.7.	Effect of NO on the pyrolysis of $t\text{-}C_4H_9I$	93.
4.8.	Relative rates of pressure change and iodine production at different surface	94.
4.9.	Model calculation of rate constants at 190.0°C	97.
4.10.	Model calculation of rate constants at 219.2°C	98.
4.11.	Model calculation of rate constants at 239.0°C	99.

Tables

		Page.
4.12.	Data for the Arrhenius plot; allyl bromide unpacked vessel	100.
4.13.	Data for the Arrhenius plot; isobutene unpacked vessel	101.
5.1.	Determination of the ratio $\frac{P_f}{P_o}$ in the pyrolysis of n-propyl iodide	114.
5.2.	Kinetic results for the pyrolysis of n-C_3H_7I	119.
5.3.	Data for the Arrhenius plot; n-C_3H_7I pyrolysis	122.
5.4.	Production of i-propyl iodide during the induction period	124.
5.5.	Effect of NO on the pyrolysis of n-C_3H_7I	126.
5.6.	Effect of propylene and air on the pyrolysis of n-C_3H_7I	127.
5.7.	Addition of i-propyl iodide and t-butyl iodide to the pyrolysis of n-C_3H_7I	130.
5.8.	Co pyrolysis of n-C_3H_7I and C_2H_5I and analysis of products by gas chromatography	133.
6.1.	The kinetic data from the pyrolysis of ethyl iodide	147.
6.2.	Data for the Arrhenius plot; ethyl iodide pyrolysis	150.
6.3.	Comparison of the Arrhenius parameters with the previous workers; ethyl iodide pyrolysis	151.
6.4.	Effect of propylene on the pyrolysis of ethyl iodide	156.
6.5.	Effect of the constant concentration of propylene on the C_2H_5I pyrolysis	157
6.6.	Kinetic data for the cyclohexene inhibition of ethyl iodide pyrolysis	169.
6.7.	Data for the cyclohexene inhibition ;ethyl iodide pyrolysis	170.

LIST OF FIGURES

Figure		Page.
Figure 1:	A plot of the Arrhenius activation energies of simple alkyl halide pyrolyses against their heterolytic bond dissociation energies	24.
Figure 2:	A schematic diagram of the thermostat and the reaction vessel	42.
Figure 3:	A cross section of the packed reaction vessel	44.
Figure 4:	The details of the pressure measuring device	45.
Figure 5:	A schematic diagram of the apparatus	48.
Figure 6:	The gas chromatography apparatus	52.
Figure 7:	The N.M.R., spectrum of purified t-butyl iodide	57.
Figure 8:	A typical pressure-time curve for the pyrolysis of t-butyl iodide at 201.0°C	67.
Figure 9:	A typical pressure-time curve for the pyrolysis of t-butyl iodide at 229.0°C	68.
Figure 10:	Two typical curves for iodine production during the pyrolysis of t-butyl iodide	69.
Figure 11:	Pressure-time and iodine-time curves from the t-butyl iodide pyrolysis on the same scale; Temp. 229.0°C	70.
Figure 12:	Pressure-time and iodine-time curves from the t-butyl iodide pyrolysis on the same scale; Temp. 201.0°C	71.
Figure 13:	A typical first order log plot for the $t\text{-}C_4H_9$ iodide pyrolysis. $[RI]_o$ = 44.2 mm.; Temp. 229.0°C	72.
Figure 14:	An autocatalytic rate plot for the pyrolysis of t-butyl iodide. $[RI]_o$ = 44.2 mm.; Temp. 229.0°C	73.
Figure 15:	Arrhenius plots for the first order reaction in the pyrolysis of t-butyl iodide on different surfaces	102.

Figure		Page.
Figure 16:	Arrhenius plots for $k_{1.5}$ on the two surfaces; t-butyl iodide pyrolysis	103.
Figure 17:	Arrhenius plot for the first order rate in an isobutene-carbon coated vessel in comparison with those of the previous workers; t-butyl iodide pyrolysis	104.
Figure 18:	Typical pressure-time curves for the pyrolysis of n-propyl iodide at 310.0°C	116.
Figure 19:	Corresponding log plots for the curves in figure 18	117.
Figure 20:	A typical iodine-time plot for the pyrolysis of n-propyl iodide at 330.8°C. Pressure changes shown by triangles	118.
Figure 21:	Arrhenius plot from n-propyl iodide pyrolysis compared with that of Jones and Ogg	123.
Figure 22:	A typical chromatogram showing the separation of i-propyl iodide from the n-compound. Temp. 307.0°C; time of pyrolysis 2½ minutes, pyrolysis of n-propyl iodide	125.
Figure 23:	A typical pressure-time curve for the pyrolysis of C_2H_5I. $[RI]_o$ = 60.5 mm.; Temp. 364.0°C	145.
Figure 24:	A typical first order log plot for the pyrolysis of C_2H_5I. $[RI]_o$ = 75 mm.; Temp. 364.0°C	146.
Figure 25:	Arrhenius plots for the C_2H_5I pyrolysis using different reaction vessel surfaces	152.
Figure 26:	Arrhenius plot for the C_2H_5I pyrolysis compared with the results of Benson and Lee	153.
Figure 27:	Ethyl Iodide pyrolysis, a typical chromatogram showing the separation of C_2H_6 and C_2H_4	155.
Figure 28:	A plot for the production of ethylene when different concentrations of C_3H_6 are added to different concentrations of C_2H_5I. Pyrolysis. Temp. 347.8 C	160.

Figure		Page.
Figure 29:	Plot of ethane concentration against time for a varying concentration of C_3H_6 and a constant concentration of C_2H_5I. Pyrolysis of C_2H_5I	161.
Figure 30:	Pyrolysis of C_2H_5I; plot of the rate of ethane production against propylene	162.
Figure 31:	Pyrolysis of C_2H_5I; plot of the $\frac{Rate_{C_2H_6}}{C_3H_6}$ against $\left[C_2H_5I\right]^2$	
Figure 32:	Pyrolysis of C_2H_5I; plot of $\left[C_2H_4\right]$ against $\frac{\left[C_3H_6\right]_o}{\left[C_3H_6\right]_o - \left[C_2H_6\right] + \left[C_2H_4\right]}$	167.

SECTION - 1

ABSTRACT AND INTRODUCTION

1.1. Abstracts:

Pyrolysis of t-butyl iodide

The pyrolysis of t-C_4H_9I has been carried out in a conventional static system in the temperature range 190°-240°C. The reaction has been found to be heterogeneous as reported by previous authors. The chief products are isobutene and hydrogen iodide together with some isobutane and iodine. The latter pair together represented less than 10% of the total product. The reaction does not go to completion but the equilibrium

$$t\text{-}C_4H_9I \underset{-1}{\overset{1}{\rightleftharpoons}} C_4H_8 + HI$$

is rapidly established. The stoicheiometry of the iodine producing process is simply

$$t\text{-}C_4H_9I + HI \xrightarrow{1.5} C_4H_{10} + I_2$$

The pressure-time data obey first order kinetics up to about 25% reaction. The iodine producing process has been found to fit an autocatalytic rate law of the type -

$$\frac{d(I_2)}{dt} = k_{1.5}(I_2)^{\frac{1}{2}}(C_4H_9I)$$

Homogeneity tests revealed that the iodine producing process is completely homogeneous and that the first order process is partially heterogeneous.

In an attempt to find values for the homogeneous first order rates, the effects of different reaction vessel surfaces on the pyrolysis have been studied. The carbonaceous coating produced by the decomposition products of isobutene, gave the rate which was the least heterogeneous. The Arrhenius parameters for the two rates in the isobutene coated vessel are:

$$E_1 = 38.33 \text{ K.Cals} \quad ; \quad \log_{10} A_1 = 13.53 \text{ Sec.}^{-1}$$

$$E_{1.5} = 31.1 \text{ K.Cals} \quad ; \quad \log_{10} A = 9.76 \text{ mm.}^{-\frac{1}{2}} \text{Sec.}^{-1}$$

A mechanism has been proposed for the pyrolysis.

Pyrolysis of n-propyl iodide

The pyrolysis of $n\text{-}C_3H_7I$ has been investigated in the above system in the temperature range of 307°-360°C. Reports of previous authors, regarding the order of the reaction and the stoicheiometry, have been confirmed. The rate law

$$\frac{-d(n\text{-}C_3H_7I)}{dt} = k'_{1.5}(n\text{-}C_3H_7I)\ (I_2)^{\frac{1}{2}}$$

is seen to be obeyed from about 5% to about 70% decomposition. The Arrhenius parameters are also in excellent agreement with

those of Jones and Ogg, who however, were unable to propose a satisfactory mechanism.

	E (K.Cals)	$\log_{10}A$ ($mm.^{-\frac{1}{2}}Sec.^{-1}$)
Jones and Ogg	37.9	10.06
Present work	38.4	10.18

The appearance of an induction period which decreases with rise of temperature and shows only small dependence on initial concentration has been interpreted as due to the intermediate formation of i-propyl iodide.

Pyrolysis of Ethyl iodide

This compound has been pyrolysed in the same system in the temperature range of 340°-378°C. The order, the stoicheiometry and Arrhenius parameters have been found to be in good agreement with those of the previous workers. Experiments using reaction vessels having different chemical coatings showed that the decomposition is not surface active. The Arrhenius parameters in different types of reaction vessel surface are:

	Surface		E(K.Cals)	$\log_{10}A$(Sec.$^{-1}$)
Present work	(ethyl bromide) (isobutene)	average	51.02	14.24
Lee	(allyl bromide)		49.3	13.53
Benson	(Clean glass)		50.0	13.66

In order to examine the importance of any free radical processes in the pyrolysis, the effect of propylene has been studied. This inhibitor was found to have no effect on the ethylene producing reaction, but a new bimolecular reaction between the iodide and propylene was observed. The results indicate a molecular mechanism for ethyl iodide pyrolysis and rule out any appreciable radical process during the reaction.

1.2. Mechanism of homogeneous gas phase decompositions:

Three basic types of mechanism have been used in the interpretation of homogeneous gas phase decompositions. They are:-

(i) A radical non-chain mechanism

(ii) A radical chain mechanism

(iii) Isomerisation and molecular elimination reactions.

Any substance decomposes mainly by the path involving the least activation energy and this path depends on the structure of the reactant molecule and the temperature of the reaction.

The presence of free radicals in gas phase reactions was first demonstrated by Paneth[1] who noticed the formation of metallic mirrors during the pyrolyses of certain metal alkyls. A few years later Rice and Johnston[2,3] pointed out the importance of such free radicals during thermal decompositions of certain organic compounds.

(i) Radical non-chain mechanism:

This type of process is very simple and is comparatively rare. This was first discussed by Daniels[4,5] in the case of the ethyl bromide pyrolysis. Later, Lossing and Tickner[6] and Maccoll[7] used this mechanism to explain the kinetics of the pyrolyses of di-tertiary butyl peroxide and allyl bromide respectively.

If M_n are stable molecules and R_n free radicals (where n = 1, 2, 3.....etc.), the general mechanism of this type is

$$M_1 \longrightarrow R_1 + R_2 \quad \text{.....} \quad \text{(i)}$$

$$R_1 + M_1 \longrightarrow R_1H + R_3 \quad \text{.....} \quad \text{(ii)}$$

$$R_2 + R_3 \longrightarrow M_1 + M_2 \quad \text{.....} \quad \text{(iii)}$$

Step (i) involves a bond dissociation and usually is the slowest step. Such a process is of first order with an overall activation energy equal to the bond dissociation energy. Therefore, a radical non-chain process is practically possible only when the energy of activation is equal to the bond dissociation energy of the compound.

(ii) Radical chain mechanism:

This hypothesis, first developed by Rice and Herzfeld[8] involves the formation of long chains by free radicals during the thermal decomposition of organic compounds. If a steady state for the intermediate radicals is assumed,

this kind of scheme can account for the various overall kinetic order of the reaction. As an example, consider the following scheme for the decomposition of a hydrocarbon molecule M_1 -

$$M_1 \xrightarrow{k_1} R_1 + R_3 \quad \ldots\ldots\ldots\ldots \quad (1)$$

$$R_1 + M_1 \xrightarrow{k_2} R_1H + R_2 \quad \ldots\ldots\ldots\ldots \quad (2)$$

$$R_2 \xrightarrow{k_3} R_1 + M_3 \quad \ldots\ldots\ldots\ldots \quad (3)$$

$$R_1 + R_2 \xrightarrow{k_4} R_1 + M_4 \quad \ldots\ldots\ldots\ldots \quad (4)$$

$$R_1 + R_1 \xrightarrow{k_5} M_5 \quad \ldots\ldots\ldots\ldots \quad (5)$$

$$R_2 + R_2 \xrightarrow{k_6} M_6 \quad \ldots\ldots\ldots\ldots \quad (6)$$

The radical chain mechanism may conveniently be divided into three parts viz., chain initiation, chain propagation and chain termination. In the above scheme reaction (1) is the initiating step, reactions (2) and (3) the propagating step and reactions(4), (5) and (6) are different chain terminating steps. In this scheme two radicals are formed each of which will initiate a separate chain. For simplicity only one of these chains is considered here.

When a steady state concentration of R_1 and R_2 is established we may write

$$\frac{d}{dt}(R_1) = k_1(M_1) - k_2(R_1)\ (M_1) + k_3(R_2) - k_4(R_1)\ (R_2) = 0$$

and $$\frac{d}{dt}(R_2) = k_2(R_1)\ (M_1) - k_3(R_2) - k_4(R_1)\ (R_2) = 0$$

Here step (4) is considered as the terminating process.

From above,

$$R_1 = \frac{k_1}{4k_2} + \left\{\left(\frac{k_1}{4k_2}\right)^2 + \frac{k_1k_3}{2k_2k_4}\right\}^{\frac{1}{2}}$$

If the chains are very long

$$R_1 = \left(\frac{k_1k_3}{2k_2k_4}\right)^{\frac{1}{2}}$$

The overall rate of disappearance of M_1 is given by

$$-\frac{d}{dt}(M_1) = k_1(M_1) + k_2(R_1)\ (M_1)$$

If k_1 is small then the primary step is slow compared with the overall rate and this becomes

$$-\frac{d}{dt}(M_1) = k_2(R_1)\ (M_1)$$

$$= M_1 \left(\frac{k_1k_2k_3}{2k_4}\right)^{\frac{1}{2}}$$

which is of first order.

The overall activation energy E of the reaction is given by

$$E = \tfrac{1}{2}(E_1 + E_2 + E_3 - E_4)$$

E_1 is usually much larger than E_2 and E_3 and $E_4 \approx 0$, so that E is usually much smaller than E_1

The overall frequency factor A is given by

$$A = \left(\frac{A_1 A_2 A_3}{2A_4}\right)^{\frac{1}{2}}$$

It can be seen that the overall rate is made up of two parts $k_1 (M_1)$ which is the rate of initiation step and $k_1 (R_1)(M_1)$ which is the rate of disappearance of M_1 by chain steps. The ratio of these is the average chain length which is equal to

$$k_2 = \frac{(R_1)(M_1)}{k_1 (M_1)} = \left(\frac{k_2 k_3}{2k_1 k_4}\right)^{\frac{1}{2}}$$

If the terminating step is (5), then the steady state approximation leads to

$$-\frac{d}{dt}(M_1) = (M_1)^{3/2} k_2 \left(\frac{k_2}{k_5}\right)^{\frac{1}{2}}$$

a reaction of order 3/2; similarly if the chain ending step is (6) an order of 1/2 is obtained.

A chain reaction is not so easily discounted on an energy basis as a non-chain process if first order rates are obtained. The order of the overall reaction depends critically on the way in which the chains are broken. Goldfinger, Letort and Niclaus[9] treated the subject systematically and gave a table (table 1.1) listing the expected order for various initiating and terminating processes. While doing so they distinguish between two types of radical,

(i) β - radicals - which propagate chains by participation in bimolecular reactions and they do not decompose (e.g., R_1 in above scheme)

(ii) μ - radicals - which propagate chains by undergoing a unimolecular decomposition (e.g., R_2 in above scheme). The conclusion is that if the chain reaction is initiated either by a unimolecular or by a bimolecular reaction, the overall order depends upon the type of chain ending steps and is shown schematically in table 1.1.

Table 1.1. Effect of method of initiation and termination on order of reaction. M = third body.

Initiation Process	Unimolecular		Bimolecular	
Terminated by order	Triple Collisions	Simple Collisions	Simple Collisions	Triple Collisions
2			$\beta\beta$	
3/2		$\beta\beta$	$\beta\mu$	$\beta\beta$ (M)
1	$\beta\beta$ (M)	$\beta\mu$	$\mu\mu$	$\beta\mu$ (M)
1/2	$\beta\mu$ (M)	$\mu\mu$		$\mu\mu$ (M)
0	$\mu\mu$ (M)			

Which process is more important in terminating chains, depends partly upon the relative concentration of the radicals. Thus if the concentration of the radical R_1 is much higher than that of R_2, the most important chain ending process is probably the reaction between two R_1 radicals. The choice of chain ending step is of utmost importance while formulating a reaction mechanism.

Two significant aspects of gas phase reactions, which are at times useful for providing a clue to the nature of the processes taking place are

(a) the occurrence of an induction period and

(b) the effect of inhibitors on reactions.

(a) Induction period:

Induction periods are observed when the reaction rate is almost immeasurably slow at the beginning of the reaction. These induction periods have been observed in many gas phase reactions. For example, Barton and Howlett[10] noticed this phenomenon during the dehydrochlorination of 1:2 dichloroethane.

Induction periods may be the result of one of the following:-

(i) Slow attainment of the steady state concentration of radicals or atoms:

This may be due to a branched chain reaction during the process. For example, the induction period during the decomposition of 1:2 dichloroethane[10] was due to the primary processes

$$CH_2Cl\ CH_2Cl \longrightarrow C_2H_4 + Cl_2$$

$$Cl_2 + CH_2ClCH_2Cl \longrightarrow HCl + Cl + CHCl.CH_2Cl$$

(ii) Autocatalysis by an intermediate or final product:

Such induction periods are often observed in the low temperature oxidation of hydrocarbons and of many hydrocarbon derivatives, and are caused due to the biradical nature of the oxygen molecule[11] which forms a linear transition complex with the compound. For example, a hydrocarbon molecule oxidises as -

$$RH + O_2 \rightleftharpoons R\text{-}H\text{-}O_2 \longrightarrow R + HO_2$$

HO_2 is unreactive but R can combine with another oxygen molecule to give a radical RO_2 which, like oxygen can extract a hydrogen atom from the parent molecule RH and the reaction continues thus:-

$$R + O_2 \longrightarrow RO_2$$

$$RO_2 + RH \longrightarrow ROOH + R$$

The overall reaction in such oxidation is

$$RH + O_2 \longrightarrow ROOH$$

The induction period is seen due to the slow initial reaction of abstraction of a hydrogen atom from the hydrocarbon

molecule by the oxygen molecule.

(iii) The initial inhibition due to an impurity which is removed as the reaction proceeds:

Thus the $H_2 + Cl_2$ reaction may display anomalously long induction periods owing to the presence of small amounts of impurities such as NH_3, organic compounds[12], O_3[13] or O_2 which break the chains and are slowly consumed.

(b) <u>The effect of inhibitors</u>:

The most commonly applied tool for distinguishing a radical chain reaction from a molecular process is to use inhibitors which will compete with the parent molecule for the propagating radical. The action of an inhibitor is usually to react with the radical to form a stable molecule and a more stable radical[14], resulting in a marked drop in rate. The usual inhibitors for gas phase reactions are nitric oxide[15] propylene[16] and cyclohexene[17]. Nitric oxide, itself a free radical, reacts with an organic radical to form an addition complex

$$R + NO \longrightarrow RNO$$

which rearranges or decomposes. The inhibitory action of propylene can be explained by the reaction

$$R + CH_3CH=CH_2 \longrightarrow RH + CH_2-CH=CH_2$$

the allyl radical formed being stabilized by resonance will combine with itself to form diallyl rather than continue the

chain. The efficiency of cyclohexene may be due to the stability of the allylic cyclohexenyl radical formed when hydrogen atom is abstracted.

However, care must be taken in interpreting inhibition results because if chains are short and the competition by the inhibitor for the initating radical is not particularly effective, it is possible that large amounts of inhibitors will have little effect.

Hinshelwood[18] has shown that nitric oxide produces a limiting rate in certain organic decompositions and thus he believes that the maximally inhibited reaction is molecular. This conclusion, although it seems reasonable, still has some difficulties. The isotopic mixing investigations of Wall and Moore[19] and Rice and Varnerin[20] during the co-decompositions of deuterated and undeuterated compounds do not rule out the possibility of radical processes at maximum inhibition. This conclusion is not, however, absolutely firm because there remains the possibility that products formed by the reaction between free radicals and nitric oxide are still quite reactive, and able to undergo hydrogen-deuterium mixing. The mixing experiments, therefore, do not completely exclude the possibility of a molecular mechanism. Besides, the residual rate in the case of n-butane has also been interpreted as referring to a process consisting partly of a residual chain process[21,22].

Laidler and Wojciechowski[23] have suggested that organic decompositions that are fully inhibited by substances

such as nitric oxide or propylene proceed not by molecular mechanisms, but by special types of free radical mechanisms in which the inhibitor is involved in both initiation and termination. In the case of nitric oxide inhibition; initiation is considered to be by the abstraction of a hydrogen atom by NO, while termination involves reaction between the most plentiful chain carrier and either HNO or NO, depending upon whether or not H is a chain carrier. Specific mechanisms were proposed for the decompositions of paraffins, ethers and aldehydes, when inhibited by NO, and the resulting rate equations were shown to be consistent with the behavior observed experimentally.

Maccoll and co-workers[16,17] and Thomas have observed that a common limiting rate is obtained in the pyrolyses of some alkyl bromides using propylene, 2:4 dimethylpentane, cyclohexene and cyclopentadiene as inhibitors.

Holmes and Maccoll[25] have prefered propylene for alkyl iodide pyrolyses. The pyrolyses of alkyl halides is discussed in detail elsewhere in this thesis.

(iii) Isomerisation and molecular elimination reactions:

Three typical cases of such reactions are

(a) Depolymerisation of cyclobutane and isomerisation of cyclopropane[26,27]

(b) Elimination of olefins from organic esters[28], e.g., elimination of neopentyl chloride and a mixture of methyl butenes from pyrolysis of neopentyl chloroformate.

(c) Elimination of hydrogen halide from alkyl halides[29,30].

The conventional transition states for these processes are four centered and six centered and may be drawn as -

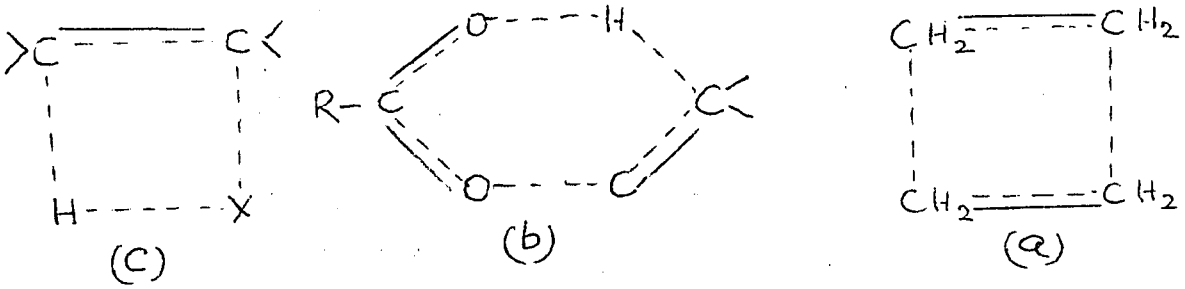

Type (c) was first discussed in connection with the pyrolyses of ethyl and tertiary butyl bromide.

If the experimental results indicate that a chain reaction is absent in the process, then it remains to differentiate between radical non-chain and molecular processes. This is usually done on energetic grounds. In the case of the former mechanism the activation energy will be equal to the homolytic bond dissociation energy. If the experimental activation energy is appreciably lower than the homolytic bond dissociation energy, then the reaction is usually assumed to be molecular.

1.3. Evidence for the molecular elimination reaction in the pyrolysis of alkyl halides:

Some alkyl halides decompose by a first order unimolecular elimination mechanism while in others duality of the mechanism is observed. In these cases reaction proceeds

simultaneously by the unimolecular mechanism and by a radical chain process. In the case of alkyl halides, the separation and identification of the molecular process is easier than other simple organic compounds. Molecular processes are usually distinguished from a radical process in the following way:-

If a source of atoms or radicals (such as a halogen or allyl bromide) sensitises the decomposition, then the mechanism is against a molecular process. On the contrary, if these sensitisers are ineffective in stimulating a chain reaction, the mechanism may be either a non-radical chain or a unimolecular elimination one.

Use of inhibitors in alkyl halide pyrolyses has been a very powerful tool for the investigation of a molecular reaction. Maccoll and co-workers found olefinic inhibitors to be efficient in the cases of alkyl bromide pyrolyses[16,17]. They noticed that different olefinic inhibitors produce the same limiting rate at maximum inhibition. The maximally inhibited rates were independent of the concentrations of different inhibitors. Thus it seems highly probable that the maximally inhibited rate is molecular because it is unlikely that different olefinic structures would produce the same limiting rate in case of any initiation or termination of chains by the inhibitors.

A molecular process can also be distinguished from a radical non-chain process on energetic grounds as described in the previous subsection.

Thus, if a reaction cannot be sensitised and the same minimum rate is produced by different inhibitors and if the activation energy is considerably lower than a bond dissociation energy, then in all probablities the reaction is molecular.

1.4. Structural effects upon the unimolecular elimination mechanism in organic halide pyrolyses:

At a constant temperature, halides, decomposing by a unimolecular mechanism and having the same organic residue R decompose at rates such that

$$k_{R-I} > k_{R-Br} > k_{R-Cl}$$

(c) Influence of the alkyl group:

Green, Harden, Maccoll and Thomas[17] showed that for the alkyl bromides, the rate of pyrolysis was dependent on the environment of the carbon-bromine bond. They found that the rate increases in going from a primary to a tertiary halide were at 380°C as -

C-H/C-Br → ↓	p	s	t
p	1	170	32,000
s	3.5	380	46,000
t	6.3	980	130,000

Thomas[24] has shown that the importance of the carbon-hydrogen environment is small i.e., allylic weakening

had little effect since the molecules

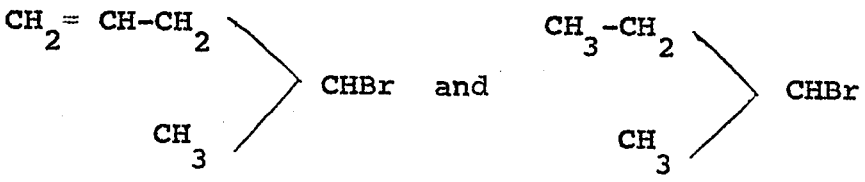

pyrolyse at the same rate. This can be interpreted as saying that the transition state contains little double bond character. Good[21] investigated the elimination of deuterium bromide from deuterated isopropyl-bromide and found that the activation energy was the same as for ordinary isopropyl bromide, but there was a slight fall in the A factor. Blades[22,31] found similar results for deuterated ethyl bromide. These results also support the importance of C-Br bond and rule out any significant role of C-H bond in determining the rate during pyrolyses. In the case of chlorides the same general picture is obtained with the exception that whereas the pyrolysis of primary bromides possesses a radical chain component[32], the monoalkyl chlorides decompose solely by a unimolecular process. However, mixed mechanisms are observed in the case of pyrolyses of compounds having more than one chlorine atom. Holmes and Maccoll[25] have shown that the relative unimolecular elimination rates in the case of secondary butyl iodide and isopropyl iodide are the same as for the corresponding chlorides and bromides. The same general picture is true for other iodides, chlorides and bromides, (table 2.2).

The unimolecular mechanism was suggested in the chlorides or bromides by Kistiakowsky[29] in 1936, but it was not proved rigorously. However, it was not further examined until 1949, when Barton[30] proposed that elimination of hydrogen halide proceeds via a four centre planar transition state i.e.,

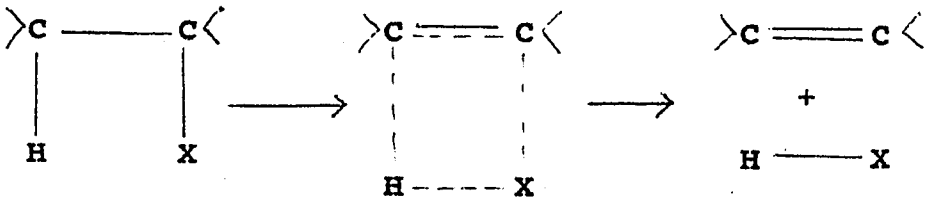

He based this scheme on two propositions:-

(a) The mechanism had to involve the arrangement of the atoms in a way which required the least energy.

(b) Examination of the gaseous elimination of H-X from certain cyclic compounds led to the conclusion that cis elimination was preferred, as determined by product analysis.

The mechanism of these decompositions was not definitely proved to be homogeneous and of unimolecular type. However, this was confirmed later[33] for (-) menthyl chloride. This decomposes by a homogeneous unimolecular mechanism and yields 3-menthene rather than 2-menthene, indicating preferential cis elimination i.e.,

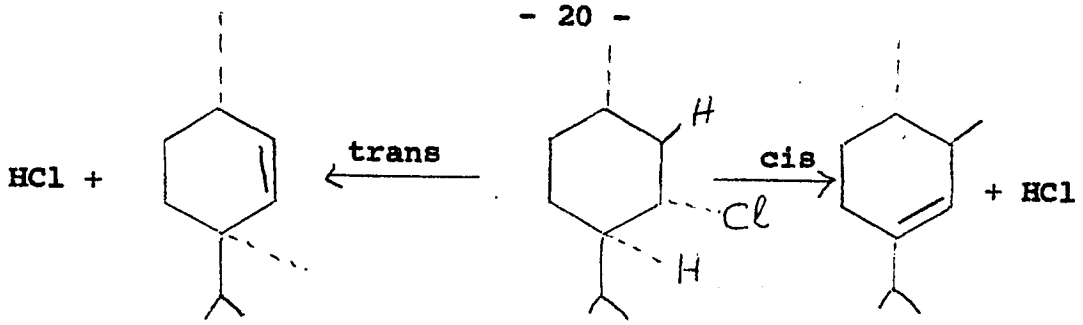

25%	unimolecular gas phase	75%
30%	E_1 in EtOH	70%

It is seen that the unimolecular elimination mechanism (E_1) in ethanol gives similar proportions of the two isomeric products[34]. It has been suggested[35] that the A factor may be expected to be well below 10^{13} due to the reduced entropy of the transition state. Green and Maccoll[36] suggested that this might not be true if the rotation is restricted to the initial state.

This picture of the transition state was accepted until 1955, when Maccoll and Thomas[37] pointed out the startling correlation of the rates of elimination in the gas phase of alkyl chlorides and bromides with the heterolytic bond dissociation energy of the carbon-halogen bond and also with the rate of SN_1 and E_1 reactions in solution (table 1.2) Maccoll's view is also supported by the same kind of trend in iodides (table 1.3).

Table 1.2. Comparison of the unimolecular activation energies E_{H-X} for the elimination of H-X, the homolytic bond dissociation energy D(R-X) and heterolytic bond dissociation energies $D(R^+X^-)$ of the carbon halogen bond.

	CH_3CH_2Cl	$(CH_3)_2CHCl$	$(CH_3)_3CCl$
E_{H-Cl}	50.8	50.5	41.4
D_{R-Cl}	80.9	82.2	78.3
$D_{R^+Cl^-}$	192.8	166.3	150.2
$\frac{D_{R^+Cl^-}}{E_{H-Cl}}$	3.17	3.29	3.63
$\frac{D_{R-Cl}}{E_{H-Cl}}$	1.33	1.67	1.89
	CH_3CH_2Br	$(CH_3)_2CHBr$	$(CH_3)_3CBr$
E_{H-Br}	53.9	47.8	42.2
D_{R-Br}	67.2	67.6	63.8
$D_{R^+Br^-}$	183.7	156.3	140.3
$\frac{D_{R^+Br^-}}{E_{H-Br}}$	3.41	3.27	3.33
$\frac{D_{R-Br}}{E_{H-Br}}$	1.25	1.42	1.51

Table 1.3. Comparison of the unimolecular activation energies E_{H-X} for the elimination of H-X, the homolytic bond dissociation energy D(R-X) and heterolytic bond dissociation energies $D(R^+X^-)$ of the carbon halogen bond
The same data for iodides as for chlorides and bromides in table 1.2.

	CH_3CH_2I	$(CH_3)_2CHI$	$(CH_3)_3CI$
E_{H-I}	49.6 (Present work)	47.96 (25)	39 (Present work)
D_{R-I}	51.2 (62)	53.0 (71)	48 (71,72)
$D_{R^+I^-}$	180.0 (38)	151 154 (39)	132 (40)
$\frac{D_{R^+I^-}}{E_{H-I}}$	3.6	3.15	3.39
$\frac{D_{R-I}}{E_{H-I}}$	1.02	1.11	1.23

There is a distinct lack of correlation with either the homolytic bond dissociation energies or with SN_2 reactions. Ingold[34] has set out in detail the evidence and arguements leading to the conclusion that SN_1 and E_1 reactions proceed as a first stage by ionisation to R^+ and X^-. Maccoll and Thomas therefore suggested that the pyrolysis of alkyl halides might be quasi heterolytic with polarisation of the carbon halogen bonds. The energy needed to accomplish this is partly reduced by the stabilizing field of the polarised hydrogen atom in the β position, i.e.,

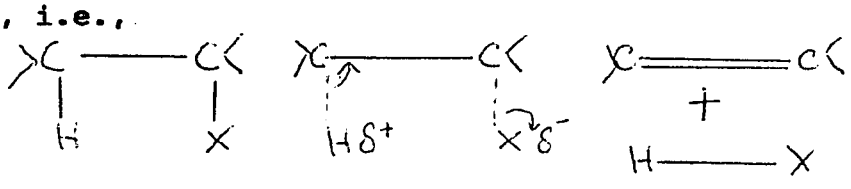

The role of the β hydrogen atom is likened to that of the solvent molecules which stabilize polar transition states in solution.

The evidence for this theory has steadily accumulated and has been set out in detail by Maccoll[41,42].

From this evidence Maccoll concluded that the transition state for gas phase eliminations from alkyl halides is best represented as a carbonium ion pair, R^+X^-. As pointed out by Ingold[43], this hypothesis cannot be ruled out on energetic grounds, and it does give a rational explanation of the observed behavior.

Maccoll supports his idea also on the following grounds -

Since no complication arises from solvation in the gas phase, a linear relationship might be expected between the activation energy for elimination, E(HX) and the heterolytic bond dissociation energy, $D(R^+X^-)$ of the carbon halogen bond. Such a plot is shown in Fig.1, for some chlorides, bromides and iodides where it is seen that the suggested relationship is quite well obeyed. In this figure Maccoll's original[42] plot is supplemented by some recent data.

Recently Benson and Bose[44] have re-examined the elimination of H-X from gas phase alkyl halides in terms of recent and less controversial results on iodides. These authors consider Maccoll's point of view as an extreme and not supportable in terms of simple models or data on isomerisation. On the contrary, they have shown that an intermediate charge separation corresponding to formal changes of + ½ and - ½ on

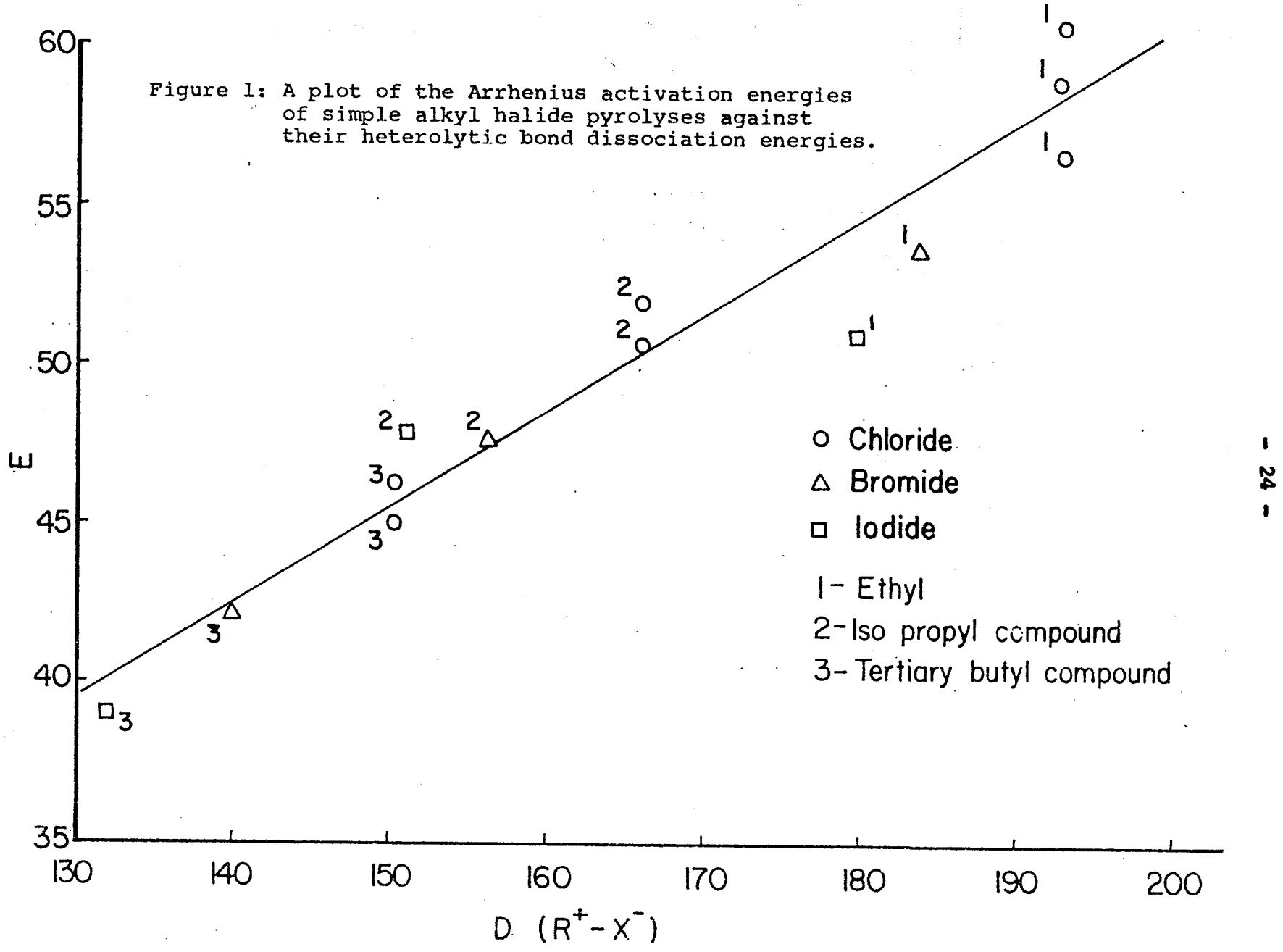

Figure 1: A plot of the Arrhenius activation energies of simple alkyl halide pyrolyses against their heterolytic bond dissociation energies.

the H and X atoms of HX appear to give quite reasonable results. Thus, they proposed a very polar transition state with very large charge separation and to which they give the name "Semi ion pair" transition state.

1.4. Surface effects in gas phase reactions:

A homogeneous gas phase reaction involves only particles (atom, molecules and ions) in the free gaseous state. Any reaction with particles adsorbed on solids or absorbed and dissolved in solids or liquids or with particles of solids or liquids is termed a heterogeneous reaction.

The surface of the reaction vessel may play a significant role in gas phase decomposition studies. Such catalysis depends on the nature of the material of the reaction vessel.

The most commonly used material for constructing a reaction vessel in gas phase kinetic study is pyrex glass or silica because of

(i) their thermal and chemical stability,

(ii) they can be suitably put into shape by blowing,

(iii) they are suitable for light transmission in photo chemical studies.

The usual method to test the homogeneity of a reaction is by increasing the surface to volume ratio of the reaction vessel. In case of glass or silica this is usually achieved by packing the reaction vessel with concentric tubes of the same material.

The surface effect is particularly prominent in the case of alkyl halide pyrolysis in glass vessels. This may be interpreted as due to the polar nature of the glass surface[45,46]. Recently, Swinbourne[47] has examined the kinetics of the catalysis of an alkyl chloride pyrolysis due to the glass surface. He believes that the catalytic action is through the activated complex.

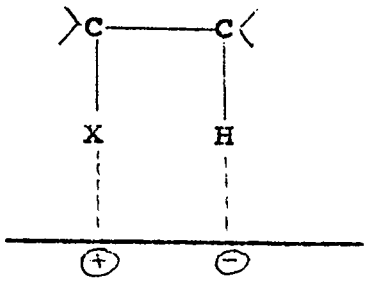

glass surface

The chlorine atom is eliminated as Cl^- and the hydrogen as H^+. The ions do not occur in a free state but the charge separation is the rate determining factor.

Heterogeneity in halide pyrolyses increases from primary to tertiary compounds.

In the case of many pyrolyses prolonged seasoning of the reaction vessel with the reaction products eliminates the wall effect and gives a reproducible and a homogeneous rate. Such seasoning produces a thin carbon coating, which acts as a non-polar skin on the polar surface of the reaction vessel. In other cases, when the substances to be studied are also polar the above procedure to obtain a homogeneous rate is not always sufficient. Thus, in recent years gas phase pyrolyses have been carried out using glass vessels coated with a fine

film of many inactive materials. Some of the coating materials employed are (i) carbonaceous deposits from the decompositions of organic chlorides[10,45,48,49], bromides[7,50,51] and olefins[52] and (ii) potassium chloride[53,54,55]. Recently, in some of these coatings, free radical concentrations have been found by E.S.R. studies[56,57]. These may themselves exert a catalytic effect, so such coatings should be used with caution.

SECTION - 2

A SURVEY OF PREVIOUS WORK ON SIMPLE ALKYL MONO-HALIDES:

2.1. Alkyl Chlorides and Bromides:

The unimolecular elimination reactions of alkyl chlorides and bromides have been exhaustively studied by Barton and co-workers and by Maccoll and others respectively. During these studies, it has been shown that all the monochlorides with β hydrogen atoms eliminate hydrogen chloride unimolecularly on pyrolysis, the absence of a chain mechanism being proved by inhibition studies; whereas the bromides decompose by molecular elimination or by a mixed mechanism. In the latter case the unimolecular reaction can be isolated by the use of inhibitors.

The Arrhenius parameters of simple alkyl monochlorides and bromides are tabulated in table 2.1. The table also gives the mechanism of reaction in respective cases of alkyl halide pyrolyses.

Table 2.1. The decompositions of organic mono-chloro and mono-bromo alkanes
X - inhibited by cyclohexene,
Y - toluene carrier technique.
The "mechanism" column refers to the process for which the Arrhenius parameters in other columns have been found.

Compound	Mechanism	E(K.Cals)	$\log_{10}A$	References
Methyl Chloride	Complex	85.0	——	58
Methyl Bromide	"	67.0 Y	——	59

Table 2.1. Cont'd

Compound	Mechanism	E(K.Cals)	$\log_{10}A$	References
Ethyl Chloride	Unimolecular	59.5	14.2	60
	"	60.8	14.6	61
	"	55.29	13.11	62
	"	56.62	13.46	63
	"	56.4	13.16	64
	"	59.0	———	58
Ethyl Bromide	"	53.9 X	13.42	17
	"	53.3 Y	13.86	22
	"	52.2	12.73	31
	"	53.76	13.25	58
	Radical non chain	53.2	14.06	50
	Unimolecular	53.7	13.19	64
	Complex	46.4	11.78	65
n-Propyl Chloride	Unimolecular	55.5	13.51	66
	"	56.57	13.87	63
n-Propyl Bromide	"	50.7 X	12.9	16
	"	50.7 Y	13.0	22
	1.5 order Chain	33.8	10.86	51
	"	42.7	13.62	61

Table 2.1. Cont'd

Compound	Mechanism	E(K.Cals)	$\log_{10}A$	References
i-Propyl Chloride	"	52.16	13.1	63
	"	50.5	13.4	61
	"	51.1	13.64	64
i-Propyl Bromide	"	47.7 Y	13.6	22
	"	47.8	13.62	67
	"	47.0	12.74	68
n-Butyl Chloride	"	57.9	14.5	69
	"	57.0	14.0	66
	"	56.55	13.98	63
n-Butyl Bromide	"	50.9 X	13.18	16
	1.5 order Chain	48.00	——	68
s-Butyl Chloride	Unimolecular	49.6	13.62	70
	"	50.55	13.91	63
s-Butyl Bromide	"	43.8	12.63	16
	"	45.5	13.04	71
	"	45.4	13.18	72
	"	46.5 X	13.53	72
i-Butyl Chloride	"	56.85	14.02	73
	"	56.32	13.90	63
i-Butyl Bromide	"	56.4 X	13.05	74
	1.5 order Chain	30.0	6.26	58

Table 2.1. Cont'd

Compound	Mechanism	E(K.Cals)	$\log_{10}A$	References
t-Butyl Chloride	Unimolecular	46.31	13.27	63
	"	45.0	13.9	73
	"	41.4	12.4	49
	"	45.0	13.77	75
	"	46.61	14.41	76
	"	46.2	13.9	77
t-Butyl Bromide	"	41.0	13.33	66
	"	42.2	14.0	74
	"	40.5	13.3	73,78
	"	41.5	13.5	74

2.2. Alkyl iodides:

The pyrolyses of alkyl iodides are not so simple as alkyl chlorides or bromides. The products are usually iodine and olefin and the corresponding paraffin in equimolar amounts. The mechanisms are not so well established and they are not invariably unimolecular.

The first kinetic study of organic iodides was carried out by Ogg[79] who studied the reactions between hydrogen iodide and methyl, ethyl and normal propyl iodides at various concentrations in the temperature range 250°-320°C. The reactions were followed by analysing for iodine spectrophotometrically and the results were found to fit the bimolecular reaction equation

$$\frac{d}{dt}(I_2) = k(RI)(HI)$$

but that k varied inversely with the hydrogen iodide concentration. The equation was modified to

$$\frac{d}{dt}(I_2) = k_1(RI)(HI) + k_2\frac{(RI)(HI)}{(HI) + I_2}$$

where k_1 represents the rate constant of the bimolecular reaction and k_2 that of the thermal decomposition of the alkyl iodide. In all three cases Ogg found E_2 (for the thermal decomposition) to be 43 K.Cals per mole. This value is very much lower than the presently accepted values. The following mechanism was proposed by Ogg to explain his results.

$$RI + HI \longrightarrow RH + I_2 \quad \ldots\ldots\ldots(1)$$

$$RI \longrightarrow R + I \quad \ldots\ldots\ldots(2)$$

$$R + HI \longrightarrow RH + I \quad \ldots\ldots\ldots(3)$$

$$R + I_2 \longrightarrow RI + I \quad \ldots\ldots\ldots(4)$$

$$I + I + M \rightleftharpoons I_2 + M \quad \ldots\ldots\ldots(5)$$

He claimed that reactions (3) and (4) are faster than (2) and that the initial step in the iodide decomposition is (2). The back reaction of (2) together with (4) can account for the very slow decompositions of iodides at the temperatures investigated.

Benson[80] and Sullivan[81] have re-interpreted these early results of Ogg. They independently came to the conclusion that the mechanism is a simple iodine atom catalysed radical reaction and that the rate determining step is

$$I + RI \longrightarrow R + I_2$$

Their overall mechanism is

$$RI \longrightarrow R + I \quad \ldots\ldots\ldots\ldots \quad (1)$$

$$I + RI \rightleftharpoons R + I_2 \quad \ldots\ldots\ldots\ldots(2,-2)$$

$$R + HI \rightleftharpoons RH + I \quad \ldots\ldots\ldots\ldots(3,-3)$$

$$I_2 \rightleftharpoons 2I \quad \ldots\ldots\ldots\ldots \quad (4)$$

Sullivan estimated the values for the activation energies of step (2) for CH_3I and C_2H_5I to be 19.8 and 16.7 K.Cals $mole^{-1}$. Using some thermodynamic estimates Benson came to the conclusion that $E_{+3}-E_{-2}$ appears to lie between 0 and 2 K.Cals $mole^{-1}$ and

that $E_2 + E_{+3} - E_{-2}$ were 20.8, 19.3 and 19.6 K.Cals mole^{-1} for CH_3I, C_2H_5I and n-C_3H_7I respectively.

In an attempt to determine the values of the bond dissociation energies, Butler and Polanyi[82] pyrolysed a number of alkyl iodides using a flow technique and small partial pressures. They measured the amount of iodine produced and in a few cases hydrogen iodide.

Ogg and co-workers[83,84,85,86] have shown that for n-propyl, n-butyl, i-propyl, s-butyl and i-butyl iodides both the unimolecular elimination of halogen acid and iodine catalysed decompositions are possible. These authors were unable to prove unequivocally the mechanism of these pyrolyses.

Iodine atom reactions, conspicuous surface effects and the weak carbon iodine bonds make these systems kinetically more complex. Two types of processes seem reasonable in these decompositions -

(i) the unimolecular elimination of hydrogen iodide which is of first order and

(ii) an autocatalytic reaction between an iodine atom and the alkyl iodide which is of order 1.5.

In some systems only one of these two is rate determining whereas in others, a mixed mechanism comprising both the processes is observed.

Besides unimolecular elimination of hydrogen iodide the first order process may also be reconciled with a radical non chain process where homolysis of the carbon-iodine bond takes place as the rate determining step. However, this possibility can often be ruled out on energetic grounds,

since the activation energy must be equal to the bond dissociation energy D(C-I) in the iodide. This is not usual in iodides and as such the elimination process seems almost certain for the first order decompositions of iodides.

Lately, Benson and co-workers[87,88,89,90] and Holmes and Maccoll[25] have taken a keen interest in iodide systems in gas phase and some of the ambiguities about their nature of decomposition seem to be removed. Tsang[64] has tried to verify some previous data on alkyl iodide pyrolyses by using a single pulse shock tube and comparative rate technique. The pyrolytic results to date are summarised in table 2.2.

Table 2.2. Activation energy for the thermal decomposition of alkyl iodides compared with the bond dissociation energies.

Compound	D(R-I) K.Cals/mole	(Ref.)	E(R-I) K.Cals/mole	order	$\log_{10}A$	References E	References log A
Methyl iodide	53.5	63	54.0	-	-	82	
	54.0	93,94					
Ethyl iodide	51.3	82	52.2	1	-	82	
	53.0	94	50.0	"	#13.36 *13.66	87	
	51.0	93	49.3	"	*13.53	95	
			51.02	"	*14.24	(this work)	
n-propyl iodide	53.3	82	50.0	$\frac{3}{2}$	-	82	
	54.0	93	37.9	"	10.06	83	
			38.4	"	10.18	(this work)	

Table 2.2. Cont'd

Compound	D(R-I) K.Cals/mole	(Ref.)	E(R-I) K.Cals/mole	order	$\log_{10}A$	References E	log A
i-propyl iodide	53.0	93	46.1	1	-		82
	51.0	94	42.9	"	*13.2		85
			47.9	"	*14.79		96
			43.5	"	#12.96		89
			45.1	"	;13.67		64
n-butyl iodide	54.0	82	49.0	$3/_2$	-		84
s-butyl iodide	39.4	91	47.9	1	*15.2		25
i-butyl iodide	-		37.8	$3/_2$	-		97
t-butyl iodide	48.0	87,88	45.1	1	-		82
			36.4	"	+12.52		90
			38.08	"	;13.73		64
			38.33	"	*13.53		(this) (work)

\# Unimolecular elimination of HI

* Over all first order values from direct pyrolyses

\+ Estimated on the basis of reverse addition of HI + olefin iodide

; Shock wave studies and comparative rate technique estimation for unimolecular elimination of HI

Holmes[91] and also Benson[92] believe that the behavior of iodides is probably governed by the relative rates of the following three reactions -

(a) $RI \longrightarrow HI + \text{olefin}$

- the first order unimolecular elimination

(b) $I + RI \longrightarrow R + I_2$

or

$I + RI \longrightarrow R^1I + HI$

- an autocatalytic decomposition

(c) $RI + HI \longrightarrow RH + I_2$

- bimolecular reaction removing HI

The rapid reaction (c) maintains the hydrogen iodide at a very low stationary state concentration. Mechanism (a) appears to govern the pyrolyses of ethyl iodide and iodides containing a β-methyl group while mechanism (b) holds for iodides without a β-methyl group.

2.3. Relative rates of pyrolysis of simple alkyl chlorides, bromides and iodides:

Holmes and Maccoll[25] reported that isopropyl and secondary butyl halides (chlorides and bromides) decompose similarly and their rate ratios i-propyl/s-butyl are also similar. Their view point is also supported by the similar trend observed also in case of other halides. Table 2.3 shows the correlation of rates of pyrolysis of various halides on substitution whereas table 2.4 gives the relative rates of halides having the same organic residue R.

Table 2.3. Relative rates of pyrolysis of alkyl halides of methylated series.
Temperatures for the comparison are chosen so as to give the rate equal to 10^{-4} sec.$^{-1}$ for the ethyl compound.
References for rates are given in the parenthesis.

X →	Cl		Br		I	
R ↓	(449.3°C)		(403.6°C)		(338.0°C)	
C_2H_5	1	(63)	1	(17)	1	(this work)
i-C_3H_7	135	(61)	191	(67)	44	(25)
s-C_4H_9	417	(63)	309	(16)	118	(25)
t-C_4H_9	14460	(75)	12600	(74)	6920	(this work)

The above table also indicate that the rate relationship

tertiary 〉 secondary 〉 primary

for the gas phase unimolecular elimination of alkyl halides is similar to that for SN_1 or E_1 reactions in solution, thereby suggesting a similar mechanism.

Table 2.4. Relative rates of halides having the same organic residue.
Temperatures chosen give the rate for chloro compound equal to 10^{-4} sec.$^{-1}$.

X→	Cl	Br	I
R ↓	(441.1°C) 1 (61)	9	360
C_2H_5	(435.0°C) 1 (63)	7 (17)	330 (this work)
i-C_3H_7	(361.0°C) 1 (61)	14 (67)	186 (25)
s-C_4H_9	(343.6°C) 1 (63)	13 (16)	166 (25)
t-C_4H_9	(280.0°C) 1 (75)	8 (74)	240 (this work)

SECTION - 3

DESCRIPTION OF THE APPARATUS AND EXPERIMENTAL TECHNIQUE

3.1. General outline:

During experimental studies of the kinetics of homogeneous gas reactions, the rate of change of concentration of a reactant or product is usually determined under isothermal conditions. Two general methods have been used for this purpose:

(a) The static method in which substances are allowed to remain in the reaction vessel and the rate of reaction is measured either continuously as the reaction proceeds (e.g., by spectrophotometry or pressure change) or after definite time intervals (e.g., by analysis of products)

(b) The dynamic or flow method in which the reactants are caused to flow through the reaction vessel and the rate of the reaction is determined by comparison of the influent and effluent vapours.

The former method is more common in kinetic studies and is also the method employed in the present investigation.

3.2. The thermostat and the reaction vessel

The thermostat consisted of two concentric electrically heated tubes, each of 12" length. The ceramic outer tube was of 4" diameter and ½" thick while the thickness and diameter of the steel inner pipe was ½" and 3" respectively. The inner

portion of the steel pipe was lagged with thick, uniformly moulded asbestos to fit the reaction vessel evenly and make the latter free of any strain. The exterior of the ceramic tube was wound with 48 turns of nichrome heating ribbon. Each turn of winding was separated from the next by about 0.5 cm. In order to control the uniformity of the temperature gradient along the whole length of the reaction vessel, the windings were divided into three equal and separate circuits namely the bottom winding B, the middle winding M and the top winding T (Fig.2). The ribbons were attached to the ceramic by means of porcelain cement and the ends of each circuit were insulated from each other with the help of ceramic beads. Each winding was connected to a powerstat. The voltage of each powerstat was adjusted to produce zero temperature gradient along the reaction vessel.

The furnace was contained in a quarter inch transite sheet box of dimension 12"x12"x16". The furnace assembly is shown in figure 2.

The temperature was recorded by means of an iron-constantan thermocouple, one end of which was kept in a narrow tubular well inside the reaction vessel (Fig.2) and the other end was connected to a thermocouple potentiometer which could read to 0.01 millivolt. The cold junction was at $0^{o}C$.

The temperature was controlled by means of a thermo-electronic temperature regulator which employed a chromel-alumel thermocouple. The thermocouple was placed near the bottom of the reaction vessel. A mercury plunger electronic

relay was used in conjunction with the thermoelectronic regulator. The relay was connected to the thermoregulator via the powerstat used for heating the M circuit.

The cylindrical reaction vessel was (Fig.2) made of pyrex glass and was of capacity about 175 c.c. The length and the outer diameter of the vessel were 10cm., and 5cm., respectively. The vessel had two outlets consisting of 2mm. capillary tubes and a 8cm. long thermocouple well A. One outlet of the reaction vessel was joined to the vacuum line by means of 2mm. capillary tubing and the other outlet was joined to the spoon gauge G. The spoon gauge together with its long lever l was housed in a glass casing C. The ground mouth of the casing was vacuum sealed by means of a ground lid (Fig.4) with the help of grease. This casing of the gauge was also connected to the vacuum line in order to evacuate the outer side of the gauge. To prevent any condensation of iodine the spoon gauge was kept heated by placing it inside the furnace as shown in figure 2.

The packed reaction vessel was of the same size and shape and was packed with thin concentric pyrex tubes. The ends of the tubes used for packing were fire polished. A cross section of such a packed vessel is shown in figure 3.

The temperature gradient in the reaction vessel was checked from time to time and never exceeded 0.2°C. During the kinetic investigation, the hot end of the thermocouple was placed always about 5cm., inside the thermocouple well A.

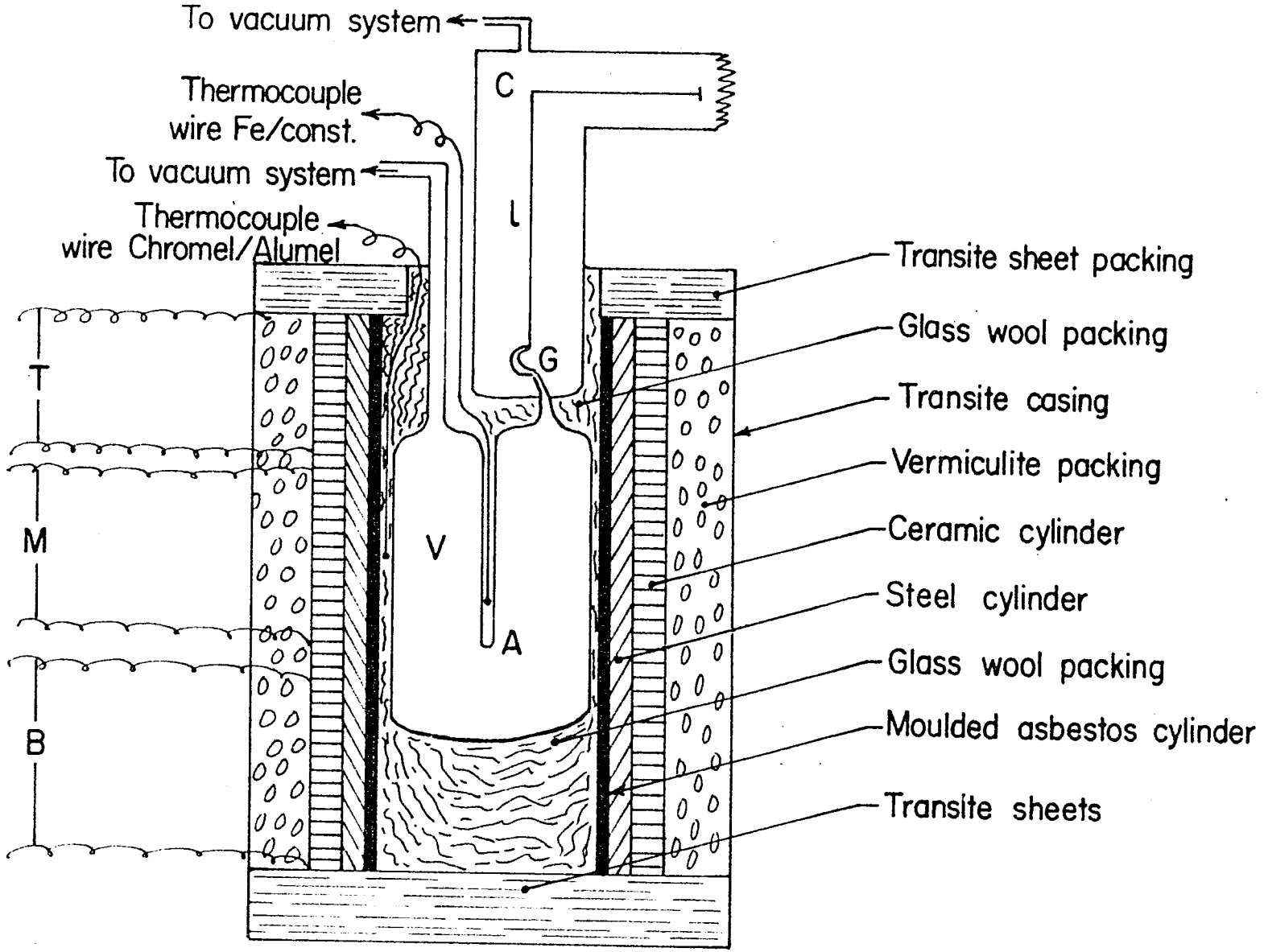

Figure 2: A schematic diagram of the thermostat and the reaction vessel.

3.3 The pressure measurement:

Pressure measurement was accomplished by means of a spoon gauge G, (Fig.2) made of pyrex glass, which was connected to the reaction vessel V. The details of the pressure measuring device are shown in figure 4. The tip of the long glass lever 1 of the spoon was kept touching a horizontal compass needle N which was mounted on a steel pin. The pin rested vertically in the hole of a small capillary head H, which was glued to the lower side of the spoon gauge casing C, by means of "araldite". Another thin pin welded to the needle N, rested in another capillary head H' which was glued to the upperside of the casing. A small mirror M was attached to the supporting pin of the compass needle also by means of "araldite". The pressure difference between the sides of the spoon gauge moved the lever which in turn displaced the magnetic needle and hence the mirror. Light from lamp L falling on the mirror reflected the movement on the scale S'. After setting the magnet and the mirror in position, the ground cover disc was put on and the both sides of the gauge were evacuated. The vacuum in the system helped to keep the cover disc in position. A small magnet m, fixed on the outer side of cover disc by means of wax, kept the compass needle N always touching the lever 1 and supplied a restoring force to the needle.

The gauge was calibrated against a Hg manometer as follows:-

Both sides of the spoon gauge were thoroughly evacuated. The light spot was adjusted to the zero of the scale.

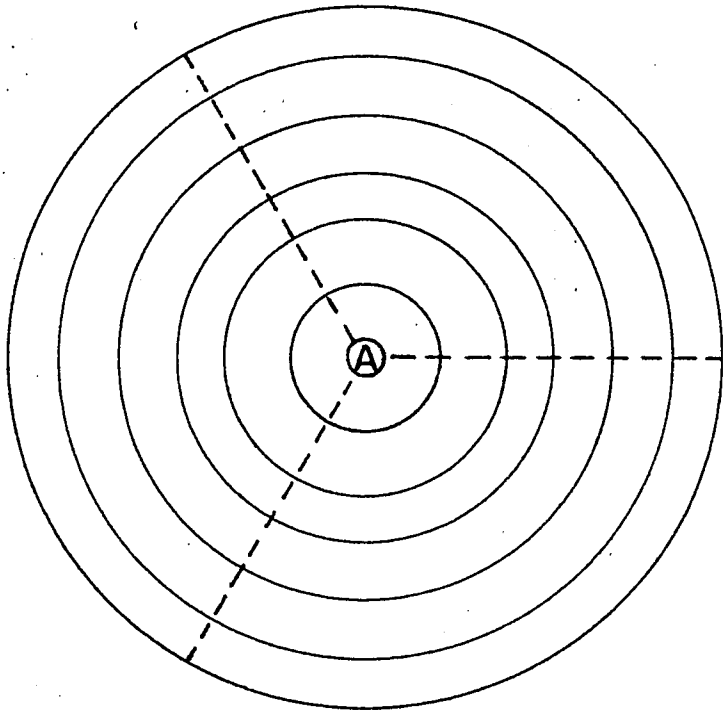

Figure 3: A cross section of the packed reaction vessel.

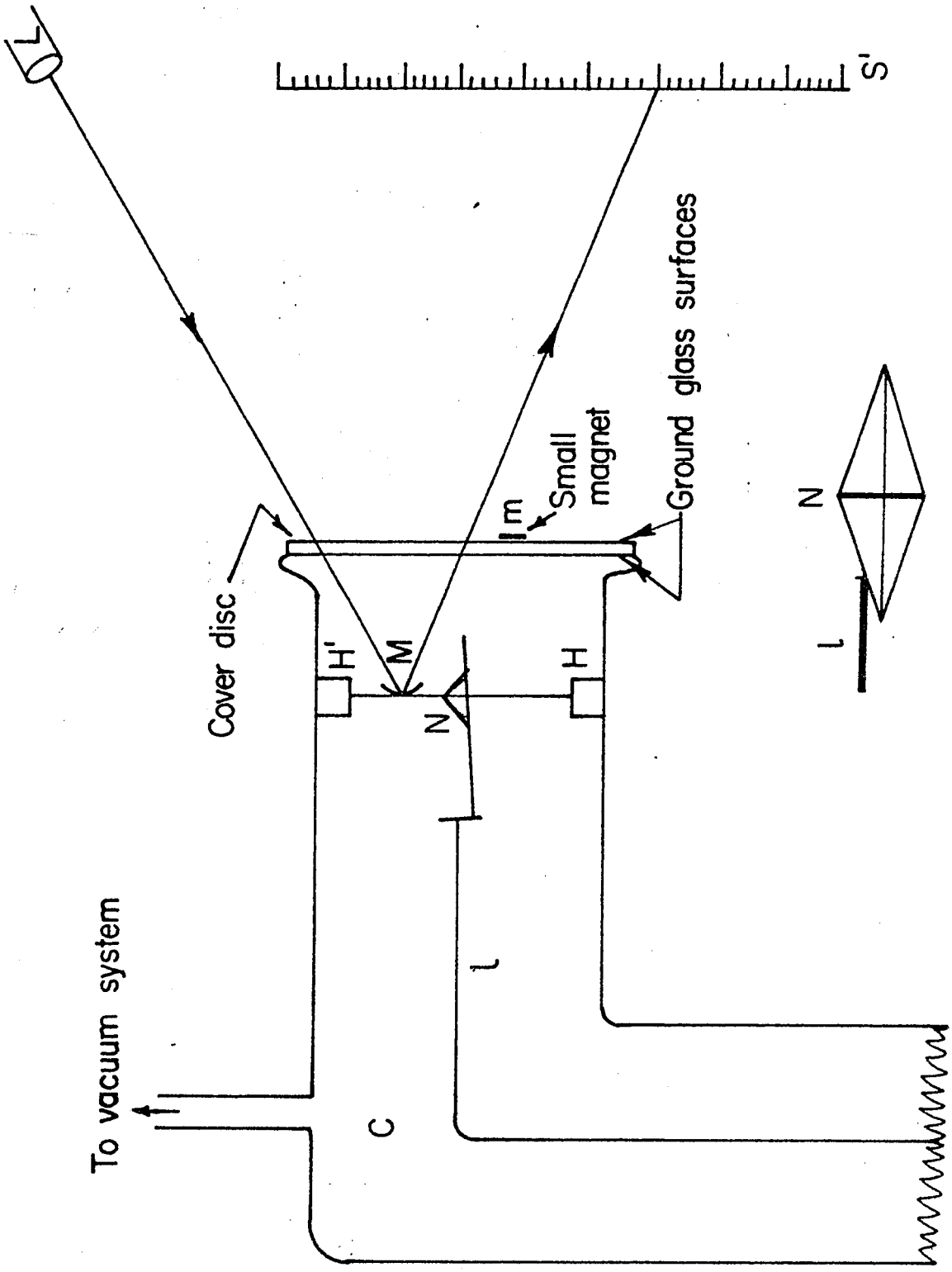

Figure 4: The details of the pressure measuring device.

Nitrogen gas was admitted to the reaction vessel while the outer side of the gauge was still evacuated. This caused a deflection of the light spot on S'. Now leaving this gas in the reaction vessel the rest of the system was completely evacuated. Then nitrogen was admitted to the outside of the gauge so as to bring the light spot back to zero on S'. The pressure reading in the manometer attached to the outer side of the gauge corresponded to the scale reading caused by the gas in the reaction vessel. This process was repeated for several different deflections and a calibration curve was drawn. Calibration had to be checked from time to time, and particularly, if the position of outside magnet m was changed for any reason. The sensitivity of the gauge could be varied from 1.3 to 4.0 small scale divisions to 1 mm. of Hg, with different settings of the compass needle N and outer magnet m.

3.4. The Vacuum System:

A conventional static vacuum system made of pyrex glass was used. The schematic diagram is shown in figure 5. All taps (1,2,3.....etc.) were of high vacuum type and all the traps (T_1,T_2,T_3.....etc.) were removable types made with "Quickfit" joints. Silicone high vacuum grease was used throughout the system. The main manifold consisted of a straight, 20mm. wide tube between taps 6 and 7. Four large bulbs ($V_1V_2V_3V_4$) for storing different reactants, two Hg manometers M_1 and M_2 and Edwards "Vacustat" gauge P were joined to the main manifold and separated from the latter by different

taps. V_1 and V_2 were used for storing alkanes and alkenes while in V_3 and V_4, HI and NO were stored respectively. "Quickfit" male joints $S_1S_2S_3$ etc., were attached to the system to serve as outlets. They were used to admit air or nitrogen to the system or to transfer substances to and from the system.

The reaction vessel was connected to the vacuum line through tap 8; 2mm. capillary tubing being the connecting link between the reaction vessel and tap 8. A finger tube t ½" long and having a bore of 6mm., was joined to the system by means of a capillary tube, between tap 8 and the reaction vessel. This side arm t was used, when necessary for distilling the reactants before entering to the reaction vessel. A large removable glass bulb V_5 was also connected between tap 8 and reaction vessel by means of capillary tube. This bulb was separated from the system by capillary stopcock 9 and ordinary stop cock 11. This bulb contained some basic absorbents and was used to separate hydrogen iodide and iodine from the products in the t-C_4H_9I pyrolysis. The total dead space between taps 8,9 and the reaction vessel, was estimated to be not more than 2% of the reaction volume. The casing of the spoon gauge, which also contained the accessories for the pressure measuring device, was connected to the system between taps 4 and 5.

A 4" long and 1cm. wide storage tube S used for iodide sample storage was separated from the system by tap 12. Iodide was always stored in S, after distilling from S_3 and degassing several times at liquid nitrogen temperature.

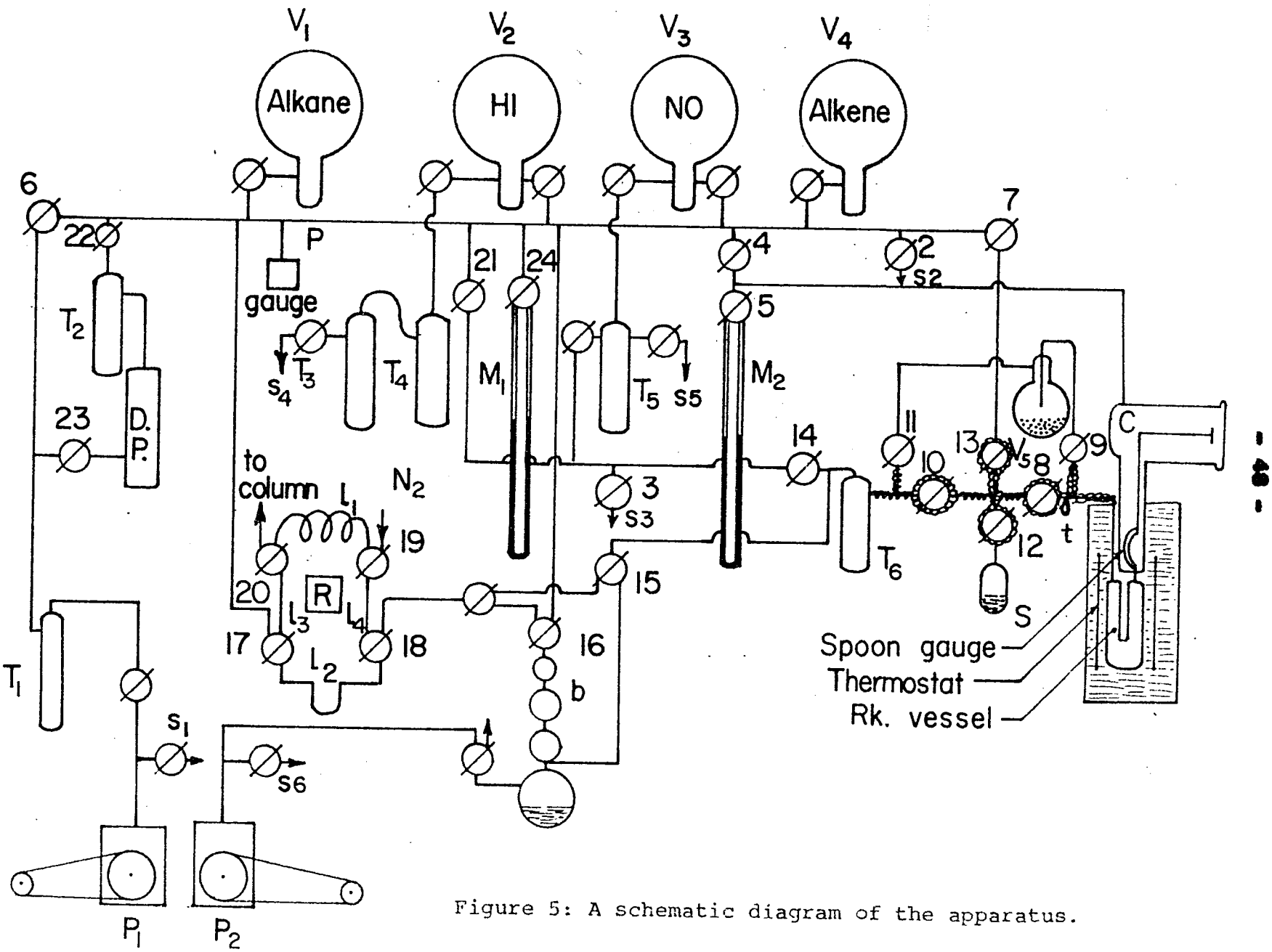

Figure 5: A schematic diagram of the apparatus.

The glass tubing and taps (9,11,12 and 13) between the furnace and the titration trap (T_6) were electrically heated to 90°C by means of nichrome heating ribbon, lagged with asbestos. This auxiliary heating was controlled by a 2 ampere variable powerstat. The side arm t was heated by covering it with a similarly heated glass tube which could be removed from position when liquid nitrogen was required there. The purpose of this heating was to prevent condensation of iodine before entering the titration trap and to facilitate distillation of low vapour pressure substances from the reaction vessel and adjoining tubing.

Coolants used were liquid nitrogen, propanol-liquid N_2 mixture, acetone-CO_2 mixture, ice-HCl, ice-salt and ice-water mixture and these were used according to need and convenience.

The gas chromatography apparatus R and gas burette were separated from the system by three way taps 15,16 and 17. A pump P_2 was employed for the gas burette.

The system was evacuated by means of Edwards high vacuum "Speedivac" model 25C20A pump P_1. The complete evacuation was facilitated by a mercury diffusion pump (D.P.) joined to the system between taps 22,23. The pressure was read on an Edwards 'Vacustat' gauge. The "sticky" vacuum indicated by the gauge was estimated to be sufficient (10^{-4}-10^{-5}mm.) to start any run.

Air was never allowed to enter the reaction vessel until it was to be out for the change because a trace of O_2

could alter the nature of reaction. When taps 8 or 9 needed regreasing, pure N_2 was admitted to the reaction vessel.

3.5 Chromatographic apparatus

The essentials of the apparatus are shown in figure 6. Samples entering through the tap 18 were condensed in a capillary U tube U and passed to the column and cell through tap 20. Four three-way taps were positioned such that the length of the tube l_1 (between taps 20 and 19) was equal to sum of the tubes l_3 (between taps 20 and 17), l_2 (between taps 17 and 18) and l_4 (between taps 18 and 19). Dry nitrogen as carrier gas was always passed through l_1 to the main column, and through l_5 to reference column. Thus when nitrogen flow was diverted through l_2, l_3 and l_4 in order to force the sample into the main column the resistance to flow remained the same. This ensured that the base line was unchanged and the peaks on the recorder were unaffected by the change of course of nitrogen flow. The flow of nitrogen was regulated with the help of a "Speedivac" pressure controller placed between N_2 cylinder and the tap 19. Both columns were of the same length, packed with the same material and placed in the same theromostat at $0^{\circ}C$.

The columns were made of copper tubing of quarter inch outer diameter and were packed with 60-80 mesh chromosorb P or silica gel. "Kovar" seals were used to join metal to glass. The cell used was a "Gow-Mac" tungsten catharometer and the recorder was a "Nesco" graphic recorder model JY 120-1.

The cell was operated by a freshly charged 12 volt battery. About 160 milli-ampere current was optimum for the functioning of the cell.

3.6. Procedure for a typical run:

The system was completely evacuated to a "sticky" vacuum. The iodide in the storage vessel S was degassed at liquid nitrogen temperature before each run. Iodide vapour was introduced into the reaction vessel by opening taps 12 and 8 and keeping taps 9, 10 and 13 closed. For most of the runs S was kept at room temperature but it was warmed with hot water when a larger pressure of vapour was required. When the desired pressure of iodide was indicated on the scale S', taps 8 and 12 were closed and a stop watch was started. Pressure changes were noted at different times. At the end of each run, products were condensed in the titration trap T_6 at liquid nitrogen temperature either directly or via V_5 to absorb HI and I_2 as the experiment required. I_2 was separated from the gaseous product at the temperature of acetone - carbon dioxide mixture ($-78^{o}C$). The I_2 was dissolved in KI solution and titrated with 0.02N thiosulphate solution. The gaseous products were either pumped off or were analysed by GLC.

If a very large initial concentration of iodide was required, some iodide was distilled into the side arm t at liquid nitrogen temperature, tap 8 was closed and the distillate vaporised rapidly by a Bunsen flame. The side arm was again covered with its heater. In the case of the runs with an

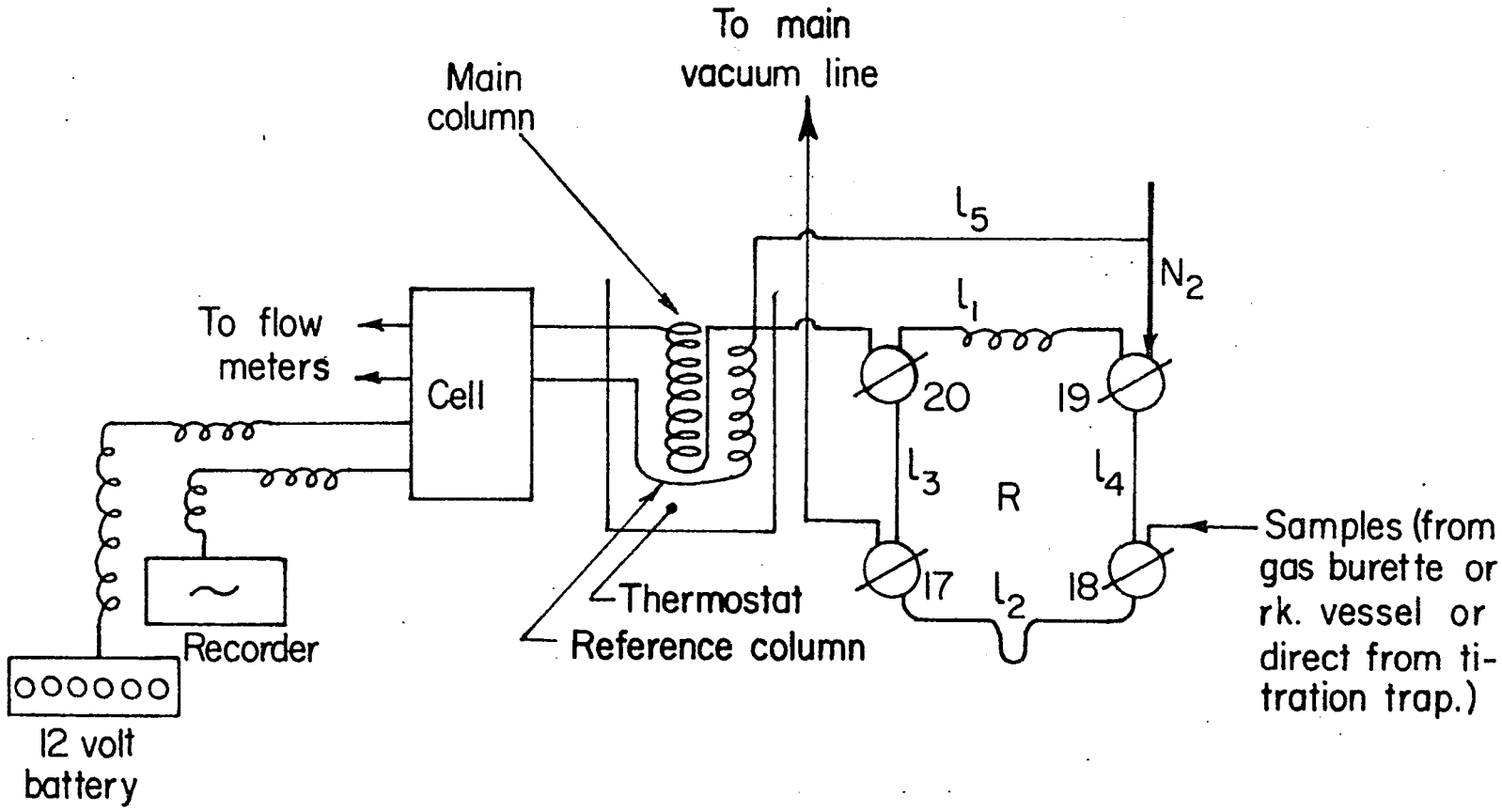

Figure 6: The gas chromatography apparatus.

inhibitor or with any other reactant, the latter was first distilled into t which was at liquid nitrogen temperature, it was then vaporised to indicate pressure on S' and was again condensed in t. The iodide was distilled on top of it and then the mixture was vaporised quickly as before. From the difference at zero time, the initial iodide pressure was found.

3.7. Homogeneity tests:

Besides the usual method of increasing the surface to volume ratio, different chemical coatings were given to the reaction vessel in the following way -

Clean glass:

For these experiments a "clean glass" reaction vessel was one that had been washed with chromic acid, thoroughly rinsed with distilled water and dried in vacuo.

Allyl bromide carbon:

About 200 mm. of pure allyl bromide vapour were decomposed at 360°C for two hours to produce a thin carbonaceous coating.

Ethyl bromide:

500 mm. of pure ethyl bromide vapour for 24 hours at 480°C.

Isobutene carbon:

400 mm. of research grade isobutene were decomposed

at 490°C for 4 days. A thin, shiny carbonaceous coating was produced.

Potassium chloride:

Before joining to the system, the "clean" reaction vessel was rinsed with a 15% solution of KCl, as suggested by Quinn[98].

When a carbon coating had to be changed, the reaction vessel was cut from the system and annealed at 450°C. Now, the reaction vessel was again cleaned in the usual way to be used again.

3.8. Preparation, purification and storage of materials:

Besides the usual criteria of purity such as boiling points and refractive index, N.M.R and GLC were also used when appropriate to determine the purity. Only the middle fractions were collected during distillations.

The sample of iodide was stored in S on silver powder. S was kept covered with black paper to prevent any photolysis of the iodide.

t-butyl iodide:

t-butyl iodide as supplied by Eastman Chemicals was shaken several times with 0.1N $Na_2S_2O_3$ solution containing 1% $NaHCO_3$ at -5°C, in order to remove any iodine. The colourless liquid was separated from water and then dried over anhydrous $CaCl_2$ for 12 hours, keeping the sample in a CO_2- ethyl alcohol

bath. The dried sample was distilled in an atmosphere of nitrogen at 64 mm. pressure in the dark. The sample distilled between 41.5-42.5°C. The refractive index of the middle fraction was 1.4892 at 25°C against 1.4898 as reported[99]. The purity was checked by disolving 0.4g of the iodide into 30 c.c., of alcoholic 0.1 N $AgNO_3$ solution and back titrating the excess Ag^+ using 0.1 N NH_4CNS solution. This showed the iodide to be 99.9% pure. An N.M.R. spectrum of a pure sample (Fig.7) showed only one intense peak for three CH_3 protons at about 8.5 τ value as expected. Absense of any multiplicity in the spectrum confirmed the purity. The purity was estimated to be at least 99.6%.

The iodide thus purified was stored over silver powder in vacuum sealed tubes. These tubes were covered with dark paper and kept in a refrigerator until required. When stored in S, the iodide was never allowed to be exposed to light and kept at all times frozen at liquid nitrogen temperature.

Normal propyl iodide:

Fresh reagent grade iodide as supplied by Eastman Chemicals was shaken with mercury to remove any iodine. It was fractionated in a short column. The middle fraction was collected and it had the following physical constants:

Observed		Literature Values[100]	
b.p.	102. -102.3/756 mm.	102.45/760 mm.	
n_D^{20}	1.5051	n_D^{20}	1.5055

When the sample was run on GLC R Column no peaks were observed for other iodides.

Isopropyl iodide:

Commercial iodide supplied by Eastman Chemicals was freed from traces of iodine by shaking with mercury, dried over anhydrous calcium chloride for several hours and fractionated in a short column.

Physical Constants were as follows:-

	Observed	Literature Values[101]
b.p	89.2°/755 mm.	89.45/760 mm.
n_D^{25}	1.4966	1.4970

Ethyl iodide:

Reagent grade iodide from the Matheson Coleman and Bell Co., was shaken with mercury as usual to remove any trace of iodine, dried over anhydrous $CaCl_2$ and fractionated twice to produce physical constants as follows:-

	Observed	Literature Values[102]
b.p	72.2/755 mm.	72.1/760 mm.
n_D^{25}	1.5096	1.5103

The sample when run on GLC silica gel column showed no peaks for any impurity.

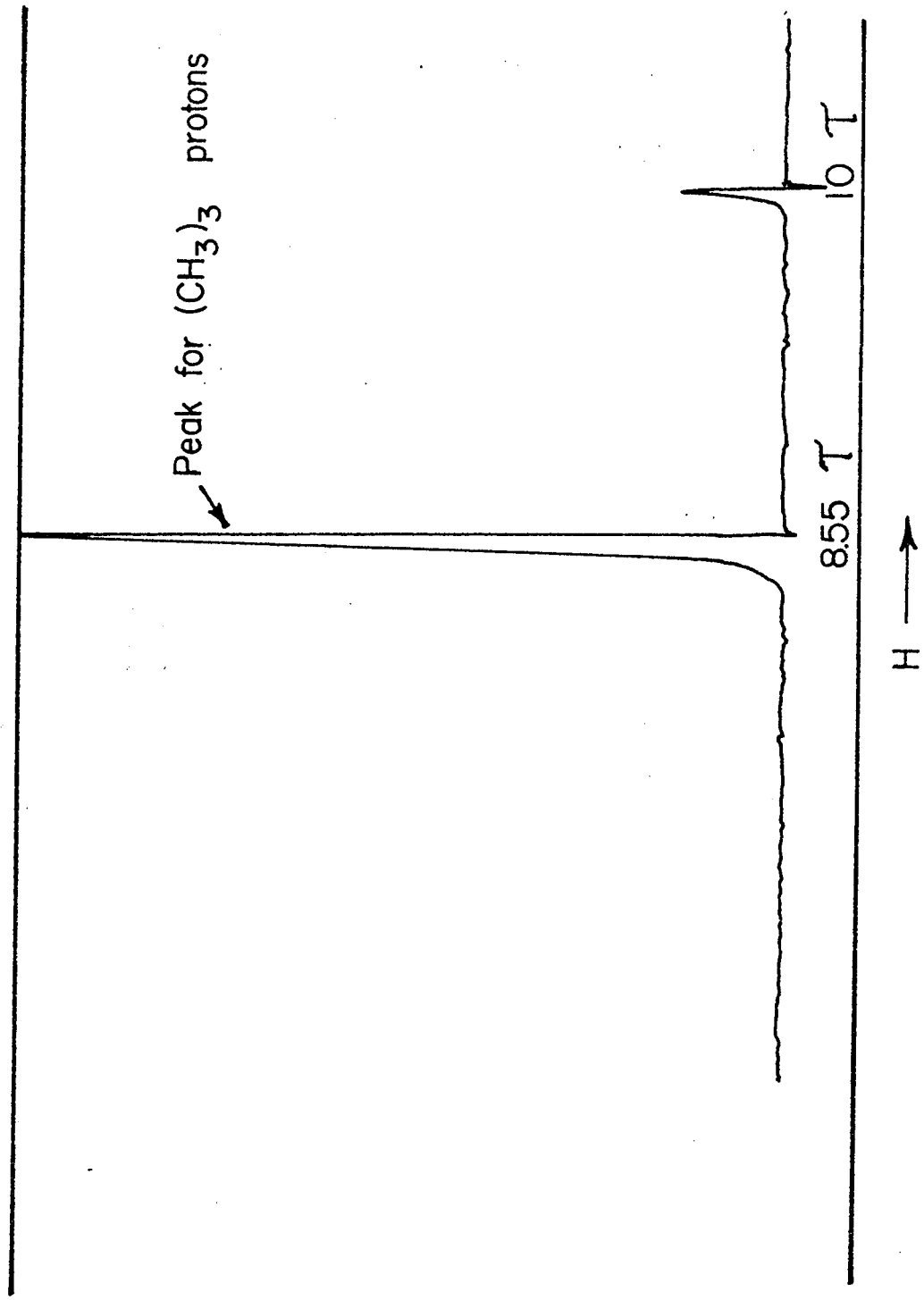

Figure 7: The N.M.R. spectrum of purified t-butyl iodide.

Normal butyl iodide:

A commercial sample from Fisher Scientific company was freed from iodine in the usual way, was dried and fractionated slowly. The middle fractions collected indicated the following physical constants.

	Observed	Literature Values[100]
b.p.	129.2 - 129.7/758 mm.	130/760 mm.
n_D^{20}	1.4997	1.5001

Iodine:

Reagent grade iodine was sublimed and degassed several times in the finger side arm (t) before use. Alternatively, iodine was collected by removing the other reaction products of an iodide pyrolysis by degassing at -20°C (ice + Conc . HCl bath).

Hydrogen Iodide:

Anhydrous hydrogen iodide was prepared by the method described by Dillon and Young[103]. Concentrated aqueous hydriodic acid solution was dropped on the phosphorous pentoxide; the gas evolved was passed through a column packed with P_2O_5 and glass wool. This column was attached to the male "Quickfit" joint S_4 of the system (see Fig.5) Hydrogen iodide was freed from any iodine by distillation from trap T_3 to trap T_4 at -78°C and then it was finally collected in a blackened storage flask V_2.

Nitric Oxide:

Pure nitric oxide gas from a cylinder supplied from Matheson Co., was passed through a silica gel U tube at -78°C attached to S_5 of the system. Nitric oxide gas energing from the U tube was condensed in T_5 at liquid N_2 temperature and was finally distilled into the storage vessel V_3.

Hydrocarbons:

These were all of research grade, in cylinders from Phillips Petroleum Co. To collect the gas, the cylinder was attached to the joint S_2 of the system by means of pressure tubing and the gas was distilled in Vacuo and degassed at liquid N_2 temperature in its storage vessel.

Allyl Bromide:

Commercial allyl bromide was shaken with three separate portions of aqueous $FeSO_4$ to remove organic peroxides, dried over anhydrous $CaCl_2$ for several hours and fractionated. Physical constants were -

	Observed	Literature Values[104]
b.p.	70.8/758 mm.	69.9/760 mm.
n_D^{20}	1.4688	1.4696

Cyclohexene:

Commercial cyclohexene was shaken with two separate portions of a saturated solution of ferrous sulphate to remove organic peroxide. It was dried over anhydrous $CaCl_2$ for 24 hours, distilled from anhydrous $CaCl_2$ and stored in a dark glass bottle over solid ferrous sulphate. The physical constants were as follows:-

	Observed	Literature Values[101]
b.p	83.0 -83.3°C/759 mm.	83.2°C/760 mm.
n_D^{25}	1.4435	n_D^{25} 1.4437

SECTION - 4

PYROLYSIS OF t-BUTYL IODIDE

4.1. Introduction:

Jones and Ogg[105] studied the pyrolysis of t-C_4H_9I and found it to be heterogeneous on clean glass and that the equilibrium

$$(CH_3)_3CI \underset{-1}{\overset{1}{\rightleftharpoons}} (CH_3)_2C = CH_2 + HI$$

was rapidly established in the temperature range 135°-190°C. They found a trace of iodine in pyrolyses above 175°C but they did not account for it.

Butler, Mandel and Polanyi[106] pyrolysed t-C_4H_9I around 400°C using a fast flow and short contact time and observed that the reaction goes chiefly via unimolecular process (1). They also observed that the iodine produced was much less than HI. Butler and Polanyi[82] estimated D(C-I) in tertiary butyl iodide to be 45.1 K.Cals. However, this value is [redacted] less than the presently accepted value of 48 K.Cals[93]. In order to obtain the Arrhenius parameters of the homogeneous reaction (1), Benson and Bose[90] studied the kinetics of the simple bimolecular reverse reaction (-1) between 200°-244°C. This, they assumed to be homogeneous under their experimental conditions. They followed the kinetics by pressure change. Iodine was analysed spectrophotometrically. Analysis of the gaseous product by GLC (R column) revealed the presence of

i-butane only and iodine formed corresponded very well with the pressure change. They said that t-C_4H_9I is formed only in a small stationary state concentration due to its rapid reaction with excess HI;

$$i\text{-}C_4H_8 + HI \longrightarrow t\text{-}C_4H_9I \quad \ldots\ldots\ldots \text{slow,}$$

$$t\text{-}C_4H_9I + HI \longrightarrow i\text{-}C_4H_{10} + I_2 \ldots\ldots\ldots \text{rapid.}$$

The first reaction is thus rate determining. Their rate constants together with the relevant thermodynamic data were used to calculate

$$E_1 = 36.4 \text{ K.Cals/mole}$$

and $\log_{10}A_1 = 12.52 \text{ Sec.}^{-1}$.

The present pyrolytic investigation was undertaken in the temperature range 190°-240°C in an attempt to verify the results of Benson and Bose for the reaction (1).

Recently Tsang[64] has determined the rate constants and Arrhenius parameters for the unimolecular elimination reaction of t-C_4H_9I by shock wave studies between 650°-760°K. He used a comparative rate technique for his investigation and his Arrhenius parameters were

$$E_1 = 38.08 \text{ K.Cals/mole}$$

and $\log_{10}A = 13.73 \text{ Sec.}^{-1}$.

4.2. Experimental:

The essentials of the experimental techniques and procedures have been described in section 3.

The surface/volume ratio of the reaction vessel was altered by replacing the original vessel by a packed vessel, thereby changing the surface/volume ratio from 1.2 to 6.1 cms.$^{-1}$ in the case of the allyl bromide carbon study and from 1.2 to 7 cms.$^{-1}$ in the case of the isobutene carbon study.

Besides this usual test for homogeneity, the effects of other chemical coatings were examined. Kinetics were investigated in detail in the cases of two different pyrolytic carbon coatings, allyl bromide carbon and isobutene carbon.

4.3. Product analysis and stoicheiometry:

Iodine was separated from the products at -78°C and t-C_4H_9I was separated from the rest of the products at -130°C. The hydrogen iodide and isobutene in the products tended to recombine on condensation to reform t-C_4H_9I. An attempt was made to analyse isobutene by separating it from the rest of the products before any condensation operations. This was done by expanding the whole product into a 4 litre evacuated flask V_5 (Fig.5) containing a basic adsorbent $Mg(OCl_4)_2 + Ca(OH)_2$ as suggested by Stimson[107]. Unfortunately, some of the remaining unpyrolysed t-C_4H_9I always decomposed on the adsorbent and larger peaks than expected appeared on the chromatogram. The column consisted of a 15 feet long ¼" copper tube packed with 15% dimethyl

sulpholane on chromosorb 'P'. Other basic adsorbents such as $Ba(OH)_2$, Al_2O_3, CaO, MgO were also tried in order to eliminate the surface decomposition of t-C_4H_9I but without success. The surface sensitivity of t-C_4H_9I was also apparent from the fact that when a pure sample of the iodide was passed through the GLC column, very large isobutane and isobutene peaks appeared on the chromatogram; this was obviously due to the decomposition of the iodide on the surface of the column packing. Thus, quantitative analysis for isobutene was not possible.

However, the quantitative estimation of isobutane could be achieved after condensation of the product at liquid nitrogen temperature. The iodine and the remaining iodide were separated from the product at -78°C and -130°C respectively before passing the gaseous product through GLC column. The isobutane peaks thus recorded were in good quantitative agreement with the iodine analysed titrimetrically. The results are summarised in table 4.1.

Table 4.1: Relation between i-butane and I_2 during the t-C_4H_9I pyrolysis surface: allyl bromide carbon.

Run Number	Temp. °C	$[RI]_o$ (mm.)	Time of pyrolysis (min.)	i-butane$_1$ (mm.x10^{-1})	Iodine$_{-1}$ (mm.x10^{-1})
143	189	45	10	1.00	1.05
144	209	26	10	2.75	2.75
147	209	41	5	3.20	3.35
149	209	31	10	5.5	5.50
153	209	46	8	12.0	11.50
154	218	43	15	6.10	5.90
162	218	42	10	5.05	4.35
165	200	13.5	5	0.85	0.7
168	200	38	5	5.90	6.4
169	200	48.5	10	5.4	4.8
			Total	47.75	46.30

It was noticed that when pyrolyses were carried out in a clean glass vessel, fast and irreproducible results were obtained. However, after the reaction vessel was given a carbonaceous coating by various means the rates became slower and reproducible. Table 4.2. shows some typical pressure-change and iodine results at various times.

Table 4.2. Iodine production compared with pressure change during the pyrolysis of t-C_4H_9I. Surface: allyl bromide carbon.

Temp. °C	$[RI]_o$ (mm.)	Time of reaction (min.)	Pressure increase (mm.)	I_2 (mm.)
200	18	10	1.5	0.08
200	44	10	5.0	0.40
230	18	5	7.8	0.85
230	41	3	12.0	1.90

The analytical results suggest that two processes are occuring simultaneously during the pyrolysis, one whose stoicheiometry can be represented as

$$t\text{-}C_4H_9I \xrightarrow{k_1} C_4H_8 + HI$$

and is responsible for the pressure change and the other, iodine producing process

$$C_4H_9I + HI \xrightarrow{k_{1.5}} RH + I_2$$

The pressure time data closely obeyed first order behavior up to 25% total reaction while the slower iodine producing process showed an autocatalytic nature involving an order of one in iodide and one half in iodine which was also obeyed up to about 25% total reaction.

Figures 8-12 show different plots of pressure-time and iodine-time relationships and figures 13 and 14 are the first order log rate plot and the autocatalytic rate plot respectively for the pyrolysis of t-C_4H_9I at 229°C.

Figure 8: A typical pressure-time curve for the pyrolysis of t-butyl iodide at 201.0°C.

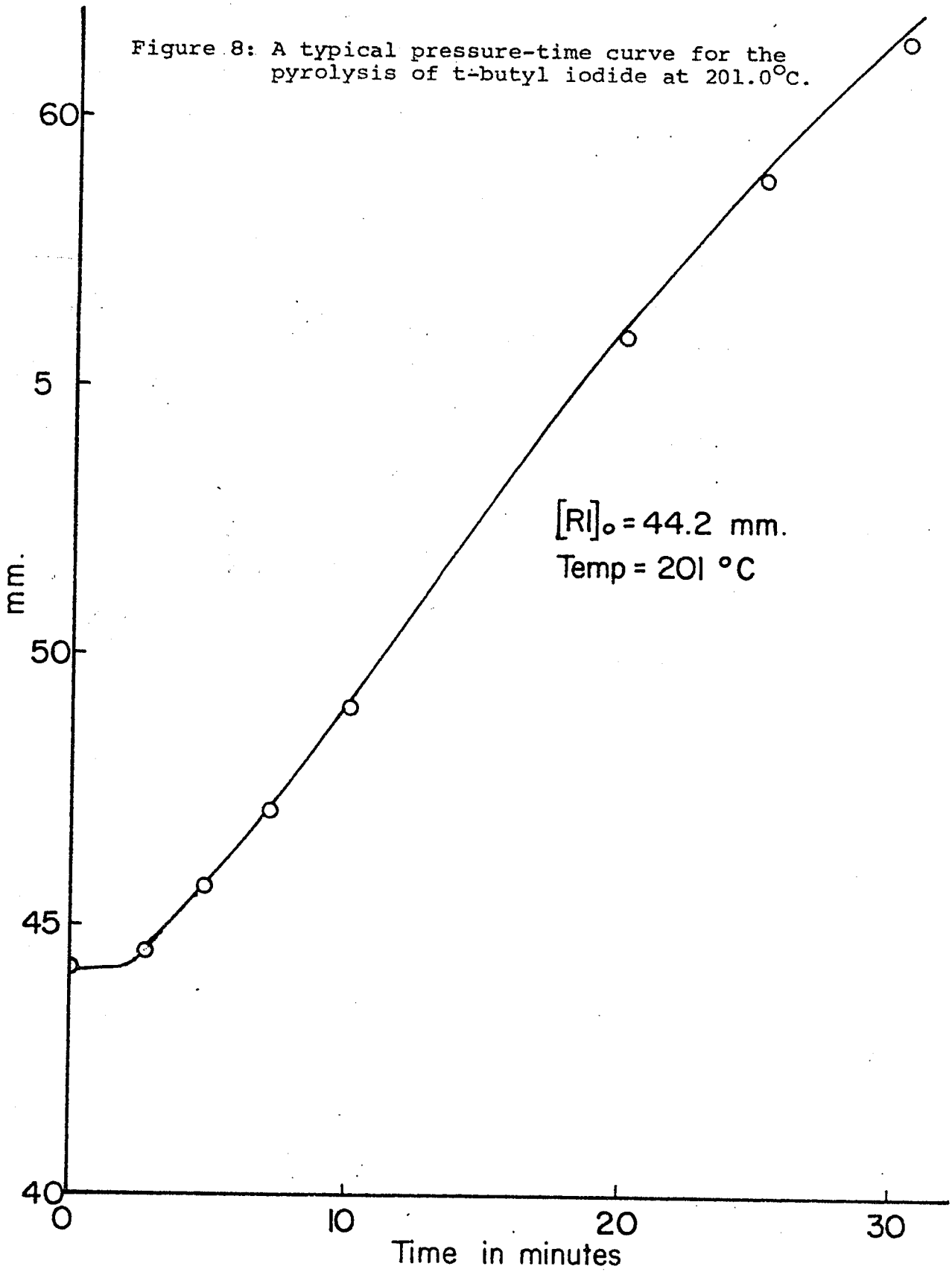

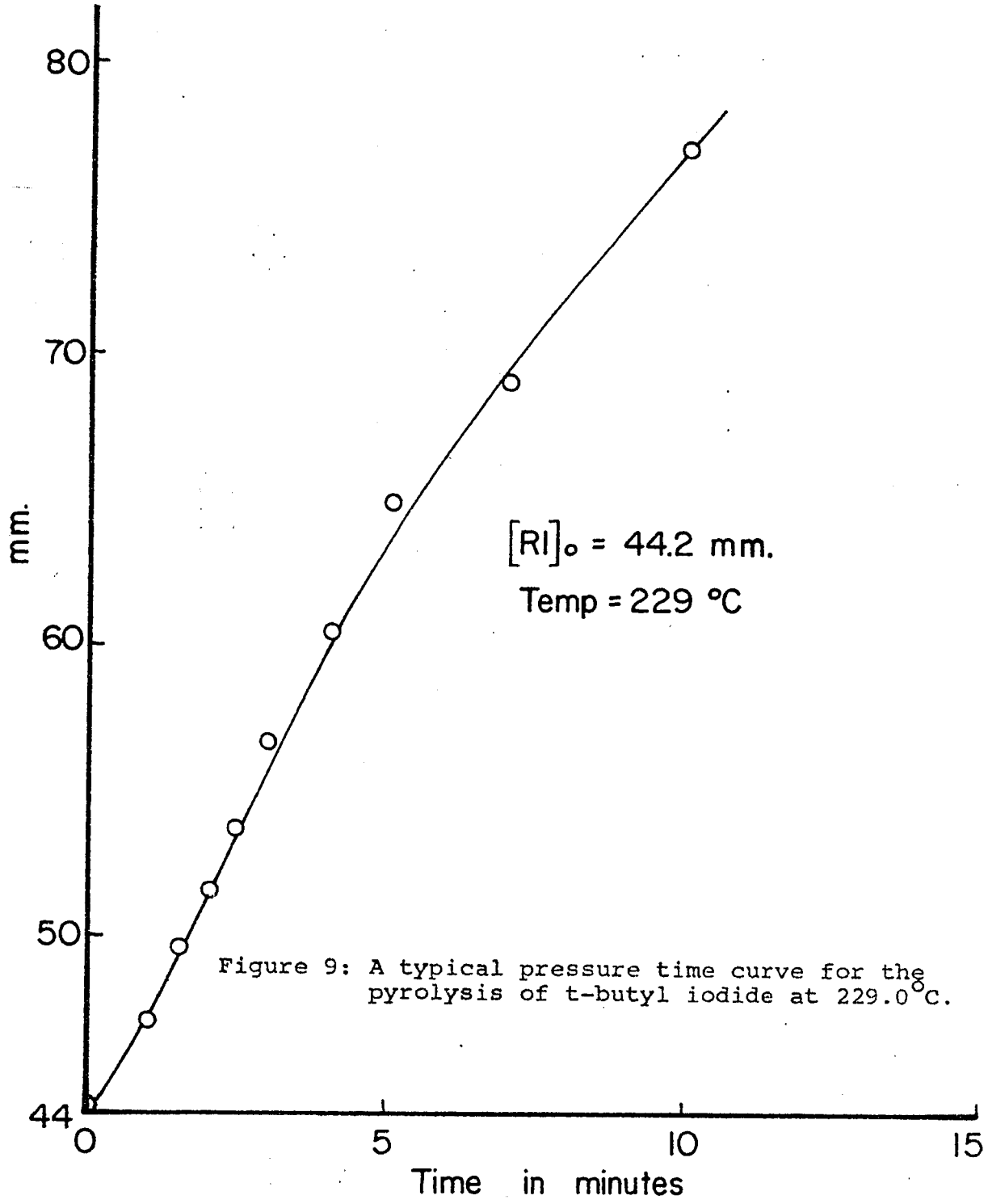

Figure 9: A typical pressure time curve for the pyrolysis of t-butyl iodide at 229.0°C.

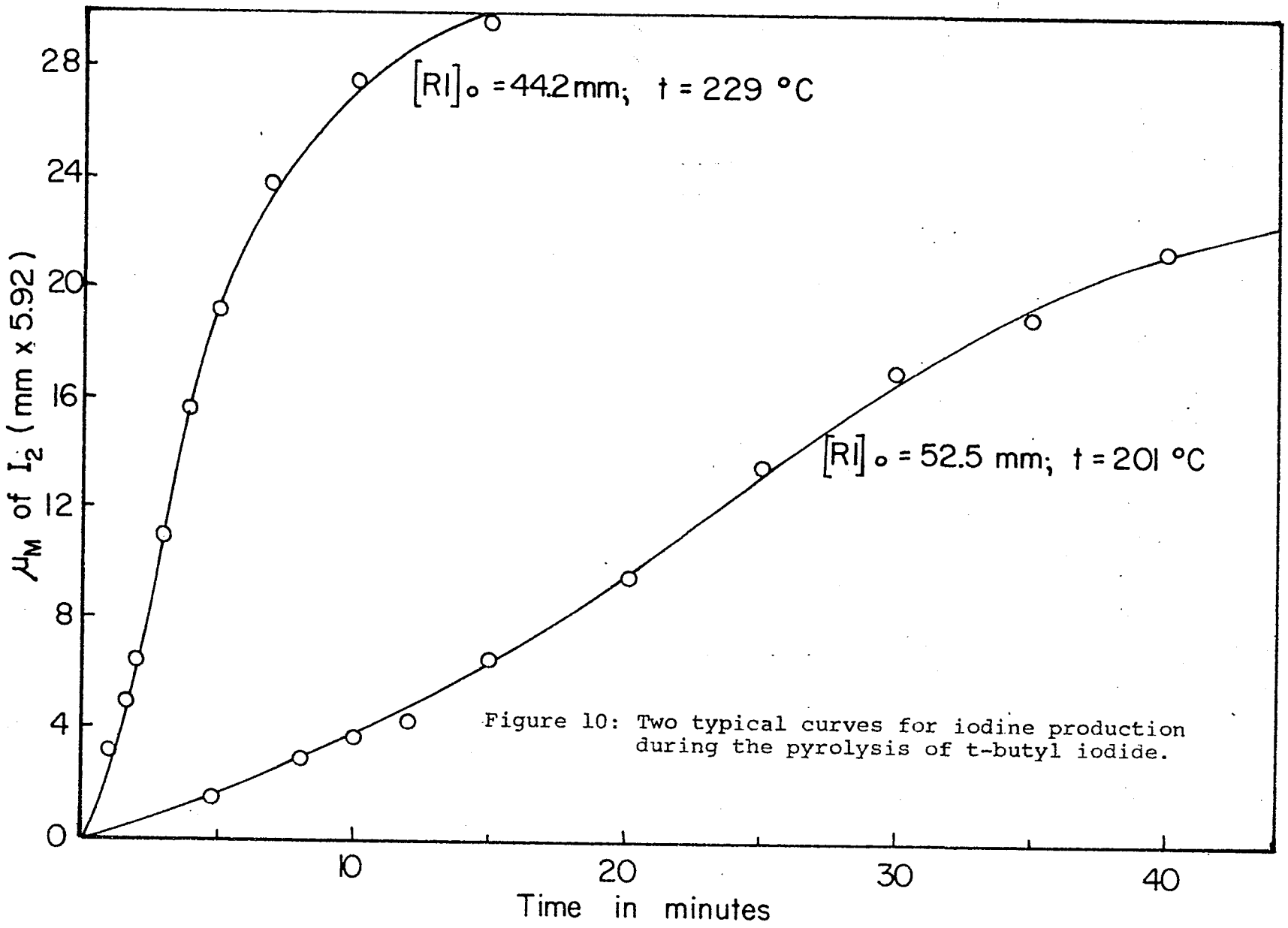

Figure 10: Two typical curves for iodine production during the pyrolysis of t-butyl iodide.

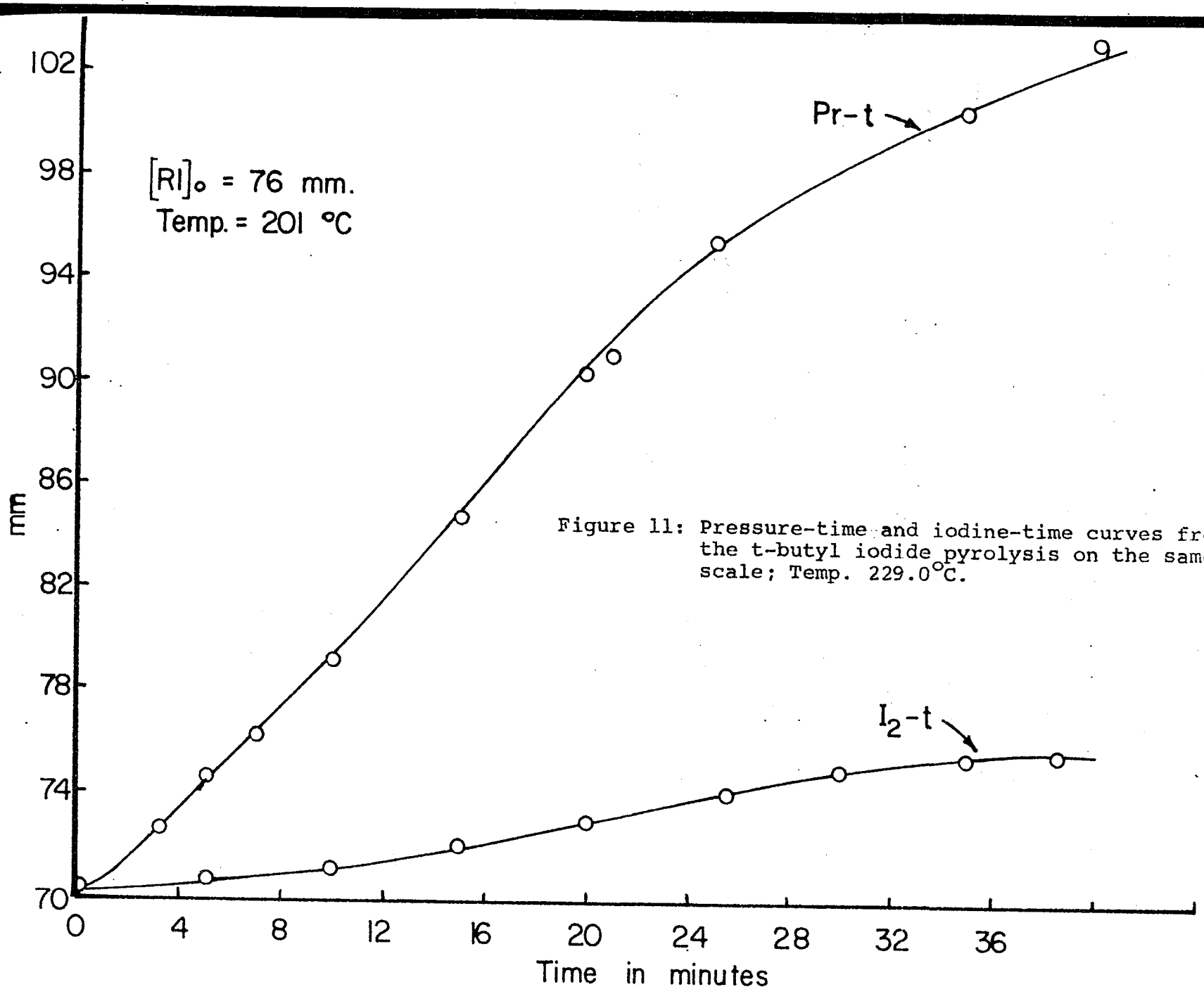

Figure 11: Pressure-time and iodine-time curves from the t-butyl iodide pyrolysis on the same scale; Temp. 229.0°C.

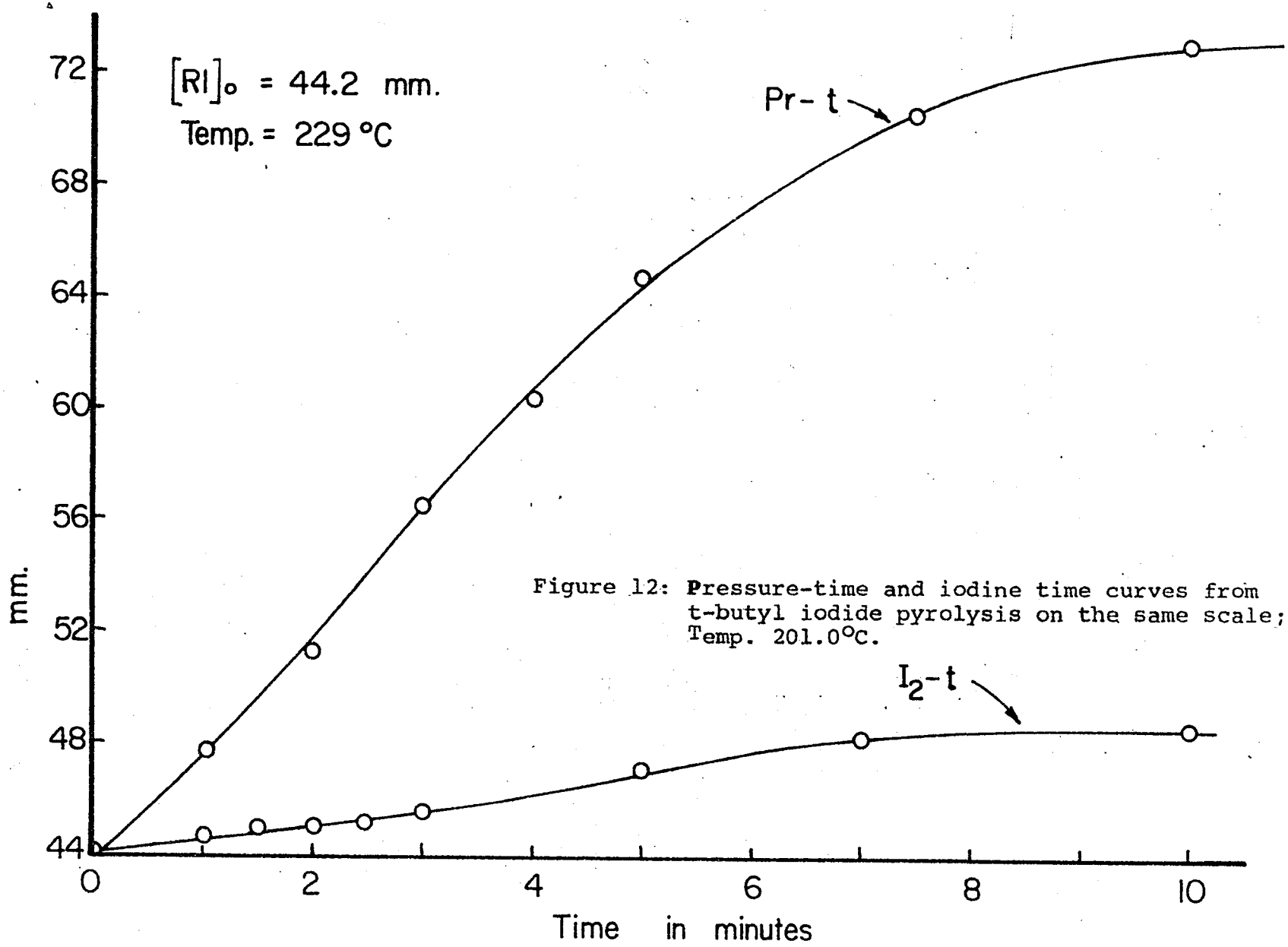

Figure 12: Pressure-time and iodine time curves from t-butyl iodide pyrolysis on the same scale; Temp. 201.0°C.

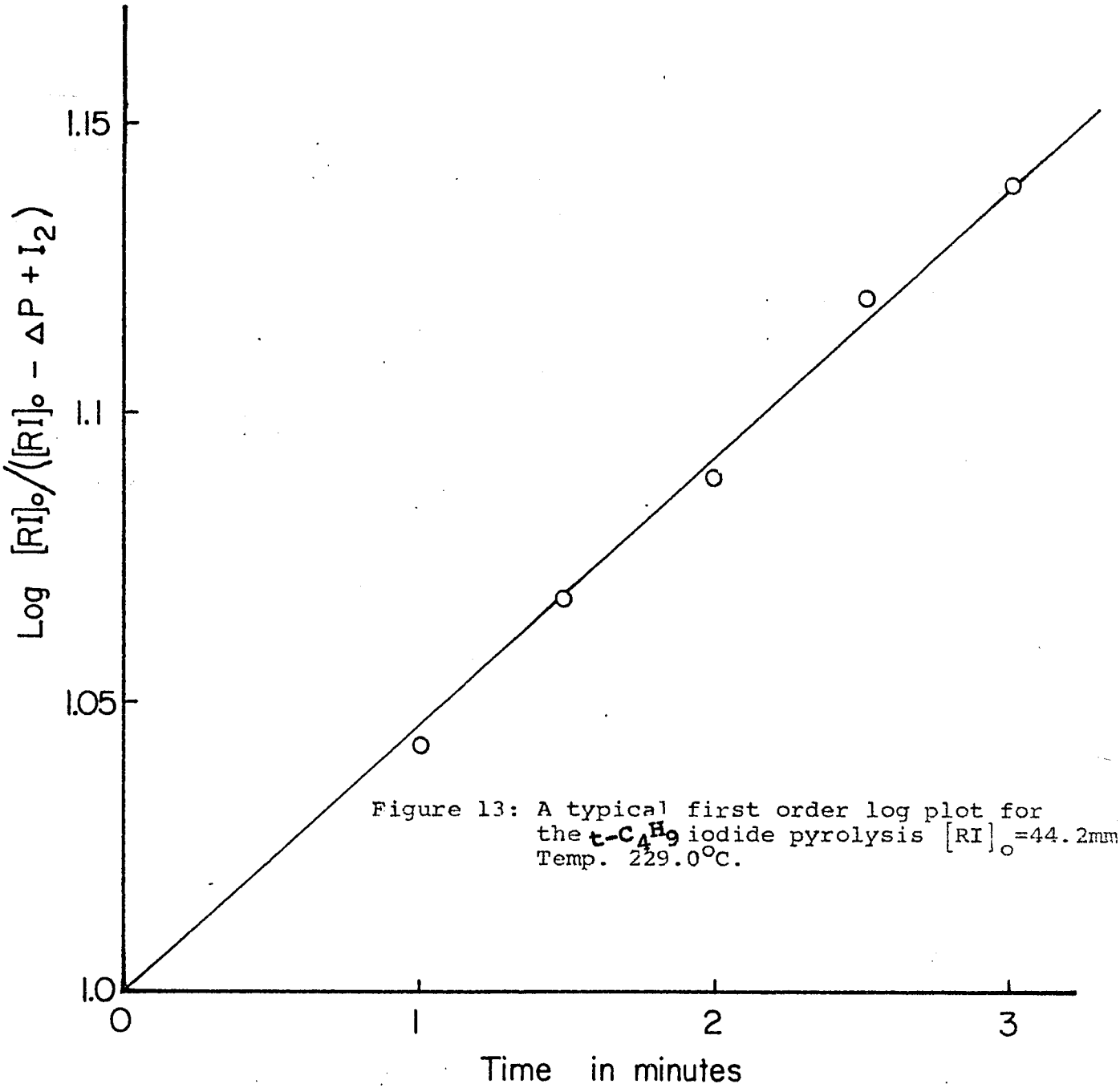

Figure 13: A typical first order log plot for the $t\text{-}C_4H_9$ iodide pyrolysis $[RI]_o$=44.2mm Temp. 229.0°C.

Figure 14: An autocatalytic rate plot for the pyrolysis of t-butyl iodide $[RI]_o$ = 44.2 mm.; Temp. 229.0°C.

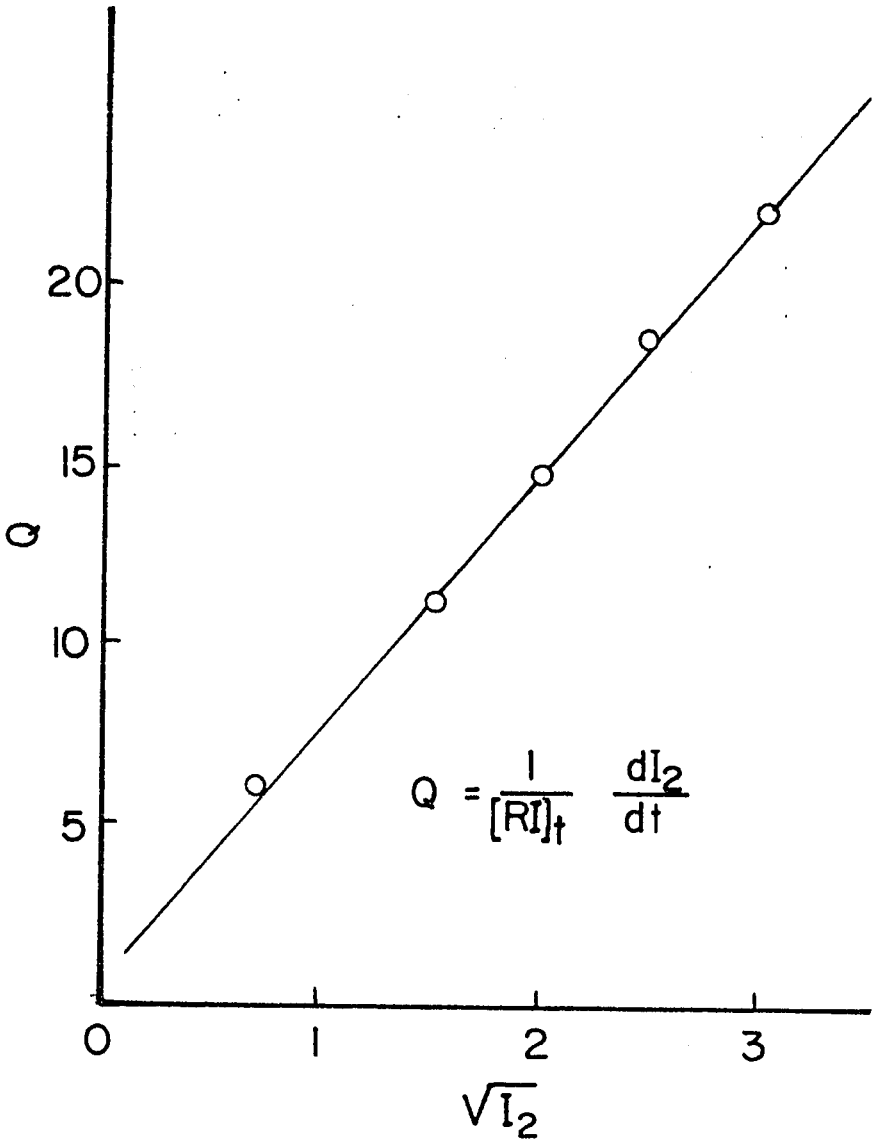

A test for the correctness of the stoicheiometry was attempted. Due to the rapid establishment of equilibrium, the chief products, i-butene and hydrogen iodide, recombined quantitatively to form the parent iodide. Thus if the products are frozen after reaction, and then revaporised, any difference between the new initial pressure and the original initial pressure will be due to the i-butane and iodine produced during the reaction. This may be explained as follows:-

Let x and y be the numbers of moles as indicated in the stoicheiometry for the two processes,

$$\underset{1-x}{t\text{-}C_4H_9I} \longrightarrow \underset{x}{C_4H_8} + \underset{x}{HI}$$

$$\underset{y}{C_4H_9I} + \underset{y}{HI} \longrightarrow \underset{y}{C_4H_{10}} + \underset{y}{I_2}$$

Now, the number of moles of $t\text{-}C_4H_9I$ at any time during the pyrolysis will be $1 - (x + y)$ moles and the olefin and HI will be similarly x and x-y moles respectively.

Upon condensation of the products at liquid nitrogen temperature x-y moles of HI will add back to x-y moles of the olefin to produce x-y moles of $t\text{-}C_4H_9I$. Thus on condensation the number of moles of different species present will be,

$$t\text{-}C_4H_9I = 1-x-y + (x-y) = 1-2y$$

$$C_4H_8 = x-(x-y) = y$$

$$C_4H_{10} = y$$

$$I_2 = y$$

and 1 + y correspond to the pressure on revaporisation. Thus the difference between the original initial pressure and the second initial pressure will be equal to the amount of iodine or i-butane produced during the reaction.

The products were frozen at liquid nitrogen temperature in the side arm of the reaction vessel and the new initial pressure was found by vaporising it quickly. The initial pressure difference agreed well with the iodine found in a similar reaction done separately. The results are summarised in table 4.3.

Table 4.3: Indirect proof of i-butane and iodine equality surface: isobutene carbon.

Rum Number	Temp. (°C)	$[RI]_o$ (mm.)	Time of pyrolysis (min.)	Pressure increase on revaporisation (mm.)	Iodide produced in a similar run (mm.)
535	198	46.7	25	-	2.5
536	198	46.3	25	2.35	-
537	202	44.7	30	-	1.75
538	202	46.0	30	1.9	-
539	224	31.5	2	-	1.2
540	224	31.3	2	1.1	-

allyl bromide carbon
unpacked vessel

4.4. Results:

(a)

Table 4.4. Kinetic results on allyl bromide carbon surface. The pressure time data are the average of several runs.

Temperature 190.0°C

Run Numbers 35-41
$[RI]_o$ = 55.7 mm.

Time (min.)	Pressure (mm.)	I_2 (mm.x10^{-1})
0	55.7	
3	56.0	
5	56.9	0.9
7	57.7	1.65
10	59.1	1.2
13	60.9	
15	61.7	4.55
17	62.4	
20	64.8	6.85
22	65.7	
25	68.2	9.35
27	68.9	
30	70.9	

$k_1 = 1.72 \times 10^{-4}$ Sec.$^{-1}$; $k_{1.5} = 2.98 \times 10^{-6}$ mm.$^{-\frac{1}{2}}$ Sec.$^{-1}$

allyl bromide carbon
unpacked vessel

Temperature 201.0°C

Run Numbers 44-52 $[RI]_o$ = 17.8 mm.			Run Numbers 53-62 $[RI]_o$ = 44.2 mm.		
Time (min.)	Pressure (mm.)	I_2 (mm.x10^{-1})	Time (min.)	Pressure (mm.)	I_2 (mm.x10^{-1})
0	17.8		0	44.2	
5	18.4	0.40	3	44.8	
8	19.0		5	45.7	1.05
10	19.4	0.90	8	47.2	
12	19.75		10	49.0	2.3
15	20.4	1.4	15	53.1	3.8
18	21.1		20	56.9	5.5
20	21.4	2.0	25	59.0	
25	22.6	2.6	30	61.5	
30	23.6	3.35			
k_1 = 2.12x10^{-4}Sec.$^{-1}$			k_1 = 2.9x10^{-4}Sec.$^{-1}$		
$k_{1.5}$ = 4.51x10^{-6}mm.$^{-\frac{1}{2}}$Sec.$^{-1}$			$k_{1.5}$ = 5.12x10^{-6}mm.$^{-\frac{1}{2}}$Sec.$^{-1}$		

allyl bromide carbon
unpacked vessel

Temperature 201.0°C

Run Numbers 63-72 $[RI]_o$ = 52.5 mm.			Run Numbers 75-84 $[RI]_o$ = 70.6 mm.		
Time (min.)	Pressure (mm.)	I_2 (mm.x10^{-1})	Time (min.)	Pressure (mm.)	I_2 (mm.x10^{-1})
0	52.5		0	70.6	
3	54.7	1.7	2	72.0	
5	55.8	2.8	5	74.2	6.1
8	57.5	4.8	8	77.5	
10	59.9	6.3	10	79.3	12.8
12	61.8	7.3	12	80.5	
15	64.5	10.8	15	84.8	20.3
20	70.5	16.3	20	91.0	28.4
			25	95.5	38.8
$k_1 = 3.54 \times 10^{-4}$ Sec.$^{-1}$			$k_1 = 3.22$ Sec.$^{-1}$		
$k_{1.5} = 5.38 \times 10^{-6}$ mm.$^{-\frac{1}{2}}$Sec.$^{-1}$			$k_{1.5} = 5.20$ mm.$^{-\frac{1}{2}}$Sec.$^{-1}$		
Mean: $k_1 = 2.72 \times 10^{-4}$ Sec.$^{-1}$;			$k_{1.5} = 5.07 \times 10^{-6}$ mm.$^{-\frac{1}{2}}$Sec.$^{-1}$		

allyl bromide carbon
unpacked vessel

Temperature 210.0°C			Temperature 219.2°C		
Run Numbers 85-91 $[RI]_o$ = 19.1 mm.			Run Numbers 92-102 $[RI]_o$ = 44.1 mm.		
Time (min.)	Press. (mm.)	I_2 (mm.x10^{-1})	Time (min.)	Press. (mm.)	I_2 (mm.x10^{-1})
0	19.1		0	44.1	
2	20.0	0.5	2	46.3	2.05
3	20.3	0.85	3	47.6	3.8
4	20.8	1.2	4	48.2	4.65
5	21.3	1.5	5	50.1	6.4
6	21.6	1.8	6	51.3	8.1
7	22.6		8	55.8	11.0
10	24.6	3.7	10	58.9	15.45
13	26.7		12	62.6	
15	27.8	4.6	15	66.3	
18	29.6		20	70.9	
20	30.4	5.0			

Run Numbers 102-111 $[RI]_o$ = 43.8 mm.		
Time (min.)	Press. (mm.)	I_2 (mm.x10^{-1})
0	43.8	
1	45.4	2.6
2	47.4	5.6
3	50.4	8.8
4	53.9	12.45
5	55.4	16.5
7	61.2	23.2
10	67.8	34.2
12	70.8	
15	73.3	41.6
20	74.3	44.7

$k_1 = 5.0 \times 10^{-4}$ Sec.$^{-1}$ $k_1 = 5.5 \times 10^{-4}$ Sec.$^{-1}$ $k_1 = 12.67 \times 10^{-4}$ Sec.$^{-1}$

$k_{1.5} = 14.95 \times 10^{-6}$ mm.$^{-\frac{1}{2}}$ Sec.$^{-1}$ $k_{1.5} = 13.15 \times 10^{-6}$ mm.$^{-\frac{1}{2}}$ Sec.$^{-1}$ $k_{1.5} = 26.5 \times 10^{-6}$ mm.$^{-\frac{1}{2}}$ Sec.$^{-1}$

Mean: $k_1 = 5.25 \times 10^{-4}$ Sec.$^{-1}$

$k_{1.5} = 14.05 \times 10^{-6}$ mm.$^{-\frac{1}{2}}$ Sec.$^{-1}$

allyl bromide carbon
unpacked vessel

Temperature 229.0°C

Run Numbers 114-120
$[RI]_o$ = 18.7 mm.

Time (min.)	Pressure (mm.)	I_2 (mm.x10^{-1})
0	18.7	
0.5	19.2	0.8
1	20.0	1.45
2	21.5	3.05
3	23.0	4.65
4	25.0	6.4
5	26.5	8.2
7	29.1	11.95
8	30.0	
10	31.5	16.7

$k_1 = 20.62 \times 10^{-4}$ Sec.$^{-1}$

$k_{1.5} = 46.49 \times 10^{-6}$ mm.$^{-\frac{1}{2}}$ Sec.$^{-1}$

Run Numbers 121-127
$[RI]_o$ = 44.2 mm.

Time (min.)	Pressure (mm.)	I_2 (mm.x10^{-1})
0	44.2	
1	47.6	5.7
1.5	49.6	8.9
2	51.4	11.4
2.5	53.8	15.35
3	56.4	19.65
4	60.2	24.7
5	64.4	33.9
7	69.0	42.7
11	77.0	48.2

$k_1 = 20.58 \times 10^{-4}$ Sec.$^{-1}$

$k_{1.5} = 48.61 \times 10^{-6}$ mm.$^{-\frac{1}{2}}$ Sec.$^{-1}$

Mean: $k_1 = 20.1 \times 10^{-4}$ Sec.$^{-1}$; $k_{1.5} = 47.55 \times 10^{-6}$ mm.$^{-\frac{1}{2}}$ Sec.$^{-1}$

allyl bromide carbon
unpacked vessel

Temperature 239.0°C

Run Numbers 128-132
$[RI]_o$ = 18.1 mm.

Time (min.)	Pressure (mm.)	I_2 (mm.x10^{-1})
0	18.1	
0.5	18.7	1.38
1	20.3	2.65
1.5	21.2	4.4
2	22.9	6.6
3	25.7	11.85
4	27.9	
5	29.2	

$k_1 = 31.33 \times 10^{-4}$ Sec.$^{-1}$

$k_{1.5} = 68.0 \times 10^{-6}$ mm.$^{-\frac{1}{2}}$ Sec.$^{-1}$

Run Numbers 133-136
$[RI]_o$ = 44.8 mm.

Time (min.)	Pressure (mm.)	I_2 (mm.x10^{-1})
0	44.8	
0.5	48.1	2.0
1	52.2	4.0
1.5	56.3	6.05
2	59.1	8.5
3	65.0	
4	67.4	
5	70.8	

$k_1 = 27.67 \times 10^{-4}$ Sec.$^{-1}$

$k_{1.5} = 74.5$ mm.$^{-\frac{1}{2}}$ Sec.$^{-1}$

Mean: $k_1 = 28.88 \times 10^{-4}$ Sec.$^{-1}$; $k_{1.5} = 71.25 \times 10^{-6}$ mm.$^{-\frac{1}{2}}$ Sec.$^{-1}$

allyl bromide carbon packed vessel

Temperature 200.0°C

Run Numbers 187-192 $[RI]_o$ = 20.5 mm.			Run Numbers 193-199 $[RI]_o$ = 53.3 mm.		
Time (min.)	Pressure (mm.)	I_2 (mm.x10^{-1})	Time (min.)	Pressure (mm.)	I_2 (mm.x10^{-1})
0	20.5		0	53.3	
1	21.8		1	55.5	
2	23.9	0.3	3	59.7	1.65
4	25.3	0.5	4	62.0	
5	26.3	0.7	5	64.5	2.65
6	27.0		6	67.5	
7	28.0	1.05	7	70.0	3.90
9	29.8	1.35	8	72.5	4.5
11	31.0		9	75.2	
13	32.5		10	77.5	5.65
			12	81.3	7.40
$k_1 = 10.8\text{x}10^{-4}$ Sec.$^{-1}$			$k_1 = 9.8\text{x}10^{-4}$ Sec.$^{-1}$		
$k_{1.5} = 6.9\text{x}10^{-6}$ mm.$^{-\frac{1}{2}}$ Sec.$^{-1}$			$k_{1.5} = 4.86\text{x}10^{-6}$ mm.$^{-\frac{1}{2}}$ Sec.$^{-1}$		
Mean: $k_1 = 10.3\text{x}10^{-4}$ Sec.$^{-1}$;			$k_{1.5} = 5.88\text{x}10^{-6}$ mm.$^{-\frac{1}{2}}$ Sec.$^{-1}$		

allyl bromide carbon packed vessel

Temperature 220.0°C

Run Numbers 201-205 $[RI]_o$ = 22.8 mm.			Run Numbers 206-212 $[RI]_o$ = 55.0 mm.		
Time (min.)	Pressure (mm.)	I_2 (mm.x10^{-1})	Time (min.)	Pressure (mm.)	I_2 (mm.x10^{-1})
0	22.8		0	55.0	
1	24.7	0.75	1	58.6	3.0
1.5	25.8	1.2	1.5	60.9	4.7
2	26.8	1.6	2	58.6	6.4
2.5	27.8		2.5	65.8	8.55
3	28.7	2.45	3	68.6	10.7
4	30.5	3.5	4	71.8	15.4
5	32.3	4.9	5	75.0	23.1
7	35.1	6.2			
10	37.9	7.90			
$k_1 = 18.6\text{x}10^{-4}$ Sec.$^{-1}$			$k_1 = 19.2\text{x}10^{-4}$		
$k_{1.5} = 33.0\text{x}10^{-6}$ mm.$^{-\frac{1}{2}}$ Sec.$^{-1}$			$k_{1.5} = 28.6\text{x}10^{-6}$ mm.$^{-\frac{1}{2}}$ Sec.$^{-1}$		
Mean: $k_1 = 18.9\text{x}10^{-4}$ Sec.$^{-1}$;			$k_{1.5} = 30.8$ mm.$^{-\frac{1}{2}}$ Sec.$^{-1}$		

allyl bromide carbon packed vessel

Temperature 230.0°C Run Numbers 215-219 $[RI]_o$ = 22.5 mm.			Temperature 240.0°C Run Numbers 220-224 $[RI]_o$ = 22.5 mm.		
Time (min.)	Pressure (mm.)	I_2 (mm.x10^{-1})	Time (min.)	Pressure (mm.)	I_2 (mm.x10^{-1})
0	22.5		0	22.5	
0.5	23.8		0.5	24.4	2.0
1	25.3	1.75	1	26.5	4.0
1.5	27.5	2.85	1.5	28.7	6.7
2	28.9	3.9	2	30.8	9.3
2.5	31.0		2.5	32.5	12.0
3	33.0		3	34.5	14.7
4	35.7				
5	37.8				
$k_1 = 30.62 \times 10^{-4}$ Sec.$^{-1}$			$k_1 = 38.7 \times 10^{-4}$ Sec.$^{-1}$		
$k_{1.5} = 60.1 \times 10^{-6}$ mm.$^{-\frac{1}{2}}$ Sec.$^{-1}$			$k_{1.5} = 88.8 \times 10^{-6}$ mm.$^{-\frac{1}{2}}$ Sec.$^{-1}$		

isobutene carbon
unpacked vessel

(b)

Table 4.5: Kinetic results on isobutene carbon surface.
The pressure-time data are the average of several runs.

Temperature 200.0°C			Temperature 208.0°C		
Run Numbers 310-320 $[RI]_o$ = 50.0 mm.			Run Numbers 321-327 $[RI]_o$ 50.5 mm.		
Time (min.)	Pressure (mm.)	I_2 (mm.x10^{-1})	Time (min.)	Pressure (mm.)	I_2 (mm.x10^{-1})
0	50.0		0	50.5	
3	50.15	0.65	1	50.95	0.3
5	50.35	1.15	1.5	51.25	0.5
7.5	50.6	1.95	2	51.5	0.65
10	50.8	2.85	2.5	51.75	0.9
15	51.65	5.15	3	52.0	
20	52.45	8.3	4	52.5	
22	52.9	10.0			
$k_1 = 0.58 \times 10^{-4}$ Sec.$^{-1}$			$k_1 = 1.63 \times 10^{-4}$ Sec.$^{-1}$		
$k_{1.6} = 4.57 \times 10^{-6}$ mm.$^{-\frac{1}{2}}$ Sec.$^{-1}$			$k_{1.5} = 7.8 \times 10^{-4}$ mm.$^{-\frac{1}{2}}$ Sec.$^{-1}$		

isobutene carbon
unpacked vessel

Temperature 214.3°C			Temperature 216.8°C					
Run Numbers 346-350 $[RI]_o$ = 50.5 mm.			Run Numbers 351-354 $[RI]_o$ = 39.9 mm.			Run Numbers 355-358 $[RI]_o$ = 52.4 mm.		
Time (min.)	Press. (mm.)	I_2 (mm.x10^{-1})	Time (min.)	Press. (mm.)	I_2 (mm.x10^{-1})	Time (min.)	Press. (mm.)	I_2 (mm.x10^{-1})
0	50.5		0	39.9		0	52.4	
1	50.9	0.45	1	40.1		1	52.7	2.1
1.5	51.5	0.8						
2	52.0	1.3	2	40.2	3.0	2	53.0	4.6
2.5	52.6		3	40.9	3.8	3	53.4	7.55
3	52.9	3.1	4	41.7		4	54.5	10.68
			5	42.9	9.5	5	57.0	
			6	43.7	12.1	6	58.8	
			7	45.6		7	60.9	
			9	47.2		9	62.85	
			10	49.1		10	63.0	
$k_1 = 2.99\text{x}10^{-4}$ Sec.$^{-1}$			$k_1 = 4.43\text{x}10^{-4}$ Sec.$^{-1}$			$k_1 = 2.3\text{x}10^{-4}$ Sec.$^{-1}$		
$k_{1.5} = 26.0\text{x}10^{-6}$ mm.$^{-\frac{1}{2}}$ Sec.$^{-1}$			$k_{1.5} = 11.4\text{x}10^{-6}$ mm.$^{-\frac{1}{2}}$ Sec.$^{-1}$			$k_{1.5} = 11.2\text{x}10^{-6}$ mm.$^{-\frac{1}{2}}$ Sec.$^{-1}$		

Mean: $k_1 = 3.5\text{x}10^{-4}$ Sec.$^{-1}$; $k_{1.5} = 11.3\text{x}10^{-6}$ mm.$^{-\frac{1}{2}}$ Sec.$^{-1}$

isobutene carbon
unpacked vessel

Temperature 220.0°C

Run Numbers 359-362
$[RI]_o$ = 21.5 mm.

Time (min.)	Pressure (mm.)	I_2 (mm.x10^{-1})
0	21.5	
1	21.7	
2	22.05	1.05
3.5	22.35	1.95
5	22.70	3.15
6	23.15	4.10

$k_1 = 1.98 \times 10^{-4}$ Sec.$^{-1}$

$k_{1.5} = 13.4 \times 10^{-6}$ mm.$^{-\frac{1}{2}}$ Sec.$^{-1}$

Run Numbers 363-366
$[RI]_o$ = 42.0 mm.

Time (min.)	Pressure (mm.)	I_2 (mm.x10^{-1})
0	42.0	
1	42.3	1.3
2	42.8	2.95
3	43.0	4.65
5	44.2	8.15
7	45.3	12.95

$k_1 = 2.30 \times 10^{-4}$ Sec.$^{-1}$

$k_{1.5} = 17.8 \times 10^{-6}$ mm.$^{-\frac{1}{2}}$ Sec.$^{-1}$

Mean: $k_1 = 2.14 \times 10^{-4}$ Sec.$^{-1}$;

$k_{1.5} = 15.6 \times 10^{-6}$ mm.$^{-\frac{1}{2}}$ Sec.$^{-1}$

Temperature 224.2°C

Run Numbers 367-370
$[RI]_o$ = 31.5 mm.

Time (min.)	Pressure (mm.)	I_2 (mm.x10^{-1})
0	31.5	
0.5	31.9	0.75
1	31.25	1.10
1.5	32.75	1.50
2	33.10	1.90

$k_1 = 5.12 \times 10^{-4}$ Sec^{-1}

$k_{1.5} = 29.30 \times 10^{-6}$ mm.$^{-\frac{1}{2}}$ Sec.$^{-1}$

Run Numbers 371-375
$[RI]_o$ = 46.0 mm.

Time (min.)	Pressure (mm.)	I_2 (mm.x10^{-1})
0	46	
0.5	46.5	0.5
1	46.75	0.90
1.5	47.1	1.25

$k_1 = 4.77 \times 10^{-4}$ Sec.$^{-1}$

$k_{1.5} = 30.2 \times 10^{-6}$ mm.$^{-\frac{1}{2}}$ Sec.$^{-1}$

Mean: $k_1 = 4.95 \times 10^{-4}$ Sec.$^{-1}$;

$k_{1.5} = 29.75 \times 10^{-6}$ mm.$^{-\frac{1}{2}}$ Sec.$^{-1}$

isobutene carbon
unpacked vessel

Temperature 229.0°C

Run Numbers 379-385
$[RI]_o$ = 19.0 mm.

Time (min.)	Pressure (mm.)	I_2 (mm.x10^{-1})
0	19.0	
1	19.6	1.25
2	20.1	2.65
3	20.7	4.25
4	21.3	6.05

$k_1 = 6.97 \times 10^{-4}$ Sec.$^{-1}$

$k_{1.5} = 29.32 \times 10^{-6}$ mm.$^{-\frac{1}{2}}$ Sec.$^{-1}$

Run Numbers 386-391
$[RI]_o$ = 39.2 mm.

Time (min.)	Pressure (mm.)	I_2 (mm.x10^{-1})
0	39.2	
1	40.05	2.65
2	41.25	6.05
2.5	41.5	8.00
3	41.9	10.00

$k_1 = 5.95 \times 10^{-4}$ Sec.$^{-1}$

$k_{1.5} = 28.6 \times 10^{-6}$ mm.$^{-\frac{1}{2}}$ Sec.$^{-1}$

Mean: $k_1 = 5.38 \times 10^{-4}$ Sec.$^{-1}$; $k_{1.5} = 28.96 \times 10^{-6}$ mm.$^{-\frac{1}{2}}$ Sec.$^{-1}$

Temperature 193.0°C

Run Number 392
$[RI]_o$ = 53.2 mm.

Time (min.)	Pressure (mm.)
0	53.2
2	53.3
5	53.9
10	54.05
15	54.8

$k_1 = 0.447 \times 10^{-4}$ Sec.$^{-1}$

Temperature 235.0°C

Run Number 393
$[RI]_o$ = 48.7 mm.

Time (min.)	Pressure (mm.)
0	48.7
1	49.55
2	52.8
3	54.85
4	56.9
5	59.8
7	63.9
9	67.45
10	69.2

$k_1 = 10.52 \times 10^{-4}$ Sec.$^{-1}$

isobutene carbon packed vessel

Temperature 226.5°C			Temperature 213.0°C		Temperature 201.0°C	
Run Numbers 394-397 $[RI]_o$ = 29.4 mm.			Run Number 400 $[RI]_o$ = 30.5 mm.		Run Number 402 $[RI]_o$ = 41.0 mm.	
Time (min.)	Pressure (mm.)	I_2 (mm.x10^{-1})	Time (min.)	Pressure (mm.)	Time (min.)	Pressure (mm.)
0	29.4		0	30.5	0	41.0
0.5	29.95	0.5	1	31.5	1	41.3
1	30.65	1.25	1.5	32.0	2	42.1
1.5	31.4	2.05	2	32.5	3	42.7
			2.5	33.1	4	43.7
					5	44.95
k_1 = 9.44x10^{-4}Sec.$^{-1}$			k_1 = 6.53x10^{-4}Sec.$^{-1}$		k_1 = 3.07x10^{-4}Sec.$^{-1}$	
$k_{1.5}$ = 38.0x10^{-6}mm.$^{-\frac{1}{2}}$Sec.$^{-1}$						

Iodine could not be analysed during the runs 392, 393, 400 and 402. The respective rate constants for the first order reaction were calculated on the basis of the iodine expected at these temperatures in allyl bromide vessels. The iodine producing process has been found to be homogeneous (Fig.15).

(c) Other Results:

Effect of hydrogen iodide

Several kinetic determinations were made to study the effect of added hydrogen iodide on the pyrolysis. The pressure-time relationship did not alter very much but iodine production was slightly increased. The decomposition temperature of HI is much higher[108,109] than the temperature range of the present investigation. Typical pressure-time results are shown below and the results are summarised in table 4.6.

Temperature 199.5°C Surface: allyl bromide carbon				Temperature 216.0°C Surface: isobutene carbon			
Run Number 20 $[RI]_o$ = 35.5 mm. HI = 0		Run Number 21 $[RI]_o$ = 36.5 mm. HI = 66.5 mm.		Run Number 420 $[RI]_o$ = 31.4 mm. HI = 0		Run Number 421 $[RI]_o$ = 28 mm. HI = 14.1 mm.	
Time (min.)	Pressure (mm.)	Time (min.)	Pressure (mm.)	Time (min.)	Pressure (mm.)	Time (min.)	Pressure (mm.)
0	35.5	0	103.0	0	31.4	0	42.1
1	35.7	1.5	104.8	1	31.7	1	44.0
3	36.4	2	105.6	2	32.0	2	44.9
5	37.25	3.5	105.85	3	32.4	3	45.75
7	38.6	5.5	107.8	5	33.15	5	46.05
10	40.7	7.5	108.7	7	38.1	7	47.9
15	44.6	10	110.0	10	39.9	10	50.15
		15	113.0				

Table 4.6. Effect of HI on t-C_4H_9I pyrolysis.

Temp. (°C)	Surface	HI added (mm.)	Reaction time (min.)	Initial iodide (mm.)	$\triangle P$ (mm.)	I_2 (mm. x 10^{-1})
200	allyl bromide	0	50	15.5	11.2	5.75
		25	50	16.0	11.0	8.6
"	"	0	30	33.5	13.5	16.05
		54.8	30	30.5	15.5	23.55
		0	30	29.5	7,7	12.7
"	"	70	30	25.3	9.8	19.45
"	"	0	15	35	9.0	10.65
		66.5	15	36.5	9.0	15.7
216	isobutene	0	10	31.4	7.95	20.2
		14.1	10	28	8.5	28.0

Effect of nitric oxide:

The effect of NO on the pyrolysis was inconclusive. The pressure-time relationship was slightly affected, but there was an increase in iodine production. A typical pressure-time result with or without NO is shown below and the results for more runs are summarised in table 4.7.

Temperature 220.0°C; allyl bromide carbon

Run Number 22 $[RI]_o$ = 26.0 mm. NO = 0.		Run Number 23 $[RI]_o$ = 25.0 mm. NO = 91.98 mm.		Run Number 24 $[RI]_o$ = 27.75 mm. NO = 2.15 mm.	
Time (min.)	Pressure (mm.)	Time (min.)	Pressure (mm.)	Time (min.)	Pressure (mm.)
0	26.0	0	116.9	0	29.9
0.5	28.25	0.5	117.5	0.50	31.15
1	30.5	1	118.3	1.0	32.45
1.5	32.5	1.75	119.50	1.5	33.35
2	34.65	2	120.55	2	34.65
2.5	36.8	2.5	123.8	2.75	36.35
3	38.0	3	126.60	3	36.8
3.5	40.25	3.5	129.2	3.50	37.9
4.5	41.35	4.5	130.0	4	38.95
5	42.0	5	130.3	4.5	40.25
7	43.7	6	130.1	5	41.55
10	44.4	7.5	129.45	6	43.5
		10	128.55	7	44.85
				8	46.1
				9	46.75
				10	47.2

Table 4.7. Effect of NO on the pyrolysis of t-C_4H_9I. Temp. = 220.0°C; allyl bromide carbon surface.

Runs 25-34

$[RI]_o$ (mm.)	NO (mm.)	I_2 produced ($\times 10^{-1}$ mm.)	Time of reaction (min)
26.0	0	8.75	10
27.75	2.0	13.7	"
24.5	13.9	22.8	"
22.0	5.0	12.65	"
25.0	23.8	32.3	"
25.0	11.2	19.65	"
23.2	22.2	25.45	"
22.5	22.1	20.7	"
23.7	21.5	27.20	"

Effect of different surfaces:

Table 4.8 summarises the relative rates of pressure change and iodine production during the pyrolysis of t-C_4H_9I at 220.0°C in reaction vessels having different chemical coatings.

Table 4.8: Relative rates of pressure change and iodine production at different surfaces.

Run Numbers 252-285

Surface	U-unpacked P-packed	Temp. (°C)	$[RI]_o$ (mm.)	Time (min.)	$\triangle P$ (mm.)	I_2 (mm.x10^{-1})
Clean glass	U	220.0	44.0	3	10.3	8.5
	P	"	"	3	19.5	12.3
	U	219.0	44.0	3	9.0	7.2
	"			5	12.5	15.4
Allyl bromide carbon	U	219.2	43.0	3	6.8	8.8
	"	"	"	5	11.0	16.5
	P	219.0	43.0	3	15.5	11.4
	"	"	"	5	25.5	19.2
Ethyl bromide carbon	U	220.0	44.5	3	4.9	8.9
	"			5	8.1	15.1
Isobutene carbon	U	220.0	44.0	3	1.1	4.6
	"		"	5	2.2	8.3
	P		"	3	2.1	
	"		"	5	3.3	

The kinetics were investigated in detail on two of the above surfaces viz., allyl bromide and isobutene carbons.

4.5. Discussion of Results and Mechanism.

The pressure-time curves, particularly at lower temperatures, showed a small induction period. Thereafter results corresponded well with first order behavior. The shape of the pressure-time curves did not alter with the nature of the surface and may be characteristic of the iodide.

The autocatalytic shape of the iodine-time curves also was not affected by the nature of the surface.

Principles of Calculations.

The kinetic calculations are based on the following mechanism for the two processes in the pyrolysis.

$$C_4H_9I \xrightarrow{k_1} C_4H_9 + HI \qquad \ldots\ldots\ldots\ldots \quad (1)$$

$$\left.\begin{aligned} I + C_4H_9I &\longrightarrow C_4H_9 + I_2 \\ C_4H_9 + HI &\longrightarrow C_4H_{10} + I \end{aligned}\right) \qquad \ldots\ldots\ldots\ldots \quad (2)$$

The rate of disappearance of the iodide is represented by

$$-d\left(\frac{C_4H_9I}{dt}\right) = k_1(C_4H_9I) + k_{1.5}(C_4H_9I)(I_2)^{\frac{1}{2}}$$

and the rate of production of iodine is

$$d\left(\frac{I_2}{dt}\right) = k_{1.5}(C_4H_9I)(I_2)^{\frac{1}{2}}$$

The pressure change $\triangle P$ is due only to step (1). The amount of the iodide remainirg will be given by $[RI]_o-(\triangle P+I_2)$, since the pressure change is always accompanied by some iodine production in step (2). In order to find the value of k_1, the logarithm of $[RI]_o-(\triangle P+I_2)$ was plotted against time and the rate constant k_1 was found from the initial slope. Also, $k_{1.5}$ was determined from the slope of the plot of $d\left(\frac{I_2}{dt}\right) \times \frac{1}{[RI]_t}$ against the square root of iodine. $d\left(\frac{I_2}{dt}\right)$ could be found from the slope

at different points of I_2 - t curve.

Three model calculations of rate constants for both the first order rate and the autocatalytic rate at different temperatures and concentrations are shown in tables 4.9-4.11. The conversion to mm. of iodine from moles of iodine was made on the basis of the assumption that iodine behaved as an ideal gas.

Table 4.9: Model calculation of rate constants

Temperature = 190.0°C
$[RI]_o$ = 55.7 mm.
= 337 micro moles.

Volume of reaction vessel = 175 c.c.
1 mm. = $\frac{273.2 \times 44.6 \times 175}{463.2 \quad 760}$ = 6.05 micro moles

Time (min.)	I_2 (micro moles)	$(I_2)^{\frac{1}{2}}$ (micro moles)	$\frac{dI_2}{dt}$ (from slope)	$\triangle P$ (mm.)	$\triangle P+I_2$ (micro moles)	$\triangle P+I_2$ (micro moles)	$[RI]_t$ = RI $_o$ - $(P+I_2)$ micro moles	$\frac{[RI]_o}{[RI]_t} = X$	log X	$\frac{dI_2}{dt} \times \frac{1}{[RI]_t} = Q$ $\times 10^{-4}$ (min.$^{-1}$)
5	0.54	0.74	0.15	1.2	7.26	7.8	329.2	1.024	0.0103	4.5
7	1.0	1.0	0.166	2.0	12.1	13.1	323.9	1.040	0.0170	5.0
10	1.51	1.21	0.2	3.4	20.57	22.1	314.9	1.070	0.0294	6.3
15	2.75	1.66	0.266	6.0	36.3	39.05	297.95	1.131	0.0535	8.9
20	4.15	2.04	0.296	9.0	54.45	58.6	278.3	1.212	0.0835	10.8
25	5.65	2.38	0.301	12.5	75.63	81.3	255.7	1.318	0.1199	11.7

k_1 = slope of plot of log X against time in seconds X 2.303 = 1.72×10^{-4} Sec.$^{-1}$

$$k_{1.5} = \frac{\text{slope of plot of Q against } (I_2)^{\frac{1}{2}}}{60 \times (6.05)^{\frac{1}{2}}}$$

$$= 2.98 \times 10^{-6} \text{ mm.}^{-\frac{1}{2}} \text{Sec.}^{-1}$$

Table 4.10: Model calculation of rate constants.

Temperature = 219.2°C
$[RI]_o$ = 43.8 mm.
= 250.0 micro moles.

Volume of reaction vessel
1 mm. = $\frac{273.2}{492.4} \times \frac{44.6 \times 175}{760}$ = 5.71 micro moles

Time (min.)	I_2 (micro moles)	$(I_2)^{\frac{1}{2}}$ (micro moles)	$\frac{dI_2}{dt}$ (from slope)	ΔP (mm.)	ΔP (micro moles)	$\Delta P+I_2$ (micro moles)	$[RI]_t = [RI]_o - (P+I_2)$ micro moles	$\frac{[RI]_o}{[RI]_t} = X$	log X	$\frac{dI_2}{dt} \times \frac{1}{[RI]_t} = Q$ $\times 10^{-4}$ (min.$^{-1}$)
1	1.5	1.202	1.5	1.6	9.12	10.62	240.4	1.040	.0170	62.4
2	3.2	1.79	1.7	3.6	20.52	23.82	226.3	1.105	.0433	75.1
3	5.0	2.23	1.83	6.6	37.62	42.62	207.40	1.206	.0813	88.2
4	7.1	2.67	2.15	10.1	57.57	64.67	185.35	1.349	.1300	116.0
5	9.4	3.07	2.35	11.6	66.12	75.52	174.5	1.433	.1562	134.6

k_1 = slope of plot of log X against time in seconds X 2.303 = 12.67×10^{-4} Sec.$^{-1}$

$$k_{1.5} = \frac{\text{slope of plot of Q against } (I_2)^{\frac{1}{2}}}{60 \times (5.71)^{\frac{1}{2}}}$$

$= 26.5 \times 10^{-6}$ mm.$^{-\frac{1}{2}}$ Sec^{-1}

Table 4.11: Model calculation of rate constants.

Temperature = 239.0°C
$[RI]_o$ = 18.1 mm.
= 99 micro moles.

Volume of reaction vessel = 175 c.c.
1 mm. = $\frac{273.2}{512.4} \times \frac{44.6 \times 175}{760}$ = 5.47 micro moles

Time (min.)	I_2 (micro moles)	$(I_2)^{\frac{1}{2}}$ (micro moles)	$\frac{dI_2}{dt}$ (from slope)	ΔP (mm.)	ΔP (micro moles)	$\Delta P+I_2$ (micro moles)	$[RI]_t = [RI]_o - (\Delta P+I_2)$ micro moles	$\frac{[RI]_o}{[RI]_t} = X$	log X	$\frac{dI_2}{dt} \times \frac{1}{[RI]_t} = Q$ $\times 10^{-4}$ (min.$^{-1}$)
0.5	0.7	0.836	1.42	1	5.47	6.17	92.85	1.066	0.0378	15.29
1	1.45	1.204	1.7	2.3	12.58	14.03	85.01	1.165	0.0664	20.00
1.3	2.0	1.42	1.75	3.1	16.96	18.96	80.05	1.237	0.0923	21.86
1.5	2.4	1.55	1.82	3.6	19.69	22.09	76.90	1.287	0.1096	23.66
2.0	3.6	1.877	2.56	4.8	26.26	29.86	69.15	1.432	0.1559	37.1

99

k_1 = slope of the plot of log X against time in seconds X 2.303 = 31.33×10^{-4} Sec.$^{-1}$

$$k_{1.5} = \frac{\text{slope of the plot of Q against } (I_2)^{\frac{1}{2}}}{60 \times (5.47)^{\frac{1}{2}}}$$

$$= 71.25 \times 10^{-6} \text{ mm.}^{-\frac{1}{2}} \text{Sec.}^{-1}$$

The rate constants together with relevant data for the Arrhenius plots for allyl bromide and isobutene carbon coated vessels are tabulated in tables 4.12 and 4.13 respectively.

Table 4.12: Data for the Arrhenius plot; allyl bromide vessel; Unpacked vessel.

Temp. (^{o}C)	$1/T \times 10^3$	$k_{1.5} \times 10^6$ ($mm.^{-\frac{1}{2}} Sec.^{-1}$)	$\log k_{1.5}+6$	$k_1 \times 10^4$ $Sec.^{-1}$	$\log k_1+4$
201	2.110	5.07	0.705	2.72	0.4346
190	2.159	2.98	0.474	1.72	0.2355
210	2.07	14.05	1.148	5.25	0.7202
219.2	2.032	26.5	1.432	12.67	1.1028
229	1.992	47.55	1.677	20.1	1.3032
239	1.953	71.25	1.853	28.88	1.4606
		Packed vessel: surface/volume ratio 1:6.2			
200	2.114	5.88	0.769	10.0	1.0128
220	2.028	30.8	1.489	16.85	1.2765
230	1.988	60.0	1.755	30.3	1.486
240	1.949	88.8	1.949	38.7	1.588

Table 4.13: Data for the Arrhenius plot; isobutene coated vessel; unpacked vessel.

Temp. (^{o}C)	$\frac{1}{T}x10^{3}$	$k_{1.5}x10^{6}$ (mm.$^{-\frac{1}{2}}$Sec.$^{-1}$)	log $k_{1.5}+6$	$k_{1}x10^{4}$ (Sec.$^{-1}$)	log $k_{1}+4$
193.0	2.146			.477	0.349
200.0	2.114	4.57	0.66	0.58	0.2366
208.0	2.079	7.8	0.892	1.63	0.2122
210.0	2.070	9.52	0.979	1.60	0.204
214.3	2.052			2.99	0.4757
216.8	2.041	11.4	1.0569	3.50	0.5441
220.0	2.028	15.6	1.193	2.14	0.3314
224.3	2.012	29.75	1.473	4.95	0.6335
229.0	1.991	28.96	1.4618	6.46	0.8102
235.0	1.969			10.52	1.0206
		Packed vessel; surface/volume = 7.0			
201.5	2.107			3.07	0.4871
213	2.058			6.2	.7822
226.5	2.002	38.0	1.58	8.4	0.975

The Arrhenius plots for the first order and three-halves order rate constants are shown in figures 15 and 16 respectively.

The first order rate constants depend on the surface and the process seems to be heterogeneous. The three-halves order process is independent of the conditions of surface and is

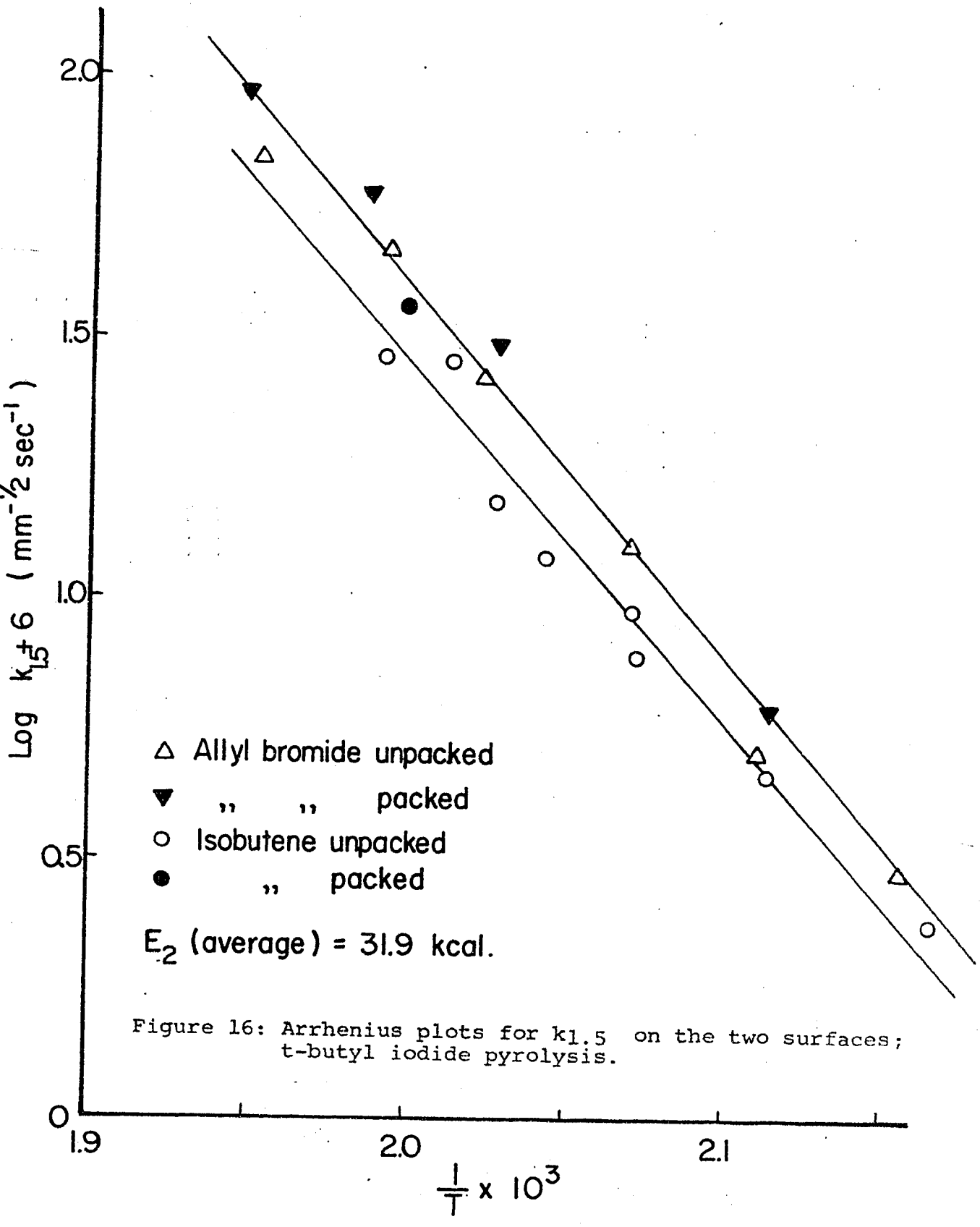

Figure 16: Arrhenius plots for $k_{1.5}$ on the two surfaces; t-butyl iodide pyrolysis.

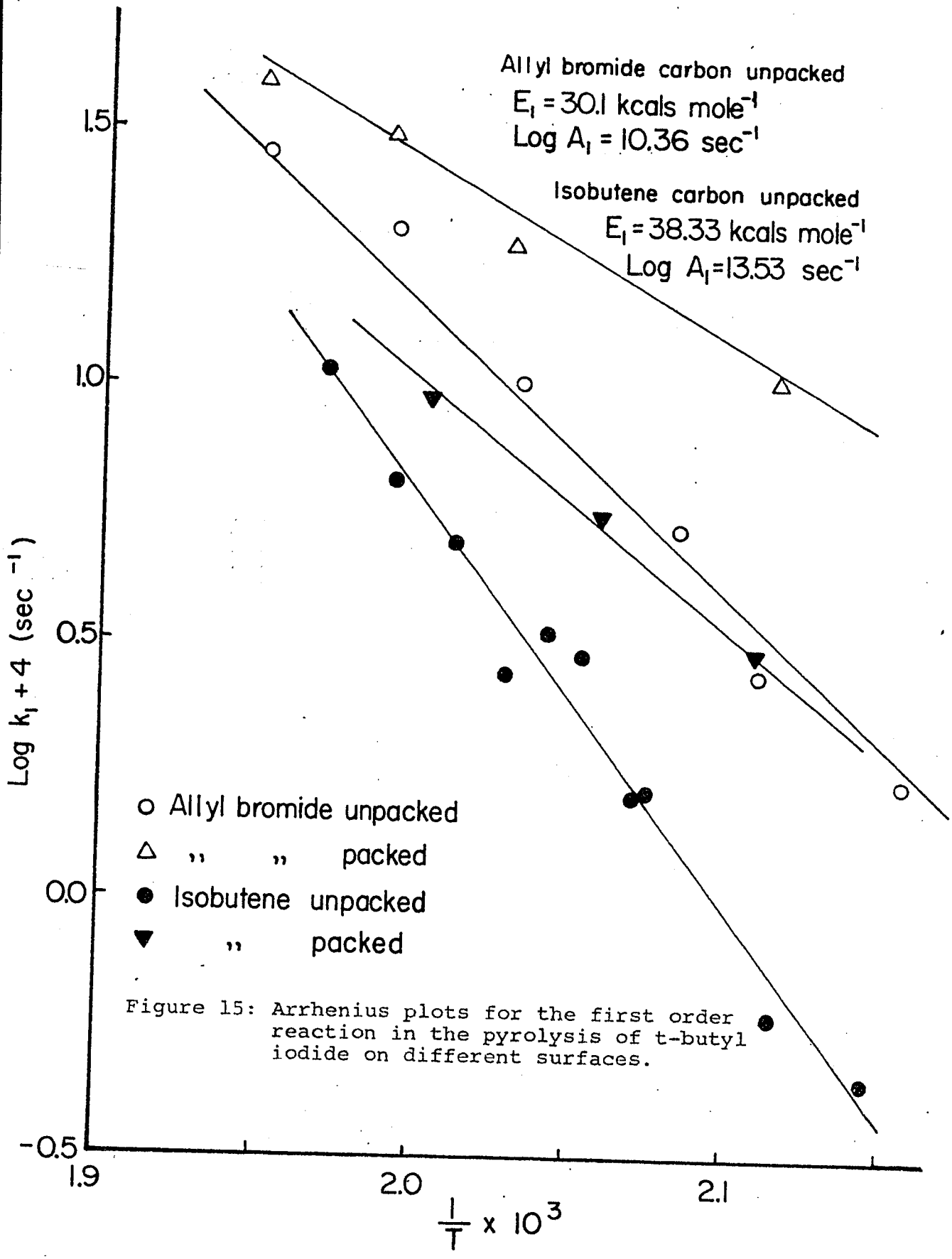

Figure 15: Arrhenius plots for the first order reaction in the pyrolysis of t-butyl iodide on different surfaces.

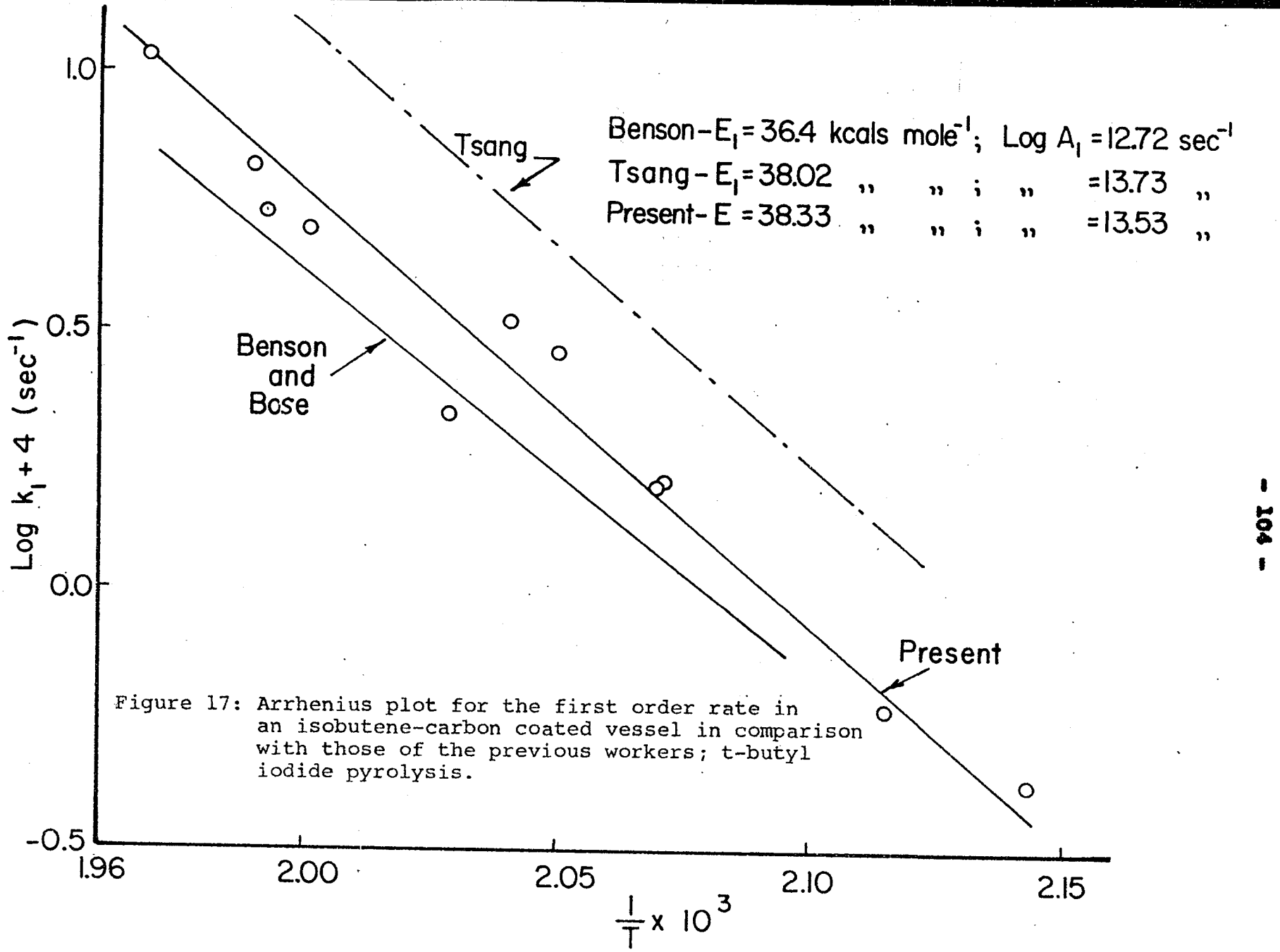

Figure 17: Arrhenius plot for the first order rate in an isobutene-carbon coated vessel in comparison with those of the previous workers; t-butyl iodide pyrolysis.

judged to be homogeneous. The values of the Arrhenius parameters for the first order reaction on isobutene carbon as calculated by the "least squares" method are very close to those of Benson and Tsang and are thought be the least heterogeneous. The Arrhenius equations for the decompositions of $t\text{-}C_4H_9I$ on isobutene carbon are

$$k_1 = 10^{13.53} \exp(38330/RT) \text{ Sec.}^{-1}$$

$$k_{1.5} = 10^{9.76} \exp(31.900/RT) \text{ mm.}^{-\frac{1}{2}}\text{Sec.}^{-1}$$

The Arrhenius plot for the first order reaction is compared with the corresponding plots of Benson and Tsang in figure 17.

Mechanism:

on the basis of the fore-going results the following mechanism for the pyrolysis of t-butyl iodide seems satisfactory.

The first order process is simply the molecular elimination of hydrogen iodide (1)

$$t\text{-}C_4H_9I \rightleftharpoons C_4H_8 + HI \qquad (1), (-1)$$

The reverse reaction (-1) becomes important at high conversions and also takes place when the products are condensed. This process is accompanied by a slower autocatalytic process, the mechanism of which is

$$I + C_4H_9I \longrightarrow C_4H_9 + I_2 \quad \ldots\ldots\ldots\ldots \quad (2a)$$

$$C_4H_9 + HI \longrightarrow C_4H_{10} + I \quad \ldots\ldots\ldots\ldots \quad (2b)$$

$$I + I + M \rightleftharpoons I_2 \quad \ldots\ldots\ldots\ldots \quad (2c)$$

and the stoicheiometry is

$$C_4H_9I + HI \longrightarrow C_4H_{10} + I_2$$

Iodine necessary for the autocatalysis was probably introduced as impurity in the system. Extrapolation of the log plots to zero time allowed calculation of the initiating concentration of iodine; these were of the order of 0.08 mm.

The homolysis of the C-I bond can be discounted on energetic grounds. The presently accepted value of $D(t\text{-}C_4H_9\text{-}I)$ of 48 K.Cal $mole^{-1}$ is well above the estimated activation energy for the homogeneous elimination process (1). However, a minute fraction of the homolysis of the C-I bond may take place to produce sufficient iodine to initiate the autocatalysis.

The possibility of reaction (-2a) and (-2b) is eliminated due to the presence of excess of hydrogen iodide in the system. The addition of hydrogen iodide does not affect the pressure change appreciably, indicating that there is no catalysis due to this compound.

The small increase in iodine production may be due to the side reaction of

$$RI + HI \longrightarrow RH + I_2$$

Nitric oxide has no conclusive effect. Some decrease in pressure change and the increase of iodine production is suggestive of the preferential reaction of HI with NO.

The results for the first order process on the isobutene carbon coated surface of the reaction vessel suggest that the activation energy for the process must be at least 38.3 K.Cals.

Benson's value of 36.4 K.Cals was based on the assumption that his system for the reverse reaction

$$C_4H_8 + 2HI \longrightarrow I_2 + C_4H_{10}$$

was homogeneous. Lately Holmes[11b] has studied this reaction and the system has been found to be heterogeneous. Morever, the reaction between HI and t-C_4H_9I to produce I_2 is not rapid and quantitative in our system contrary to Benson's findings (see table 4.6). Thus, Benson's estimated value 36.4 K.Cals for the activation energy of the unimolecular elimination reaction of t-C_4H_9I, must be doubtful. Benson supported his values on the basis of the generalisation[44] that activation energies decrease by about 7 K.Cals on every α-Me substitution. This hypothesis itself has not been found true elsewhere.[25]

The comparative rate technique employed by Tsang is unlikely to give very accurate results. Moreover, Tsang does not mention anything about the product analysis where so many difficulties were found in the present investigation. Thus his value, 38 K.Cals, is also open to doubt.

Looking towards the common trends of halides in general, it is expected from the plot of E vs. $D(H^{+}-X^{-})$ in Fig.1 that the activation energy for the homogeneous decomposition of t-butyl iodide should be about 40 K.Cals.

SECTION 5

PYROLYSIS OF n-PROPYL IODIDE

5.1. Introduction:

From his investigations of the reaction between alkyl iodides and hydrogen iodide Ogg[79] concluded that the initial step in the decomposition of n-propyl iodide is

$$n\text{-}C_3H_7I \longrightarrow n\text{-}C_3H_7 + I$$

which has an activation energy of 43.0 K.Cals. This he supposed to be the C-I bond dissociation energy. Butler and Polanyi[82] used a flow technique for the pyrolysis and estimated the value of $D(n\text{-}C_3H_7\text{-}I)$ to be 50.0 K.Cals. However, their technique was not reliable.

Glass and Hinshelwood[111] had shown that i-propyl iodide decomposed according to the equation

$$2C_3H_7I \longrightarrow C_3H_8 + C_3H_6 + I_2 \quad \ldots\ldots\ldots(1)$$

Jones and Ogg[83] studied the pyrolysis of $n\text{-}C_3H_7I$ in the temperature range 311°-354°C and reported that the stoicheiometry could be well represented by (1) as in the case of i-propyl iodide. The rate law for the pyrolysis was

$$-d\frac{(n\text{-}C_3H_7I)}{dt} = k(n\text{-}C_3H_7I)(I)^{\frac{1}{2}}$$

$$= k_1K^{\frac{1}{2}}(C_3H_7I)(I)$$

where K is the equilibrium constant for the equilibrium

$$I_2 \overset{M}{\rightleftharpoons} 2I$$

They noticed that rates were faster at the beginning of the reaction. The final to initial pressure ratio was 1.55. Their Arrhenius parameters were -

$E = 37.9$ K.Cals mole^{-1} and $\log_{10}A = 10.06$ mm.$^{-\frac{1}{2}}$Sec.$^{-1}$

Jones and Ogg discussed many possible mechanisms but because of their erroneous interpretation of the reaction between n-C_3H_7I and HI, they could not decide whether the abstraction of iodine or hydrogen takes place during the rate determining step. The mechanism chosen by Jones and Ogg is the following -

$$n\text{-}C_3H_7I \longrightarrow n\text{-}C_3H_7 + I \quad \ldots\ (i)$$

$$n\text{-}C_3H_7 + n\text{-}C_3H_7I \longrightarrow C_3H_8 + C_3H_6I \quad \ldots\ (ii)$$

$$C_3H_6I \longrightarrow C_3H_6 + I \quad \ldots\ (iii)$$

$$n\text{-}C_3H_7I \longrightarrow n\text{-}C_3H_7 + \tfrac{1}{2}I_2 \quad \ldots\ (iv)$$

$$n\text{-}C_3H_7 + I_2 \longrightarrow i\text{-}C_3H_7I + I \quad \ldots\ (v)\ \text{slow}$$

$$i\text{-}C_3H_7I \longrightarrow \tfrac{1}{2}C_3H_8 + \tfrac{1}{2}C_3H_6 + \tfrac{1}{2}I_2 \quad \ldots\ (vi)\ \text{fast}$$

$$2I + M \rightleftharpoons I_2 + M \quad \ldots\ (vii)$$

Reactions (i), (ii), (iii) and (vii) constitute the main reactions at the start. Once iodine has built up or in the presence of added iodine, reaction (iv), (v) and (vi) become important. Reaction (v) is assumed to be the rate determing

step and the decomposition of the iso-compound formed is more rapid than that of n-compound. From spectroscopic and other data they concluded in a somewhat dubious manner that $E_{(v)}$ is 13.2 K.Cals and that there is a steric factor of about 10^{-5}. This mechanism appears consistent with their results. However, their estimates of $E_{(iii)}$ and $E_{(v)}$ are unreliable.

Schumacher[112] has criticised this mechanism; in the absence of excess iodine he considers that the strongly exothermic reaction

$$2n\text{-}C_3H_7 \longrightarrow C_3H_6 + C_3H_8$$

should be considered. The mechanism would thus be

$$n\text{-}C_3H_7I \longrightarrow n\text{-}C_3H_7 + I \quad \ldots\ldots\ldots \quad \text{(i) slow}$$

$$2n\text{-}C_3H_7 \longrightarrow C_3H_8 + C_3H_6 \quad \ldots\ldots\ldots \quad \text{(viii)}$$

$$n\text{-}C_3H_7 + I_2 \longrightarrow n\text{-}C_3H_7I + I \quad \ldots\ldots\ldots \quad \text{(ix)}$$

$$2I \overset{M}{\rightleftharpoons} I_2 \quad \ldots\ldots\ldots \quad \text{(vii)}$$

This explains the retardation of the reaction by iodine as it progresses. In the presence of iodine his suggested mechanism is

$$I_2 \overset{M}{\rightleftharpoons} 2I \quad \ldots\ldots\ldots \quad \text{(x)}$$

$$n\text{-}C_3H_7I + I \longrightarrow i\text{-}C_3H_7 + I_2 \quad \ldots\ldots\ldots \quad \text{(xi)}$$

$$2i\text{-}C_3H_7 \longrightarrow C_3H_8 + C_3H_6 \quad \ldots\ldots\ldots \quad \text{(xii)}$$

This mechanism is also in agreement with experiment. It leads to a value of $E_{(xi)} = 20 \pm 2$ K.Cals[113]. The steric factor of

reaction (xi) appears to be about 5×10^{-2}. It is not possible to decide between the two mechanisms, but that of Schumacher is perhaps more plausible on general grounds although reaction (xi) seems somewhat unlikely.

Lossing, Ingold and Henderson[114] investigated the products of the pyrolysis at 650° to 850°C by means of mass spectrometry. No $n\text{-}C_3H_7$ radicals were detected, but CH_3 and C_2H_4 were major products. These obviously arise from the decomposition of n-propyl radicals at the high temperatures used.

In the light of the re-interpretation of Ogg's data for the reaction between hydrogen iodide and normal propyl iodide[80,81], Benson concluded that the rate determing step in the n-propyl iodide pyrolysis would be

$$I + n\text{-}C_3H_7I \longrightarrow C_3H_6 + HI + I$$

In another report Bose and Benson[88] claim to observe qualitatively the production of appreciable amounts of i-PrI and HI during the pyrolysis of $n\text{-}C_3H_7I$ above 300°C.

In view of the above conflicting reports about the mechanism of the pyrolysis, the present investigation was undertaken in the temperature range 307°-360°C. An induction period unobserved by any of the previous workers, was found. The same kind of induction period was also found during the pyrolysis of n-butyl iodide.

5.2. Experimental

The essentials of the experimental techniques have been described in section 3. Iodine and hydrogen iodide were

titrated in the usual way.

Formation of a tiny amount of iso-propyl iodide during the induction period was detected and estimated by GLC. A 20ft. column of 1% Apiezon grease on 60-80 glass beads was used in a Beckmann GC-2 chromatographic apparatus at 70°C to separate the n- and i- compounds. The iso compound came off the column first and so could be estimated in the presence of an enormous excess of n-propyl iodide.

5.3. Stoicheiometry and Principles of Calculations

The final to initial pressure during the pyrolysis approached 1.5 and the iodine titres were found to be closely equal to the pressure change during pyrolysis (see table). Therefore it was clear that the stoicheiometry was

$$2C_3H_7I \longrightarrow C_3H_6 + C_3H_8 + I_2$$

as also suggested by Jones and Ogg. The results obtained fitted the rate law

$$-\frac{d(C_3H_7I)}{dt} = k(C_3H_7I)(I_2)^{\frac{1}{2}}$$

On the basis of the above stoicheiometry the pressure of n-propyl iodide at any time t is given by

$$(C_3H_7I)_t = P_t = \frac{1.5P_o - P_t}{0.5}$$

and

$$(I_2)_t = (P_t - P_o) = \triangle P$$

where P_o = initial concentration of iodide in terms of pressure. Placing these values in the rate expression gives

$$\frac{dP_t}{dt} = k(1.5\ P_o - P_t)(P_t - P_o)$$

which on integration and evaluation of the integration constant becomes

$$kt = \frac{1}{(P_o)^{\frac{1}{2}}} \ln \frac{\frac{1}{2} P_o^{\frac{1}{2}} + P^{\frac{1}{2}}}{\frac{1}{2} P_o^{\frac{1}{2}} - P^{\frac{1}{2}}}$$

where P_o is the initial pressure and $\triangle P$ is the pressure change during the pyrolysis. Thus k can be evaluated from the slopes of the plots of the log function against time.

5.4: Results:

The ratio of final pressure P_f to the initial pressure P_o was determined by pyrolysing the compound until there was no further pressure change. The results were as follows (table 5.1)

Table 5.1: Determination of the ratio P_f/P_o

Run Number 5 Temp. = 310.0°C		Run Number 6 Temp. = 330.0°C		Run Number 7 Temp. = 360.0°C	
Time (min.)	Pressure (mm.)	Time (min.)	Pressure (mm.)	Time (min.)	Pressure (mm.)
0	53.5	0	60.0	0	30.6
100	73.5	50	86.0	30	42.7
300	77.5	100	87.0	60	44.2
330	77.6	130	87.0	75	44.6
				80	44.6
$\frac{P_f}{P_o} = 1.45$		$\frac{P_f}{P_o} = 1.45$		$\frac{P_f}{P_o} = 1.46$	

When the reaction vessel was given a coating of allyl bromide carbon, the pressure time curves were the same as those obtained in a clean glass vessel. This result supports the reports of previous workers[83], regarding the homogeneous nature of the reaction. Iodine titres at different times were always found to be equal to the pressure change within the limit of experimental error.

An induction period was observed which became shorter at higher temperatures; sometimes, during the induction period a slight drop in pressure was observed. A little iodine was produced during the induction period. However, very soon after the induction period the iodine and pressure measurements were equal.

No hydrogen iodide was ever detected as a product of pyrolysis. Figures 18 and 19 show typical pressure-time curves and the corresponding log plots. A typical iodine production vs. time plot is shown in figure 20. The pressure change is included for comparison.

The conversion of mm. of iodine from moles of iodine was made on the assumption that iodine behaves as an ideal gas.

The following (table 5.2) are the kinetic data from the pyrolysis of normal propyl iodide.

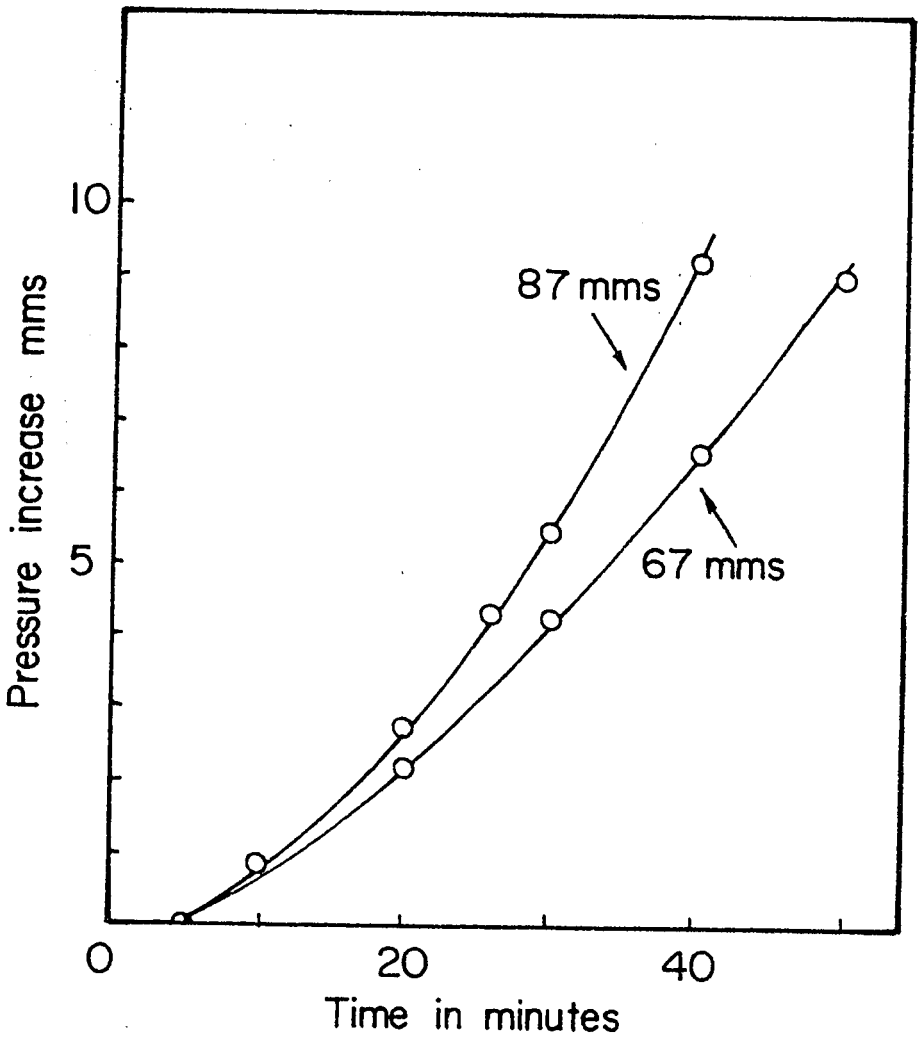

Figure 18: Typical pressure-time curves for the pyrolysis of n-propyl iodide at 310.0°C.

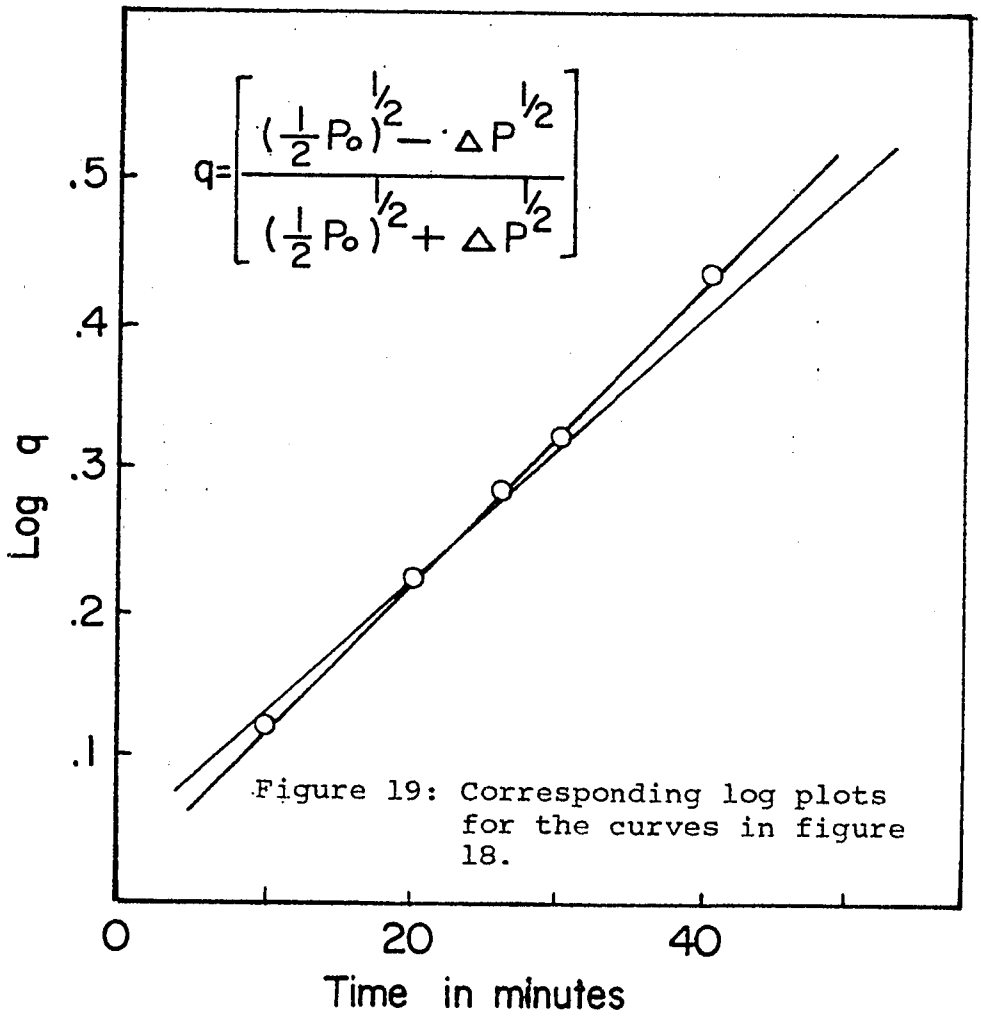

Figure 19: Corresponding log plots for the curves in figure 18.

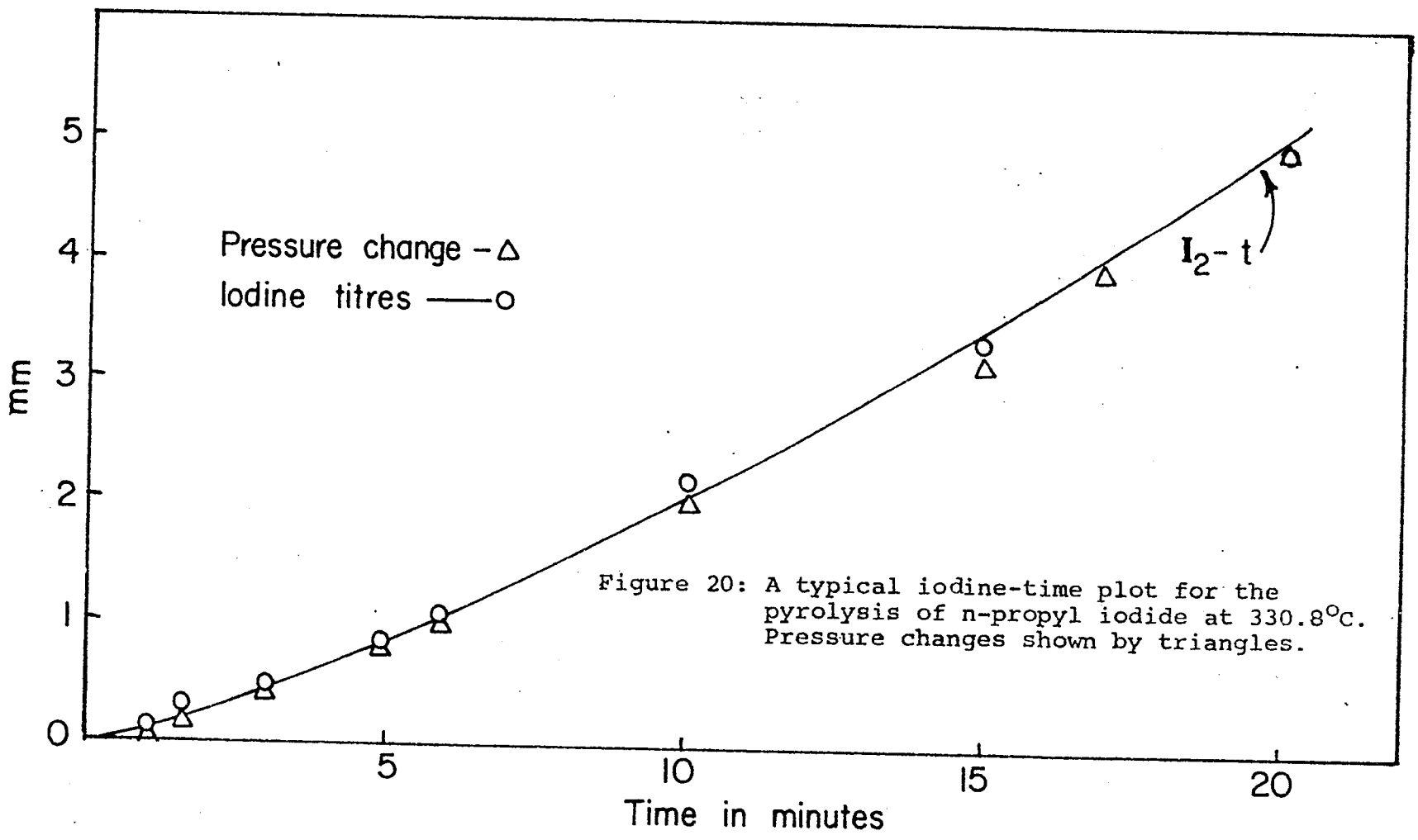

Figure 20: A typical iodine-time plot for the pyrolysis of n-propyl iodide at 330.8°C. Pressure changes shown by triangles.

Table 5.2: Kinetic results for the pyrolysis of $n\text{-}C_3H_7I$.

Temperature 310.0°C
Surface; allyl bromide carbon

Run Number 38 P_o = 67.0 mm.		Run Number 40 P_o = 87 mm.	
Time (min.)	Pressure (mm.)	Time (min.)	Pressure (mm.)
0	67.0	0	87.0
1	67.0	1	87.0
2	67.0	3	87.0
3	67.0	4	87.05
4	67.0	5	87.1
5	67.2	7	87.4
7	67.4	10	87.9
10	67.75	15	88.7
15	68.5	20	89.7
20	69.2	26	91.3
30	71.2	30	92.5
40	73.6	40	96.2
50	76.0		

Table 5.2. Cont'd

Temperature 330.8°C

Run Number 8 Surface: clean glass			Run Number 9 Surface: allyl bromide carbon		
Time (min.)	Pressure (mm.)	I_2 (mm.)	Time (min.)	Pressure (mm.)	I_2 (mm.)
0	63.3		0	62.3	
0.5	63.3	0	0.5	62.3	0
1	63.3	.05	1	62.3	.05
1.5	63.5		1.5	62.5	
3.5	64.5		2	62.8	
5	65.0		2.5	63.0	
7	65.5		4	63.6	
8	66.0		7	64.5	
9	66.7		8	65.0	
10	67.0	3.4	9	65.7	
			10	65.9	3.7

Table 5.2. Cont'd

Temperature 330.8°C
Surface; allyl bromide carbon

Run Numbers 12-17 P_o = 43.0 mm.			Run Numbers 18,19,20 P_o = 44.0 mm.			Run Numbers 22,23,24 P_o = 77.6 mm.		
Time (min.)	Press. (mm.)	I_2 ($mm.^2$)	Time (min.)	Press. (mm.)	I_2 ($mm.^2$)	Time (min.)	Press. (mm.)	I_2 ($mm.^2$)
0	43.0		0	44.0		0	77.6	
1	43.0	0.1	1	44.0	0.05	0.5	77.6	0.05
1.5	43.15	0.25	1.5	44.25		1	77.65	
3	43.45	0.5	2.5	44.5		2	78.35	
5	43.75		3	44.65	0.6	3	78.7	
6	44.0	1.05	4	45.0		5.5	80.5	2.75
10	45.3	2.35	5	45.2	1.1	7	81.5	4.0
15	46.2	3.4	7	45.7		9	83.5	
17	47.0		9	46.2		10	83.85	6.4
20	48.0	5.00	10	46.4	2.3			

Temperature 360.0°C
Surface; allyl bromide carbon

Run Numbers 28-30 P_o = 25.7 mm.			Run Number 32 P_o = 42.5 mm.			Run Number 34 P_o = 62.0 mm.		
Time (min.)	Press. (mm.)	I_2 ($mm.^2$)	Time (min.)	Press. (mm.)	I_2 ($mm.^2$)	Time (min.)	Press. (mm.)	I_2 ($mm.^2$)
0	25.7		0	42.5		0	62.0	
0.5	25.75		1	43.5		0.5	62.8	
1	26.5		2	45.0		1.0	63.8	
2	27.2		3	46.65		2.0	67.5	
3	28.0	2.2	4	48.35		3	69.2	
4	29.02		5	50.2	7.5	4	73.6	11.6
5	30.2	4.3						
7	31.7							
9	32.8	7.1						

The Arrhenius plot obtained from the average rate constants is shown in Fig.21 and the Arrhenius equation is

$$k = 10^{10.18} \exp(38400/RT)\, mm.^{-\frac{1}{2}} Sec.^{-1}$$

Jones and Ogg's plot is shown in the graph and it is seen that there is very close agreement. The data for the Arrhenius plot are given in table 5.3.

Table 5.3: Data for Arrhenius plot; $n\text{-}C_3H_7I$ pyrolysis.

Temperature (^oC)	$\frac{1}{T} \times 10^3$	$k \times 10^5$	$\log k + 5$
310.0	1.7151	6.03	0.78
330.8	1.6583	19.28	1.287
360.0	1.5798	84.70	1.928

In view of the previous work on the stoicheiometry and its confirmation in the present investigation on the basis of the $\frac{P_f}{P_o}$ ratio and the agreement between the pressure change and iodine production, propylene and propane were not analysed. However, gas chromatographic investigations were made to see if any i-propyl iodide is formed during the induction period.

At the lowest pyrolysis temperature where the induction period was the longest, the product of the reaction was condensed at liquid nitrogen temperature and was freed from the iodine by distillation at -20^oC. The colourless sample was then injected by means of a microsyringe into the chromatographic system at 70^oC. A tiny amount of i-propyl iodide was found. It increased to a maximum during the induction period. The results are shown in table 5.4.

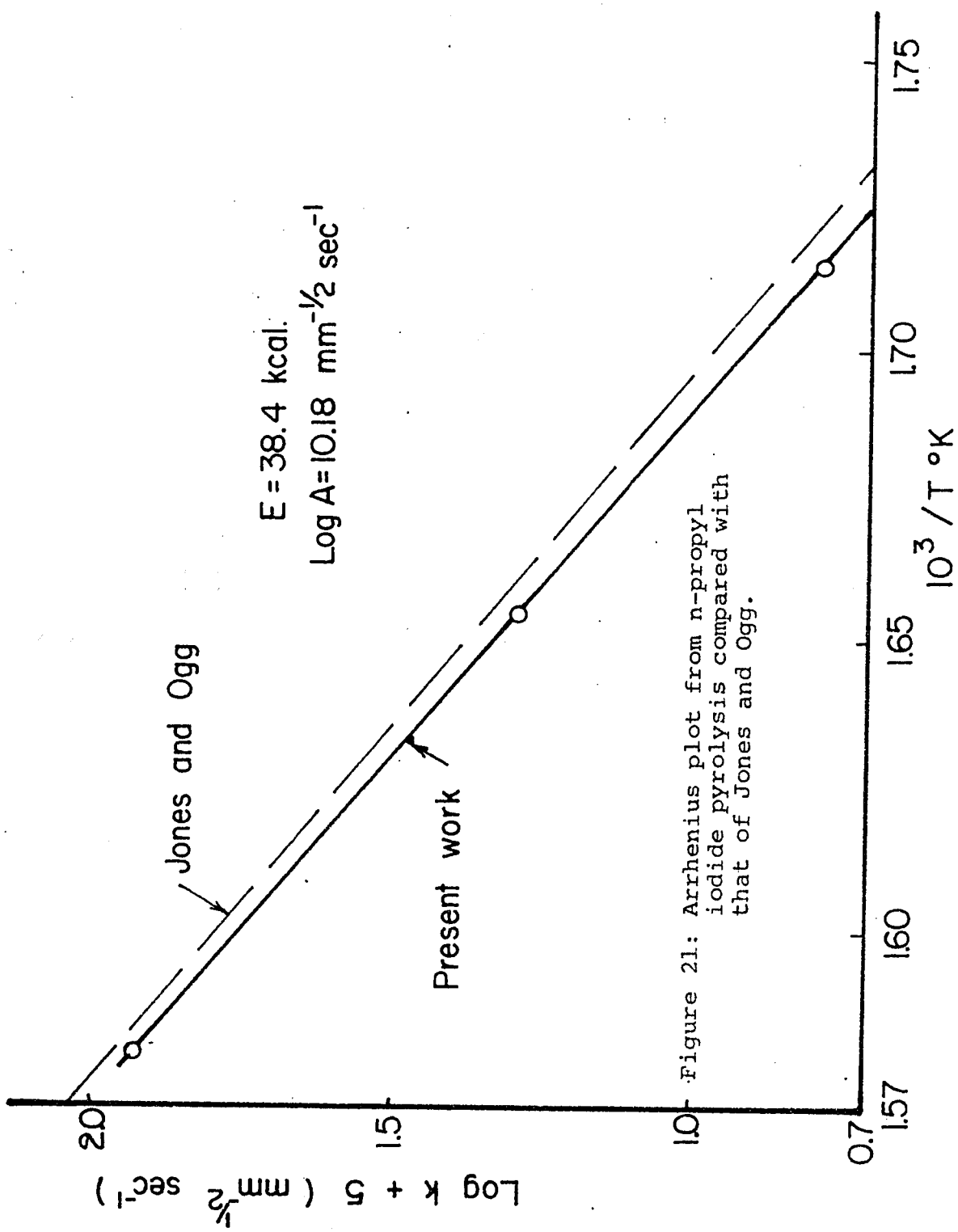

Figure 21: Arrhenius plot from n-propyl iodide pyrolysis compared with that of Jones and Ogg.

Table 5.4: Production of i-propyl iodide during the induction period.

Temperature 307.0°C

Length of the induction period 6.5 min.
$[RI]_o$ = 77 mm.; factor:- 1 mm. = 4.6 micro moles

Time (min.)	i-C_3H_7 (estimated) (micro moles)
1	0.05
2	0.1
3.5	0.2
5	0.4
7	0.35
10	0.05

A typical separation chromatogram is shown in figure 22.

Now there are two problems to be solved. One is, what is the cause of the induction period and the other is what is the rate determining step. The latter could be either

$$I + C_3H_7I \xrightarrow{A} C_3H_7 + I_2$$

or

$$I + C_3H_7I \xrightarrow{B} C_3H_6I + HI .$$

By means of the bond dissociation energies[94], $D(^{CH_3}_{ICH_2}\!\!>CH\text{-}H)$ = 95 K.Cals (estimated); D(H-I) = 71 K.Cals; $D(n\text{-}C_3H_7\text{—}I)$ = 53 K.Cals; $D(I_2)$ = 36.2 K.Cals; $E(C_3H_7 + I_2)$ = 0; and $E(HI + C_3H_6I)$ = 14 K.Cals[86], it can be shown that E_A = 34.9 K.Cals, and E_B = 38 K.Cals.

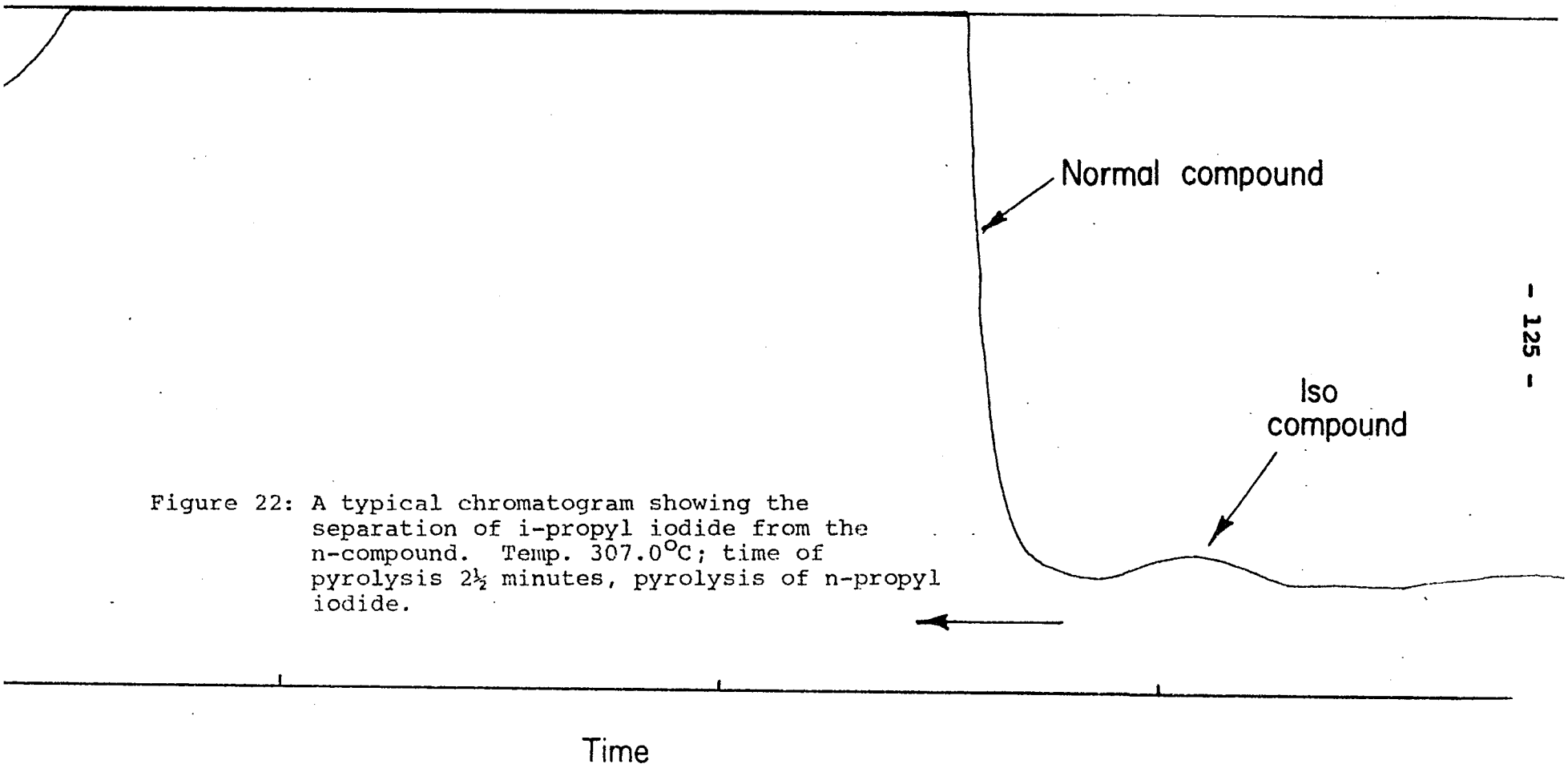

Figure 22: A typical chromatogram showing the separation of i-propyl iodide from the n-compound. Temp. 307.0°C; time of pyrolysis 2½ minutes, pyrolysis of n-propyl iodide.

The effects of a variety of substances on the induction period and on the overall pyrolysis were examined. For the induction period experiments a low temperature was chosen where the induction period was long. Results are tabulated below. Detailed discussion follows the tables.

Effect of Nitric Oxide

A few runs were carried out to see if NO had any effect on the pyrolysis. The kinetic data obtained did not show any significant effect. The results are summarised in table 5.5.

Table 5.5: Effect of NO on pyrolysis.

Temperature 330.8°C

Run Number 9 $[RI]_o$ = 62.3 mm. NO = 0		Run Number 54 $[RI]_o$ = 58.3 mm. NO = 12 mm.		Run Number 55 $[RI]_o$ 57.5 mm. NO = 35.8 mm.	
Time (min.)	Pressure (mm.)	Time (min.)	Pressure (mm.)	Time (min.)	Pressure (mm.)
0	62.3	0	70.3	0	93.3
0.5	62.3	1	70.3	1	93.35
1	62.3	2	70.7	2	93.9
1.5	62.5	3.5	71.5	3	94.9
2	62.8	5	72.0	5	95.7
2.5	63.0	7	72.9	7	97.2
4	63.6	10	74.0	10	99.6
7	64.5				
8	65.0				
9	65.7				
10	65.9				
$(I_2)_{10\ min.}$ = 3.7mm.		$(I_2)_{10\ min.}$ = 3.5mm.		$(I_2)_{10\ min.}$ = 6.5mm.	

Effects of different substances on the induction period are summarised in table 5.6.

Table 5.6: Addition of propylene and air.

Temperature 307.0°C

Run Number 60 $[RI]_o$ = 60 mm. C_3H_6 = 3 mm.		Run Number 61 $[RI]_o$ = 51.7 mm. air = 3 mm.	
Time (min.)	Pressure (mm.)	Time (min.)	Pressure (mm.)
0	63.0	0	54.9
1	62.90	1	54.75
2	62.8	2	54.70
3	62.8	3	54.7
4	62.9	5	54.8
5	62.95	6	54.8
6	63.0	6.5	54.9
7	63.1	7	54.95
8	63.15	8	55.0
$\triangle P$ = 0.15mm. I_2 = 0.5 mm.		$\triangle P$ = 1 mm. I_2 = 1.5 mm.	

Table 5.6. cont'd

Addition of I_2:

Temperature 307.0°C

Run Number 63 $[RI]_o$ = 60.9 mm. (I_2) = 0 mm.		Run Number 65 $[RI]_o$ = 59.2 mm. (I_2) = 2 mm.	
Time (min.)	Pressure (mm.)	Time (min.)	Pressure (mm.)
0	60.9	0	61.2
1	60.8	2	61.15
2	60.65	3	61.2
2.5	60.6	4	61.2
3	60.65	5	61.2
4	60.75	6	61.25
5	60.85	8	61.4
6	60.95	10	61.75
7	61.0	13	62.0
8	61.05		
$\triangle P$ = 0.15 mm. I_2 = 0.45 mm.		$\triangle P$ = 0.80 mm. I_2 = (produced) = 1.95 mm. I_2 (expected) = 2.8 mm.	

Addition of HI:

Temperature 310.5°C

Run Number 66 $[RI]_o$ = 56.3; HI = 16.0mm.		Run Number 68 $[RI]_o$ = 58.0mm.; HI = 0	
Time (min.)	Pressure (mm.)	Time (min.)	Pressure (mm.)
0	72.3	0	58.0
0.5	72.35	1	58.0
1	72.5	2	58.0
2	72.6	3	58.0
3	72.8	4	58.05
4.5	73.0	5	58.3
5	73.1	6	58.5
6	73.25	7	58.65
7	73.4	9	58.95
8	73.65	10	59.1
9	73.85		
10	74.2		
$\triangle P$ = 1.9 mm.; I_2 = 8 mm.		$\triangle P$ = 1.1 mm.; I_2 = 1.0 mm.	

Since HI removed the induction period, the effect of some alkyl iodides which produce hydrogen iodide were examined and results are shown in table 5.7.

Table 5.7: Addition of i-propyl iodide and t-butyl iodide.

Temperature 310.0°C

Run Number 75 $[RI]_o$ = 69.0 mm. $i\text{-}C_3H_7I$ = 11.3 mm.		Run Number 77 $[RI]_o$ = 68.4 mm. $i\text{-}C_3H_7I$ = 5.0 mm.		Run Number 80 $[RI]_o$ = 53.8 mm. $t\text{-}C_4H_9I$ = 18 mm.	
Time (min.)	Pressure (mm.)	Time (min.)	Pressure (mm.)	Time (min.)	Pressure (mm.)
0	80.3	0	73.4	0	71.8
0.5	81.65	0.5	73.85	0.5	71.75
1	82.65	1.0	74.65	1	71.9
1.5	83.7	1.5	75.35	2	72.6
2.5	85.35	2.0	76.2		
3.5	87.0	3.0	77.35		
5	89.2	4	78.85		
		5	80.0		
$\triangle P$ = 8.9 mm. I_2 = 8 mm. HI = 4 mm.		$\triangle P$ = 6.6 mm. I_2 = 6.8 mm. HI = 3.4 mm.		$\triangle P$ = 1.8 mm. I_2) larger HI) quantities	

Table 5.7. cont'd. Addition of ethyl iodide and n-butyl iodide.

Temperature 313.0°C

Run Number 108 $[RI]_o$ = 40.8 mm. C_2H_3I = 0 mm.		Run Number 109 $[RI]_o$ = 33.7 mm. C_2H_3I = 16 mm.		Run Number 112 $[RI]_o$ = 45.1 mm. $n\text{-}C_4H_9I$ = 55 mm.	
Time (min.)	Pressure (mm.)	Time (min.)	Pressure (mm.)	Time (min.)	Pressure (mm.)
0	40.8	0	49.7	0	50.6
1	40.8	1	49.7	2	50.6
2	40.8	1.5	49.75	3	50.6
2.5	40.8	2.5	49.75	4	50.6
3	40.8	3	49.8	5	50.6
4	40.8	4	49.85	6	50.6
5	40.85			7	50.65
				10	50.7
				12	50.9
I_2 not analysed		I_2 not analysed		I_2 = 1 mm.	

In order to confirm that hydrogen iodide plays an important part in the rate determining step during the pyrolysis of n-propyl iodide (after the induction period), the co-pyrolysis of this compound with ethyl iodide was investigated. It is believed that ethyl iodide pyrolyses according to the following mechanism

$$C_2H_5I \longrightarrow C_2H_4 + HI \quad \ldots\ldots\ldots \text{ slow}$$

$$HI + C_2H_5I \longrightarrow C_2H_6 + I_2 \quad \ldots\ldots\ldots \text{ fast}$$

and the overall stoicheiometry is -

$$2C_2H_5I \longrightarrow C_2H_4 + C_2H_6 + I_2$$

Now, if a temperature is chosen where the pyrolysis of ethyl iodide is relatively slow and n-propyl iodide is co-pyrolysed with it, then any hydrogen iodide produced from the pyrolysis of n-propyl iodide might considerably increase the production of ethane at the expense of propane. The suggested reaction scheme being

$$C_2H_5I \longrightarrow C_2H_4 + HI$$

$$I + n\text{-}C_3H_7I \longrightarrow HI + C_3H_6I$$

$$HI + n\text{-}C_3H_7I \longrightarrow C_3H_8 + I_2$$

$$HI + C_2H_5I \longrightarrow C_2H_6 + I_2$$

The increase of C_2H_6 should be equal to the decrease in C_3H_8. Further, the C_3H_6 yield should be unaffected. These will not be strictly adhered to since the co-pyrolysis will be producing extra I_2 (from ethyl iodide) which will accelerate the

n-propyl iodide pyrolysis. Two relationships follow from the proposed reaction scheme:

$$\text{Total } I_2 = (C_2H_4)_{total} + (C_3H_6)_{total}$$

$$= (C_2H_6)_{total} + (C_3H_8)_{total}$$

The results of the co-pyrolyses are tabulated in table 5.8 where these equalities are observed to be moderately obeyed.

Table 5.8: Co-pyrolysis of n-C_3H_7I and C_2H_5I and analysis of products by gas chromatography.

Temperature 318.0°C

Vol. of reaction vessel 166 c.c.; factor 1 mm. = 4.47 micro moles
Pyrolysis time 20 min.; conversion of ethyl iodide $\lesssim$ 2%

Run Number	$[RI]_o$ (mm.)	C_2H_4 (micro) (moles)	C_2H_6 (micro) (moles)	C_3H_6 (micro) (moles)	C_3H_8 (micro) (moles)	I_2 (micro) (moles)
136	C_2H_5I = 58.4 n-C_3H_7I = 0	3.75	3.8			3.8
137	C_2H_5I = 0 n-C_3H_7I = 59.4			17.7	17.7	17.75
138	C_2H_5I = 57.8 n-C_3H_7I = 59.1	3.6	11.3	not analysed for	10.8	25.7
139	C_2H_5I = 58.4 n-C_3H_7I = 59.0	3.8	11.2	19.8	10.4	24.7
140	C_2H_5I = 0 n-C_3H_7I = 59.2			17.3	17.2	17.4

Equalities from table 5.8

Equalities		Run 138	Run 139
1	Excess C_2H_6	7.5	7.4
	Decrease in C_3H_8	6.9	6.8
2	$C_2H_4 + C_3H_6$	—	23.6
	$C_2H_6 + C_3H_8$	22.1	21.6
	I_2	25.7	24.7

5.5. Discussion of results and Mechanism.

The chromatographic analysis shows that i-propyl iodide is produced in trace amounts in the induction period and disappears as the reaction proceeds.

The results in table 4.5 show that the addition of small amounts of NO did not have any appreciable effect on the pyrolysis. This result suggests that alkyl radicals are not involved in the pyrolysis. (Holmes and Maccoll[25] observed that NO had no effect on the i-propyl iodide pyrolysis at higher temperatures where the mechanism is unimolecular,

$$i\text{-}C_3H_7I \longrightarrow C_3H_6 + HI$$

However, in the lower temperature range the reaction is autocatalytic and involves i-propyl radicals -

$$I + i\text{-}C_3H_7I \longrightarrow I_2 + i\text{-}C_3H_7$$

and NO showed an appreciable effect on the rate).

That a small amount of air was ineffective in removing the induction period, suggests that oxygen is not involved in the formation of the induction period. Also no significant contribution of either iodine or propylene to the induction period was observed.

The removal of the induction period by hydrogen iodide or any hydrogen iodide producing alkyl iodide indicates some importance of this compound with regard to the induction period.

The results of the co-pyrolysis of $n\text{-}C_3H_7I$ and C_2H_5I confirm that process B above i.e.,

$$I + n\text{-}C_3H_7I \longrightarrow C_3H_6 + I + HI$$

is the rate determining step.

On the basis of the above results the following mechanism is proposed for the pyrolysis of $n\text{-}C_3H_7I$

$$n\text{-}C_3H_7I \longrightarrow n\text{-}C_3H_7 + I \quad \ldots\ldots\ldots (1)$$

$$I + n\text{-}C_3H_7I \longrightarrow C_3H_6 + I + HI \quad \ldots\ldots\ldots (2)$$

$$C_3H_6 + HI \rightleftharpoons i\text{-}C_3H_7I \quad \ldots\ldots\ldots (3)\ (-3)$$

$$i\text{-}C_3H_7I + HI \longrightarrow C_3H_8 + I_2 \quad \ldots\ldots\ldots (4)$$

$$n\text{-}C_3H_7I + HI \longrightarrow C_3H_8 + I_2 \quad \ldots\ldots\ldots (5)$$

The homolysis of the $n\text{-}C_3H_7 \text{---} I$ bond in step (1) occurs only to a small extent just to produce enough I for the autocatalysis to become rate determining.

The induction period appears to be caused by an isomerisation of $n\text{-}C_3H_7I$ to $i\text{-}C_3H_7I$ by steps (2) and (3). While a small concentration of latter is being established there should be no pressure change in the system and an induction period would be observed. After a small concentration of $i\text{-}C_3H_7I$ has been established reaction (4) competes with reaction (3) and the $i\text{-}C_3H_7I$ concentration begins to fall. The back reaction of (3) also becomes the cause of the fall of concentration of $i\text{-}C_3H_7I$. At the end of the induction period, reaction (5) takes over the reaction (4) and is responsible for the production of iodine during the overall pyrolysis. The rate of reaction (5)

is faster than the rate of reaction (4) at the same temperature as shown by the comparison of the three-halves order rate constants[25,80]. The production of iodine during the induction period is due to the disappearance of $i\text{-}C_3H_7I$ by step (4) because (-3) is slower than (4)[25].

The above explanation for the induction period is only qualitative and the exact behavior is very difficult to explain quantitatively by any simple scheme and on the basis of the observed facts. A slight fall of pressure in some cases during the induction period is also hard to explain.

There is, however, no doubt that the overall pyrolysis after the induction period comprises steps (2) and (5).

NOTE

A brief investigation of the pyrolysis of n-butyl iodide:

After knowing the nature of the n-propyl iodide pyrolysis, an obvious objective is to examine the nature of the thermal decomposition of n-butyl iodide. A few exploratory runs were done. The results showed a similar behavior as found in the pyrolysis of n-propyl iodide.

Temperature 313.0°C

Surface; isobutene carbon

Run Number 146 $[RI]_o$ = 39.6		Run Number 147 $[RI]_o$ = 85.5	
Time (min.)	Pressure (mm.)	Time (min.)	Pressure (mm.)
0	39.65	0	85.5
1	39.6	1	85.1
2	39.6	2	84.9
3	39.6	3	84.85
4	39.6	4	84.8
5	39.6	5	84.8
7	39.6	6	84.85
8	39.60	7	85.0
10	39.75	8	85.2
15	40.1	10	85.55
		12	86.1
ΔP = 0.5 mm. I_2 = 0.9 mm.		ΔP = 0.6 mm. I_2 = 3 mm.	

Addition of hydrogen iodide.

Temperature 318.0°C

Surface; isobutene carbon
HI = 11.8 mm.
RI = 60.44 mm.
Run Number 150

Time (min.)	Pressure (mm.)	Pressure change (mm.)	I_2 (mm.)
0	72.24		
1	72.00		
2	72.30		
3	72.40		
4	72.54		
5	72.69	0.45	8mm.

Ratio of final to initial pressure.

Temperature 338.0°C

Run Number 151
Surface; isobutene carbon

Time (hrs.)	Pressure (mm.)
0	46.05
3	69.08
3.5	69.74
4.0	70.72
4.25	70.72
4.75	70.72
5.0	70.72

$$\therefore \frac{P_f}{P_o} = 1.54$$

Iodine-time and pressure-time relations.

Run No.	$[RI]_o$ (mm.)	Pressure change (mm.)	I_2 (mm.)	Time (min.)	Temp. °C	Surface
152	42.1	0.35	0.5	5	328	isobutene
155	37.5	2.0	2.8	10	"	"
156	55.8	1.0	2.2	6	"	"
160	100.7	3.9	5.5	5	"	"
165	60	11.0	11.1	22	"	"
167	56.5	14.2	14.1	17	338	"
170	55.3	10.6	10.8	10	"	"

Kinetic data for the pyrolysis of $n\text{-}C_4H_9I$ at 338.5°C

Run Number 175; Surface; isobutene carbon
$[RI]_o$ = 61 mm.; 1 mm. = 4.34 micromoles.

Time (min.)	$[RI]_o$ (mm.)	$\triangle$ P (mm.)	I_2 (micromoles)
0.5	61.0	0	0.8
0.75	61.0	0	1.25
1.0	61.05	.05	1.8
1.5	61.2	0.2	2.8
2	61.45	0.45	4.1
2.5	61.65	0.65	5.6
3.5	61.8	0.8	8.7

Rate = 4.96×10^{-5} mm.$^{-\frac{1}{2}}$ Sec.$^{-1}$

The kinetics show that a rate law of the type

$$-\frac{d(n\text{-}C_4H_9I)}{dt} = k(n\text{-}C_4H_9I)(I_2)^{\frac{1}{2}}$$

is obeyed, as was observed by Jones and Ogg[83].

SECTION - 6

PYROLYSIS OF ETHYL IODIDE

6.1. Introduction:

The first pyrolysis of ethyl iodide reported in the literature was that carried out at 210°C in a sealed tube for several hours by Aronstein[115]. He stated that the decomposition at this temperature should be represented by the equation

$$2C_2H_5I \longrightarrow C_2H_4I_2 + C_2H_6$$

Kahan[116], who agreed with the above, noticed the appearance of traces of iodine over 200°C. This, he believed, might be due to a secondary reaction, thought to be the decomposition of hydrogen iodide. He concluded that his results favoured preliminary decomposition into hydrogen iodide and ethylene.

Lessig[117] carried out some exploratory pyrolyses between 300°-400°C and reported that during the pyrolysis the ratio of final to initial pressures approximated to 1.5.

Ogg[79] while investigating the reaction between ethyl iodide and hydrogen iodide below 300°C, evaluated the rate of decomposition to be

$$k = 1.82 \times 10^{13} e^{-43000/RT}$$

This value of 43.0 K.Cals, he considered equal to the bond dissociation energy of the carbon-iodine bond in ethyl iodide. The presently accepted value of D(C-I) in C_2H_5I is 52 K.Cals[93]. From his results Ogg concluded that the initial split in the decomposition is

$$C_2H_5I \longrightarrow C_2H_5 + I$$

and this is followed by

$$C_2H_5 + I \longrightarrow C_2H_5I$$

$$C_2H_5 + I_2 \longrightarrow C_2H_5I + I$$

etc.

As a result, the overall reaction is mainly due to slow secondary reactions leading to ethylene, polymers etc.

Butler and Polanyi pyrolysed ethyl iodide using a fast flow technique and a small partial pressure of C_2H_5I in the N_2 gas, in the hope of eliminating secondary reactions and suggested a value of 52 K.Cals for the bond dissociation energy. Szwarc[118] accepts this value as accurate. Butler and Polanyi measured the rate of production of iodine and hydrogen iodide produced and found that the rate constants k_{I_2} and k_{HI} were nearly equal at 492°-495°C. However, in the presence of nitric oxide at 493°C, k_{I_2} was greater than k_{HI} by a factor of 2 to 3. Thus NO had the effect of increasing the rate of formation of iodine. They concluded from their experiments, the initial step of the reaction was a combination of

(a) $C_2H_5I \longrightarrow C_2H_5 + I$

and (b) $C_2H_5I \longrightarrow C_2H_4 + HI$

Butler and Polanyi, however, point out that there are a number of puzzling complications in their results. This is not surprising in view of the fact that NO reacts with HI rapidly.

Lee[95] has investigated the pyrolysis of ethyl iodide in the temperature range 325°-380°C in a static system. He interprets his results supporting the dual mechanism of Butler and Polanyi and claims that path (b) contributes up to 66% of the pyrolysis. His arguments are based on the propylene inhibition results and his Arrhenius parameters are as follows.

$$E_{\text{unimol. elim.}} = 48.3 \text{ K.Cal mole}^{-1}$$
$$\log_{10} A = 13.02 \text{ Sec.}^{-1}$$

$$E_{\text{rad. non chain}} = 51.2 \text{ K.Cal mole}^{-1}$$
$$\log_{10} A = 13.8 \text{ Sec.}^{-1}$$

$$E_{\text{overall}} = 49.3 \text{ K.Cal mole}^{-1}$$
$$\log_{10} A = 13.53 \text{ Sec.}^{-1}$$

Benson and Bose[87] pyrolysed ethyl iodide also in a static system in the temperature range 330°-392°C and reported that the chief rate determining step is

$$C_2H_5I \longrightarrow C_2H_4 + HI$$

and this is accompanied by a fast step

$$HI + C_2H_5I \longrightarrow C_2H_6 + I_2$$

They maintain, however, the view that the radical disproportionation of the type

$$C_2H_4 + HI \longrightarrow C_2H_5 + I$$

$$C_2H_5I + I \longrightarrow C_2H_5 + I_2 \quad \text{.....} \quad \text{fast}$$

$$C_2H_5 + I \longrightarrow C_2H_4 + HI \quad \text{....(rate determining)}$$

may account for as much as 20% of the pyrolysis at the highest temperature investigated.

The results in the present investigation are based chiefly on the effect of propylene. The unimolecular elimination of HI rather than the radical mechanism is favoured.

6.2. Experimental:

The essentials of the experimental techniques are given in section 3.

Iodine was analysed titrimetrically in the usual way and hydrocarbons were estimated by GLC using a silica gel (60-80 mesh). The column, of length one foot, was made of ¼" copper and was kept at $0^{\circ}C$.

6.2. Stoicheiometry and principles of calculations.

It has already been proved by previous workers that the equation

$$2C_2H_5I \longrightarrow C_2H_6 + C_2H_4 + I_2$$

adequately represents the stoicheiometry and also that the pressures calculated from the iodine titrations agree well with the pressure increases observed.

Using the pressure-time results, the first order rate constants were calculated from the equation

$$k = \frac{2.303}{t} \log \frac{P_o}{P_o - 2\triangle P}$$

$\triangle P$ being the increase in pressure in mms. Hg after time t. Log $(P_o - 2\triangle P)$ was plotted against time and good straight lines were obtained. The first order rate fell off above forty percent decomposition. The kinetic data were obtained on different surfaces of the reaction vessel.

The area under the peaks obtained in chromatographic analyses were determined by cutting out the peak and weighing it on a sensitive balance.

6.3. Results

A typical pressure-time curve and the corresponding log plot are shown in Figs.23 and 24 respectively. Pressure-time data at different temperatures and in different conditions of surface are given in table 6.1. The data for the Arrhenius plot are tabulated in table 6.2. while the plots are shown in Figs.25 and 26. The latter plot clearly indicates the agreement of the present values of Arrhenius parameters with those of previous workers.

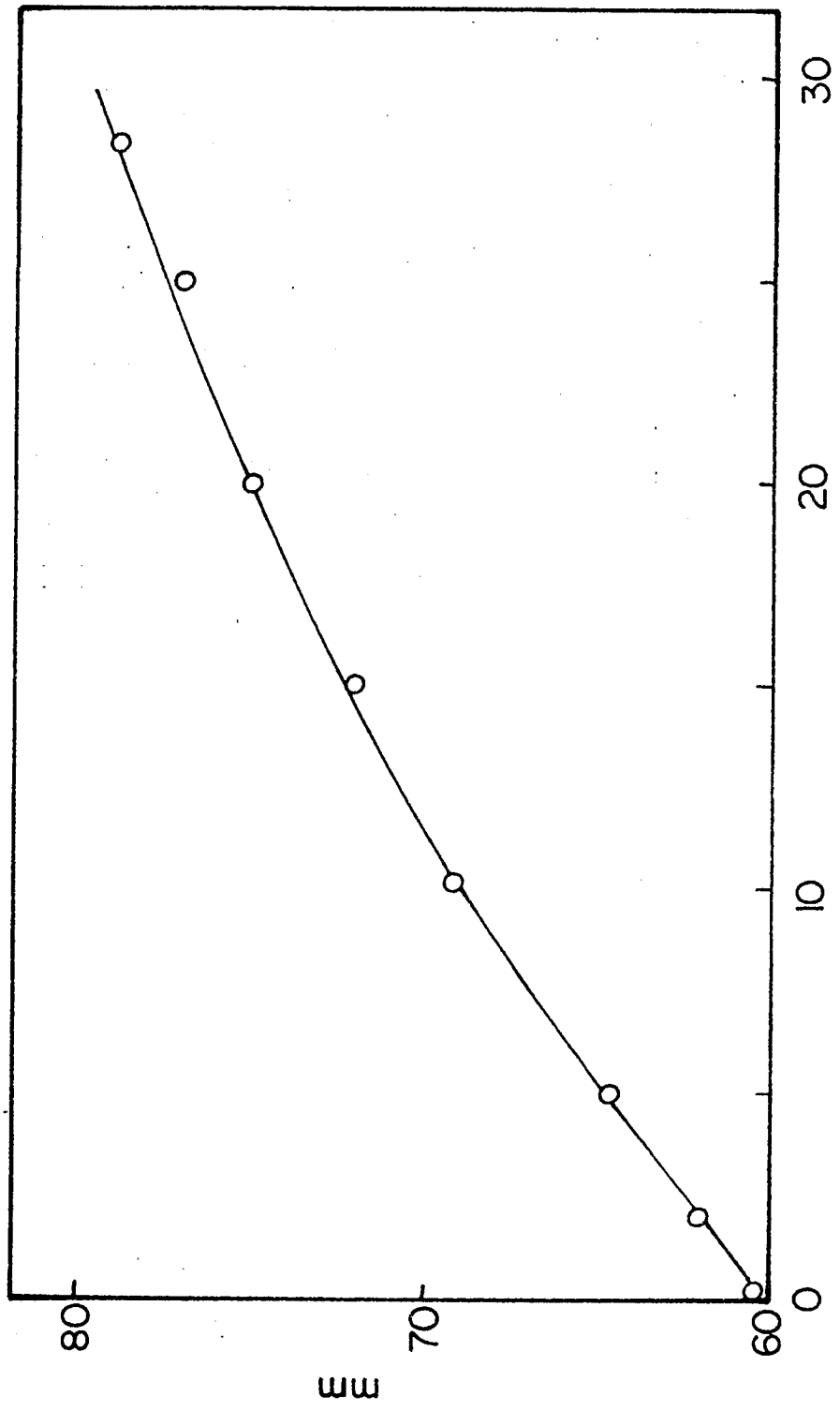

Figure 23: A typical pressure-time curve for the pyrolysis of C_2H_5I.
$[RI]_o$= 60.5 mm.; Temp. 364.0°C.

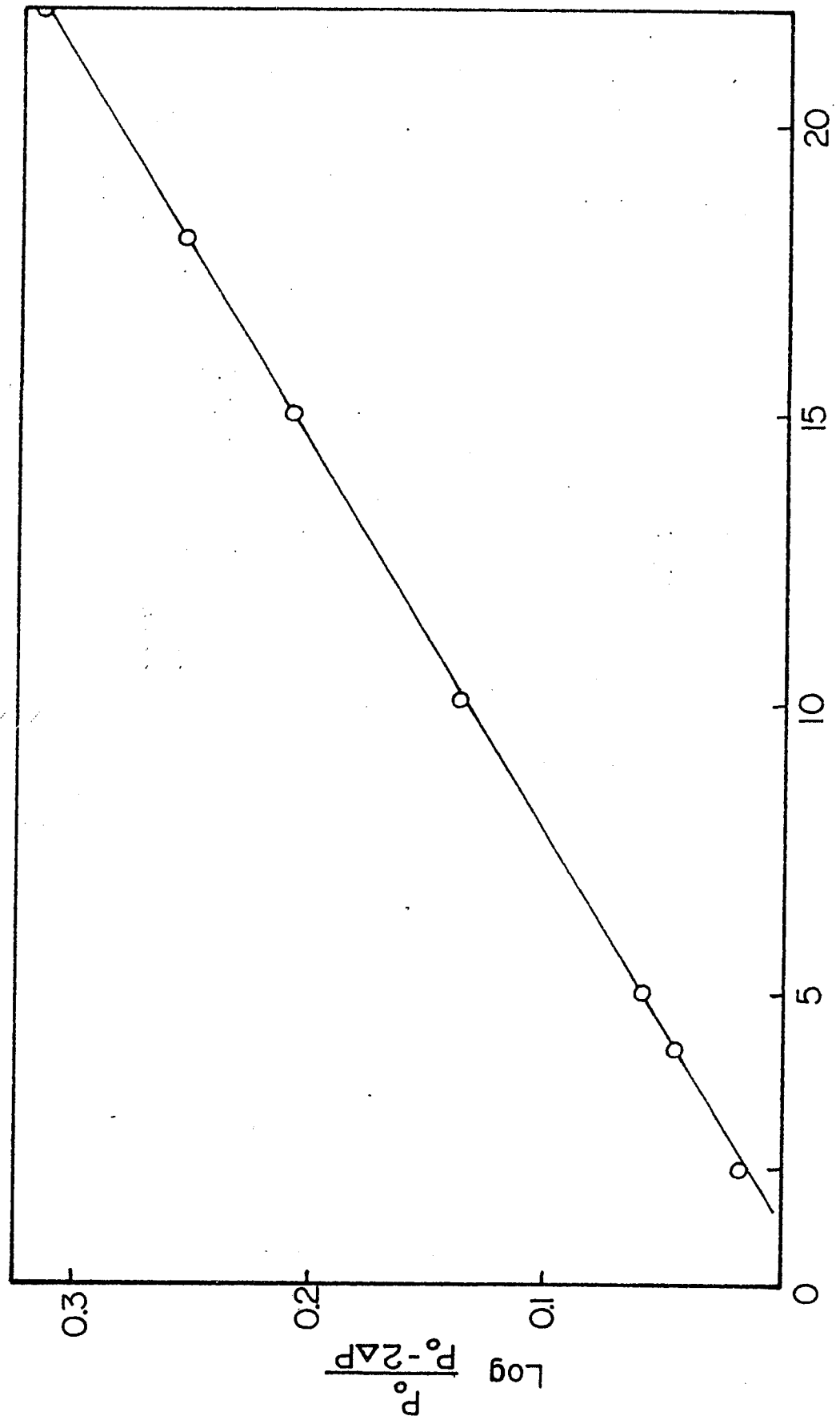

Figure 24: A typical first order log plot for the pyrolysis of C_2H_5I.
$[RI]_o$ = 75.0 mm.; Temp. 364.0°C.

Table 6.1: The kinetic data from the pyrolysis of ethyl iodide.

Temperature 350.0°C — Surface: Clean glass

Run Number 10, $[RI]_o$ = 70.0 mm.

Time (min.)	Pressure (mm.)
0	70.0
2	70.55
5	72.1
10	73.85
15	75.90

$k = 2.13 \times 10^{-4}$ Sec.$^{-1}$

Temperature 340.6°C — Surface: Isobutene carbon

Run Number 18, $[RI]_o$ = 110 mm.

Time (min.)	Pressure (mm.)
0	110.0
3	110.8
5	111.55
10	113.45
15	115.4
22	117.7

$k = 1.20 \times 10^{-4}$ Sec.$^{-1}$

Run Number 19, $[RI]_o$ = 141.5 mm.

Time (min.)	Pressure (mm.)
0	141.55
2	142.15
5	143.45
10	145.8
15	147.7
22	151.4

$k = 1.12 \times 10^{-4}$ Sec.$^{-1}$

Mean: 1.16×10^{-4} Sec.$^{-1}$

Temperature 350.4°C — Surface: Isobutene carbon

Run Number 28, $[RI]_o$ = 72.3 mm.

Time (min.)	Pressure (mm.)
0	72.3
2	72.85
5	74.30
10	76.15
15	78.15
20	80.8

$k = 2.2 \times 10^{-4}$ Sec.$^{-1}$

Run Number 29, $[RI]_o$ = 95.4 mm.

Time (min.)	Pressure (mm.)
0	95.4
2	96.15
5	98.1
10	100.95
15	103.7
20	106.7

$k = 2.3 \times 10^{-4}$ Sec.$^{-1}$

Mean: 2.25×10^{-4} Sec.$^{-1}$

Table 6.1. Cont'd

Temperature 364.0°C

Surface: Isobutene carbon

Run Number $[RI]_o$ = 60.5 mm.		Run Number $[RI]_o$ = 75.05 mm.		Run Number $[RI]_o$ = 108.0 mm.	
Time (min.)	Pressure (mm.)	Time (min.)	Pressure (mm.)	Time (min.)	Pressure (mm.)
0	60.5	0	75.05	0	108.0
2	62.0	1	75.8	1	109.5
5	64.3	2	76.55	3	112.7
10	68.55	3	77.95	5	116.0
15	71.65	5	79.25	10	122.5
20	75.05	7	82.4	12	125.4
25	77.20	10	85.75	16	130.2
30	78.9	12	87.3	18	132.5
		15	89.6	20	134.4
		20	93.0	25	138.2
		24	95.35		
$k = 5.11 \times 10^{-4}$ Sec.$^{-1}$		$k = 5.68 \times 10^{-4}$ Sec.$^{-1}$		$k = 5.48 \times 10^{-4}$ Sec.$^{-1}$	

Mean: 5.62×10^{-4} Sec.$^{-1}$

Table 6.1. Cont'd

Surface: Isobutene carbon

Temperature 369.0°C		Temperature 378.0°C			
Run Number 40 $[RI]_o$ = 58.85 mm.		Run Number 43 $[RI]_o$ = 65.4 mm.		Run Number 44 $[RI]_o$ 44.6 mm.	
Time (min.)	Pressure (mm.)	Time (min.)	Pressure (mm.)	Time (min.)	Pressure (mm.)
0	58.85	0	65.4	0	44.6
1	60.0	2	70.2	2	47.55
2	61.15	3	72.7	3.5	49.7
3	62.30	5	76.9	5	51.9
4	63.45	7	80.0	7	54.25
5	64.6	10	84.2	10	56.15
$k = 7.21 \times 10^{-4}$ Sec.$^{-1}$		$k = 14.20 \times 10^{-4}$ Sec.$^{-1}$		$k = 14.1 \times 10^{-4}$ Sec.$^{-1}$	

Mean: $1.4.15 \times 10^{-4}$ Sec.$^{-1}$

Temperature 347.2°C

Surface: ethyl bromide carbon

Run Number 48 $[RI]_o$ = 58.8 mm.		Run Number 49 $[RI]_o$ = 58.9 mm		Run Number 50 $[RI]_o$ = 60.0 mm.	
Time (min.)	Pressure (mm.)	Time (min.)	Pressure (mm.)	Time (min.)	Pressure (mm.)
0	58.8	0	58.9	0	60.0
5	59.85	5	59.75	5	61.15
10	60.95	10	61.5	11	62.8
15	62.65	15	62.9	15	63.85
20	64.25	20	64.25	20	65.2
25	65.9	25	65.75	25	66.55
$k = 1.8 \times 10^{-4}$ Sec.$^{-1}$		$k = 1.70 \times 10^{-4}$ Sec.$^{-1}$		$k = 1.82 \times 10^{-4}$ Sec.$^{-1}$	

Mean: 1.76×10^{-4} Sec.$^{-1}$

Table 6.1. Cont'd

Surface: ethyl bromide carbon

Temperature 361.0°C		Temperature 378.1°C			
Run Number 52 $[RI]_o$ = 71.0 mm.		Run Number 55 $[RI]_o$ = 60.8 mm.		Run Number 57 $[RI]_o$ = 62.0 mm.	
Time (min.)	Pressure (mm.)	Time (min.)	Pressure (mm.)	Time (min.)	Pressure (mm.)
0	72.0	0	60.8	0	62.0
2.5	74.3	2.5	65.4	5	70.95
5	76.3	5	69.95	10	77.50
6.5	77.5	7.5	73.8	12.5	79.7
7.5	78.3	10	76.9	15	81.75
10	80.4	12.5	79.1		
12.5	82.5	15	81.0		
15	84.55				
$k = 4.45 \times 10^{-4}$ Sec.$^{-1}$		$k = 11.98 \times 10^{-4}$ Sec.$^{-1}$		$k = 11.46 \times 10^{-4}$ Sec.$^{-1}$	

Mean: 11.72×10^{-4} Sec.$^{-1}$

Table 6.2: Data for Arrhenius plot

Temp. °C	$1/T \times 10^3$	$k \times 10^4$	log k + 4
Surface: isobutene carbon			
340.6	1.629	1.155	0.0625
350.4	1.604	2.25	0.3522
364.0	1.571	5.62	0.7497
369.2	1.557	7.21	0.8579
378.0	1.536	14.15	1.1510
Surface: clean glass			
350.2	1.604	2.13	0.3284
Surface: ethyl bromide carbon			
347.2	1.612	1.74	0.2455
361.0	1.577	4.45	0.6484
378.2	1.536	11.72	1.0690

The following table summarises the Arrhenius parameters together with those of Benson and Lee.

Table 6.3: Comparison of the Arrhenius parameter; ethyl iodide pyrolysis.

	E (K.Cals mole^{-1})	$\log_{10}$A (Sec.$^{-1}$)	Reaction considered
Benson and Bose	50.0	13.66	overall decomposition
	"	13.36	unimolecular elimination
Lee	49.3	13.53	overall decomposition
Present investigation: (average)	51.0	14.24	overall decomposition
ethyl bromide carbon	49.6	13.72	overall decomposition
isobutene carbon	52.1	14.54	overall decomposition

The average values for the Arrhenius parameters have been calculated by the "least squares" method using all the results. At lower temperatures there is very good agreement between results on different surfaces (Fig.25). The relatively higher rate constant at 378°C on the isobutene carbon surface causes the average values of the Arrhenius parameters to be somewhat higher than those of previous workers. Except for this one point on the Arrhenius plot, the results are in good agreement with those of other workers.

Similar rate constants on different surfaces (Fig.25) confirm the homogeneous nature of the reaction. The reaction

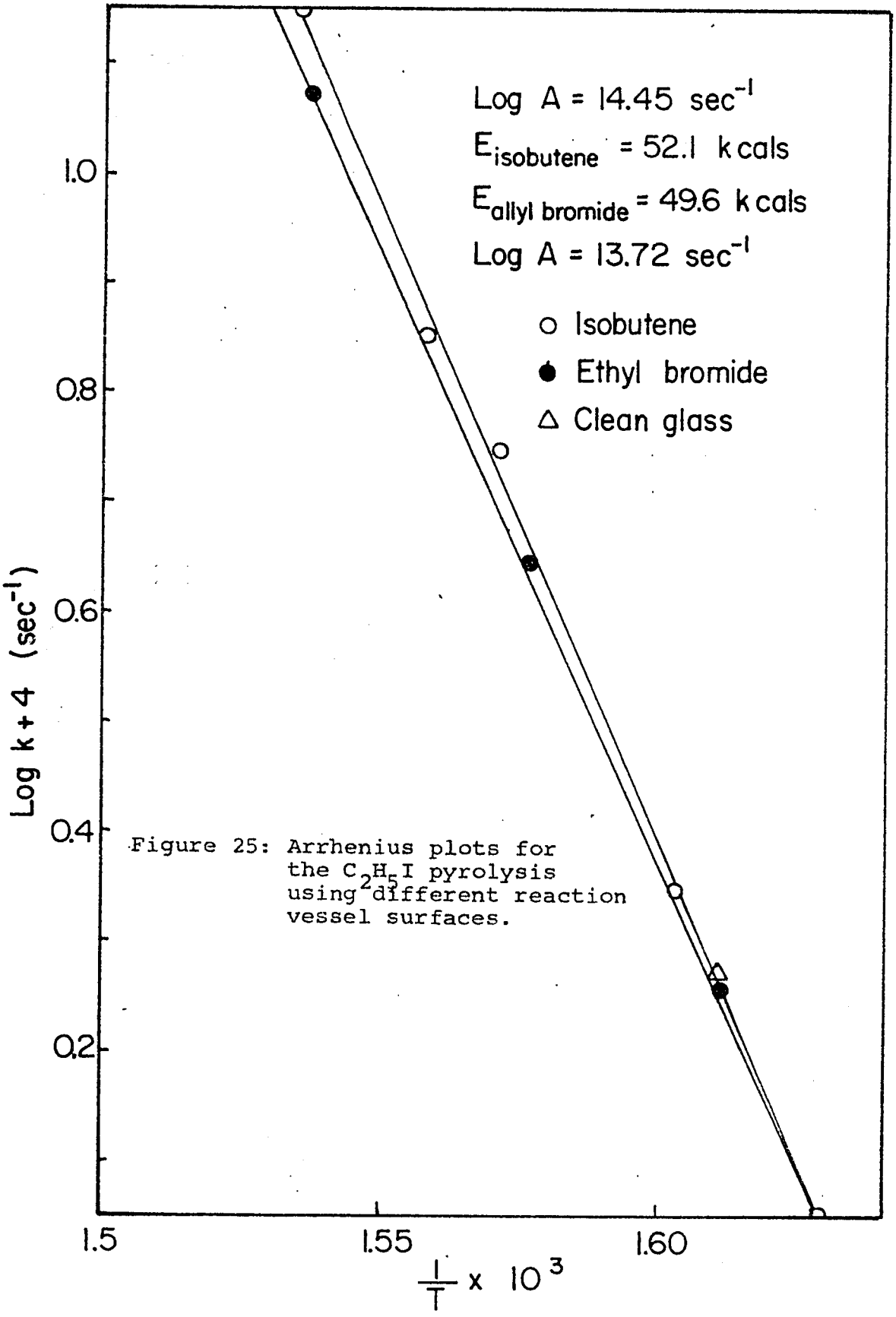

Figure 25: Arrhenius plots for the C_2H_5I pyrolysis using different reaction vessel surfaces.

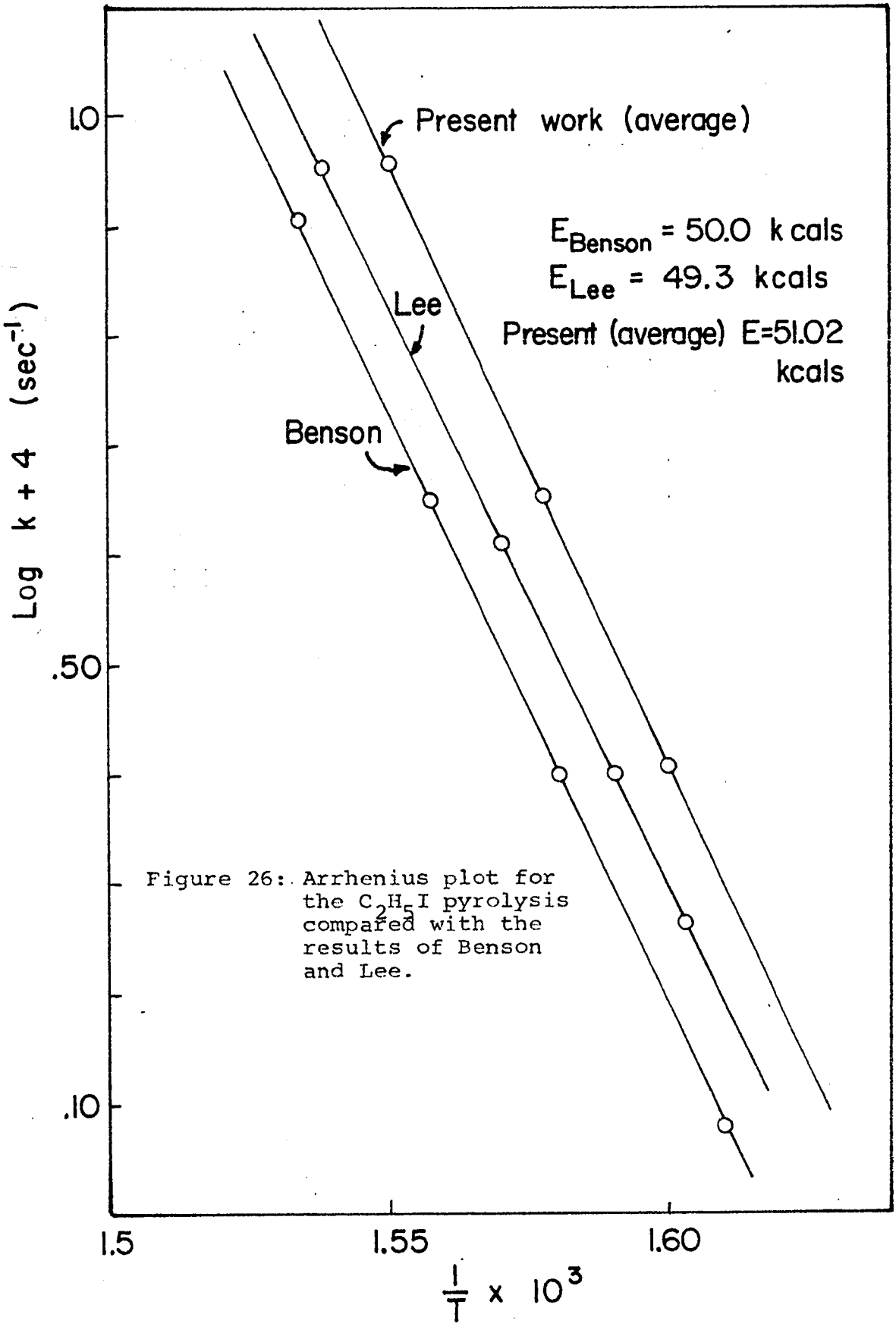

Figure 26: Arrhenius plot for the C_2H_5I pyrolysis compared with the results of Benson and Lee.

was also found to be homogeneous by Lee[95] and Benson[87]. They studied the homogeneity by changing the surface to volume ratio.

Chromatographic results:

The effect of propylene on the kinetics was investigated entirely by gas chromatographic analysis. The gaseous product was separated from iodine and excess C_2H_5I at $-78^{\circ}C$ and was passed into the column for analysis. A typical chromatogram for the separation is shown in figure 27. Propylene appeared on the chromatogram as a very broad peak with a long tail and its retention time was 20 minutes. The retention times for C_2H_4 and C_2H_6 were 3.5 and 5.5 minutes respectively. Results for different concentrations of propylene with approximately constant concentrations of C_2H_5I are summarised in table 6.4. Table 6.5 shows the results when a constant concentration of propylene is added to different concentrations of C_2H_5I.

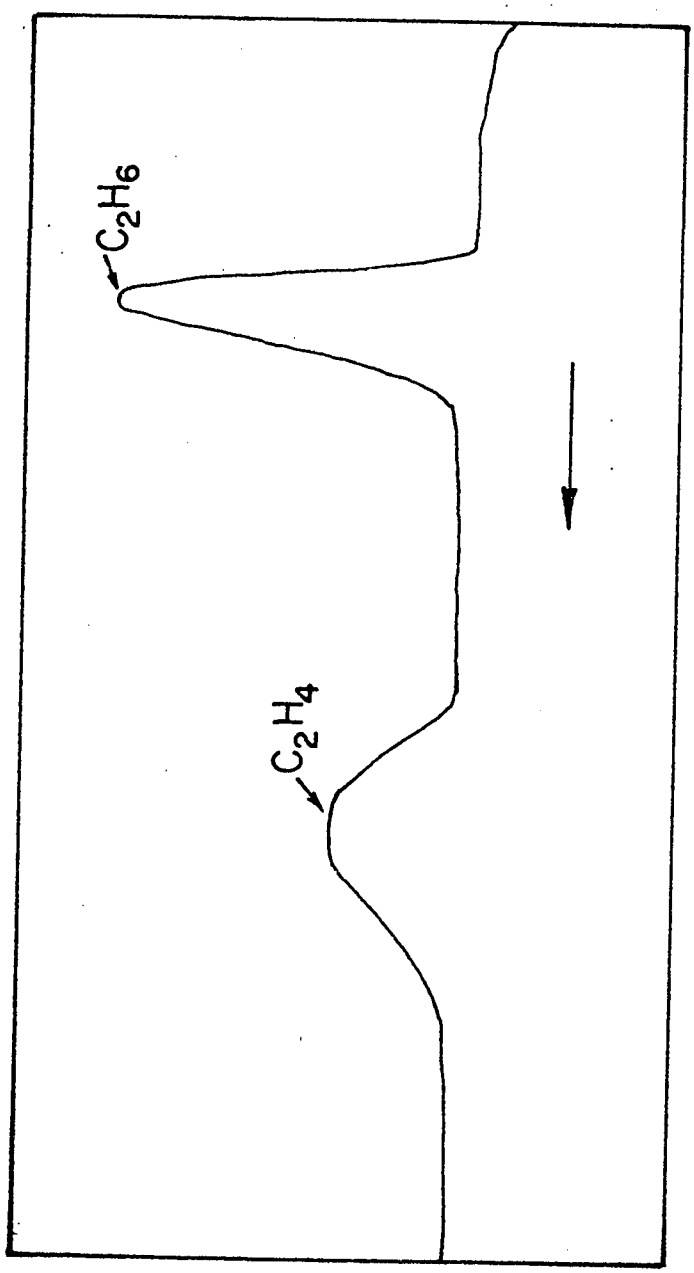

Figure 27: Ethyl iodide pyrolysis; a typical chromatogram showing the separation of C_2H_6 and C_2H_4.

Table 6.4: Effect of propylene on the pyrolysis of ethyl iodide at 347.8°C; 1 mm = 4.28 micro moles.

Run Number	Time (min.)	C_2H_5I (micro) (moles)	C_3H_6 (micro) (moles)	I_2 (micro) (moles)	C_2H_4 (micro) (moles)	C_2H_6 (micro) (moles)
86	5	247	0	4.9	5.0	5.1
116	5	221	237	8.7	6.5	9.5
108	5	237	240	9.8	5.5	8.5
120	5	252	481	14.7	2.8	9.4
94	5	209	603	13.0	——	12.5
99	7.5	247	0	8.1	7.3	7.5
100	7.5	244	0	7.7	6.8	7.3
107	7.5	252	232	14.2	8.1	12.5
118	7.5	242	241	14.3	5.9	9.7
128	7.5	216	534	18.0	2.7	11.4
73	10	239	0	11.0	12.2	12.0
77	10	242	0	12.4	11.6	10.6
82	10	231	0	10.5	10.9	11.4
92	10	247	0	12.0	11.4	10.8
112	10	243	0	11.4	10.9	10.0
80	10	216	68	12.8	10.3	12.0
74	10	223	115	14.8	13.0	14.5
81	10	201	162	15.2	10.9	15.0
71	10	231	239	19.0	12.3	20.8
93	10	260	241	20.8	11.6	18.5
117	10	223	241	19.0	10.0	18.5
83	10	250	249	19.0	10.9	21.9
75	10	198	336	18.1	9.6	18.3

Table 6.4. Cont'd

Run Number	Time (min.)	C_2H_5I (micro) (moles)	C_3H_6 (micro) (moles)	I_2 (micro) (moles)	C_2H_4 (micro) (moles)	C_2H_6 (micro) (moles)
84	10	214	349	20.2	10.4	22.1
89	10	250	402	24.7	11.1	22.7
72	10	219	450	18.3	10.5	19.1
124	10	192	488	24.4	8.1	14.8
90	10	274	504	29.0	11.8	25.3
91	10	232	559	30.8	6.1	27.1
110	12.5	245	0	14.8	14.0	14.5
111	12.5	212	239	22.0	12.2	20.1
115	12.5	264	242	24.0	13.6	22.4

Table 6.5: Effect of a constant concentration of propylene on C_2H_5I pyrolysis at 347.5°C. 1 mm. = 4.27 micro moles.

Run Number	Time (min.)	C_3H_6 (micro) (moles)	C_2H_5I (micro) (moles)	C_2H_4 (micro) (moles)	C_2H_6 (micro) (moles)	I_2 (micro) (moles)
166	10	100	55	2.0	3.8	3.55
161	10	100	71	4.2	6.35	4.85
158	10	100	86.5	5.0	10.00	6.05
170	10	100	110	5.0	10.6	7.56
168	10	100	105	6.55	12.7	8.75
157	10	100	112	6.45	10.0	7.8
163	10	100	114	5.8	12.2	8.0
159	10	100	245	13.4	19.8	16.8
162	10	100	312	16.65	25.95	23.9
167	10	100	418	20.2	30.0	34.3

6.4. Mechanism and Discussion.

Lee[95] proposed a mixed mechanism for the pyrolysis comprising a unimolecular elimination (a) and radical non chain process (b)

$$\text{(a)}\quad C_2H_5I \longrightarrow C_2H_4 + HI \quad \ldots\ldots\ldots \text{slow}$$

$$C_2H_5I + HI \longrightarrow C_2H_6 + I_2 \quad \ldots\ldots\ldots \text{fast}$$

$$\text{(b)}\quad C_2H_5I \longrightarrow C_2H_5 + I \quad \ldots\ldots\ldots \text{slow}$$

$$C_2H_5 + C_2H_5I \longrightarrow C_2H_6 + C_2H_4I$$

$$C_2H_4I \longrightarrow C_2H_4 + I$$

$$I + I + M \rightleftharpoons I_2 + M$$

His arguments were based upon the effect of propylene. In his experiments he found that the added propylene increased the ratio C_2H_6/C_2H_4, decreased the ratio P_f/P_o and increased the rate of production of iodine. Lee, however, did not analyse the absolute quantities of the hydrocarbons. He concluded that propylene should not interfere with the unimolecular elimination mechanism but would react with the ethyl radicals formed in the radical non chain reaction as follows

$$C_2H_5I \longrightarrow C_2H_5 + I$$

$$C_2H_5 + C_3H_6 \longrightarrow C_2H_6 + \text{Allyl}$$

$$\text{Allyl} \longrightarrow \tfrac{1}{2}\ (\text{Di-allyl})$$

$$I + I \overset{M}{\rightleftharpoons} I_2$$

This scheme produces neither ethylene nor a change in pressure and therefore these must result from unimolecular

elimination process. On the basis of these results he calculated

$$E_a = 48.3 \text{ K.Cals and } E_b = 51.2 \text{ K.Cals.}$$

With process (b) contributing 66% of the overall decomposition $E_{observed} = 49.3$ K.Cals.

The present chromatographic results indicate that the production of ethylene remains constant up to a C_2H_6/C_2H_5I ratio of about 2 (Fig.28). The ratio C_2H_6/C_2H_4 increased (as was also found by Lee) but it is due to an increase in C_2H_6 production, rather than a decrease in C_2H_4. The constancy of C_2H_4 production in the experiments shows that a radical process is substantially absent and it must be concluded that the process (a) is the only important decomposition reaction in the pyrolysis of ethyl iodide.

Figure 30 shows a plot of the rate of ethane production against the concentration of added propylene. The values for the rate of ethane production have been found from the slopes of the plots (Fig.29) of ethane concentration against time for a constant concentration of ethyl iodide and a varying concentration of propylene. For the latter plot an average value of 230 micro moles C_2H_5I has been taken and the values of ethane concentration have been corrected for this average value of the iodide.

The straight line dependance of the rate of ethane production (Fig.30) on the propylene suggests that the extra ethane production is first order in propylene. Thus it appears that the extra ethane is produced by a simple bimolecular reaction

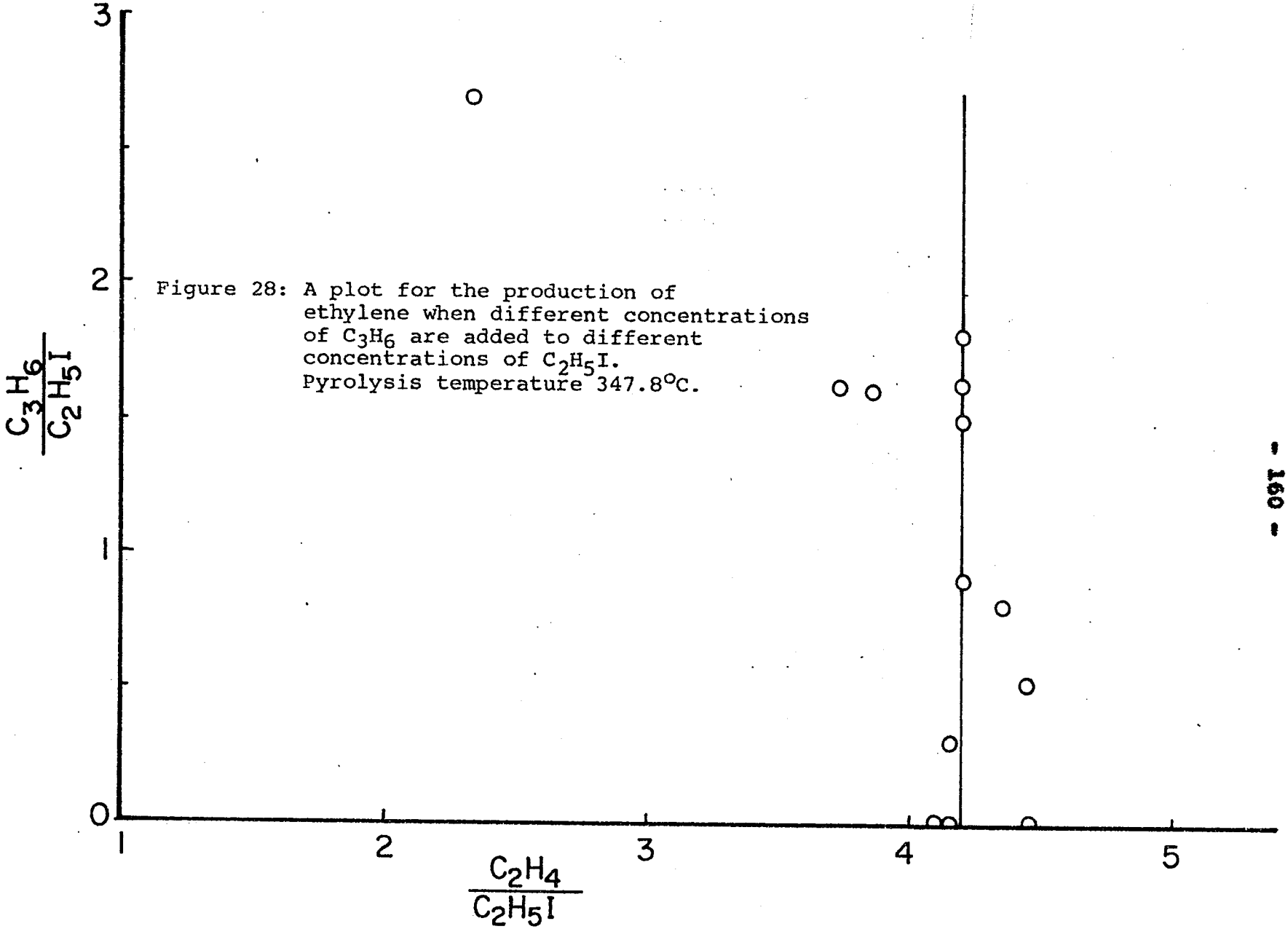

Figure 28: A plot for the production of ethylene when different concentrations of C_3H_6 are added to different concentrations of C_2H_5I. Pyrolysis temperature 347.8°C.

Figure 29: Plot of ethane concentration against time for a varying concentration of C_3H_6 and a constant concentration of C_2H_5I. Pyrolysis of C_2H_5I.

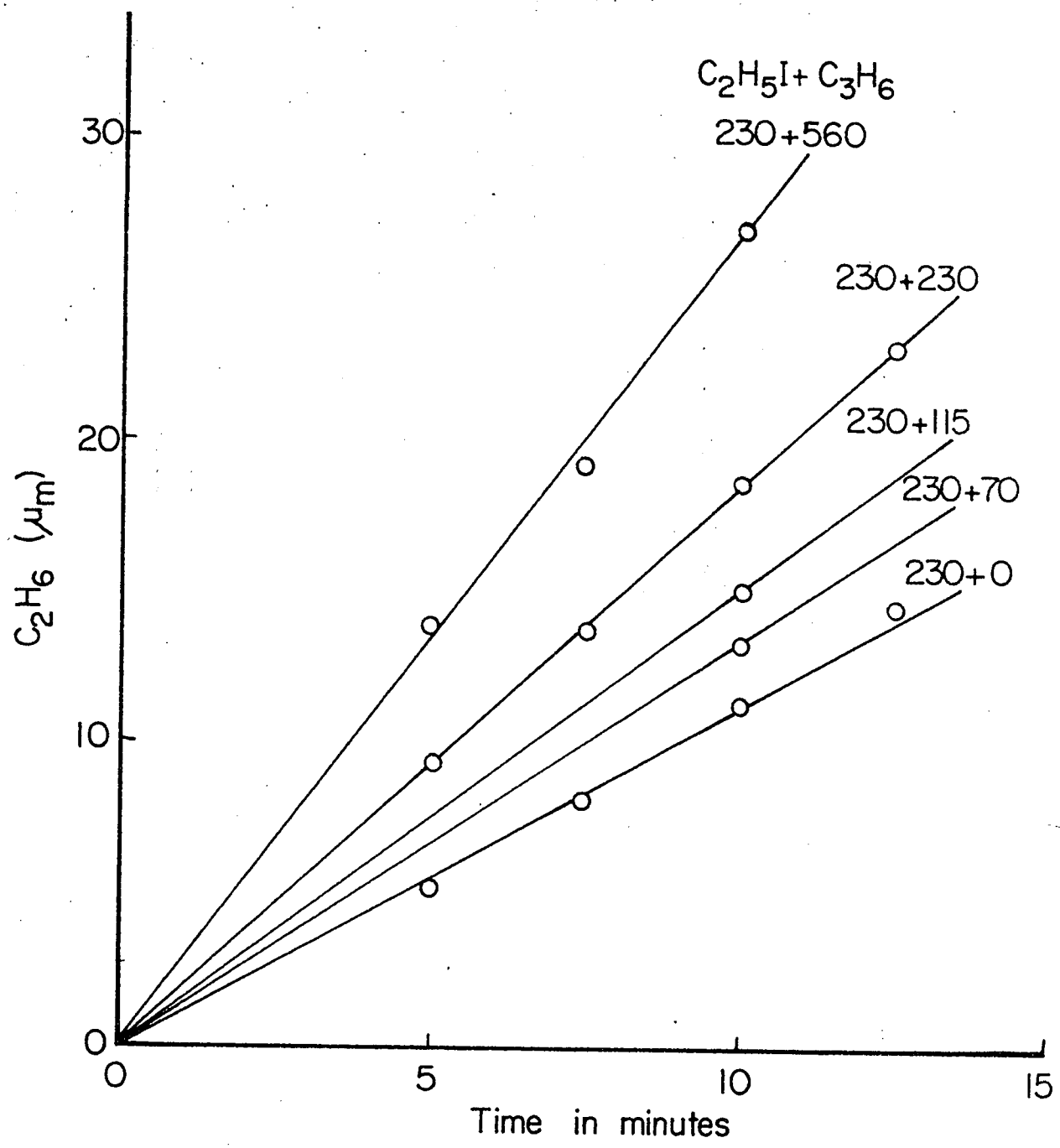

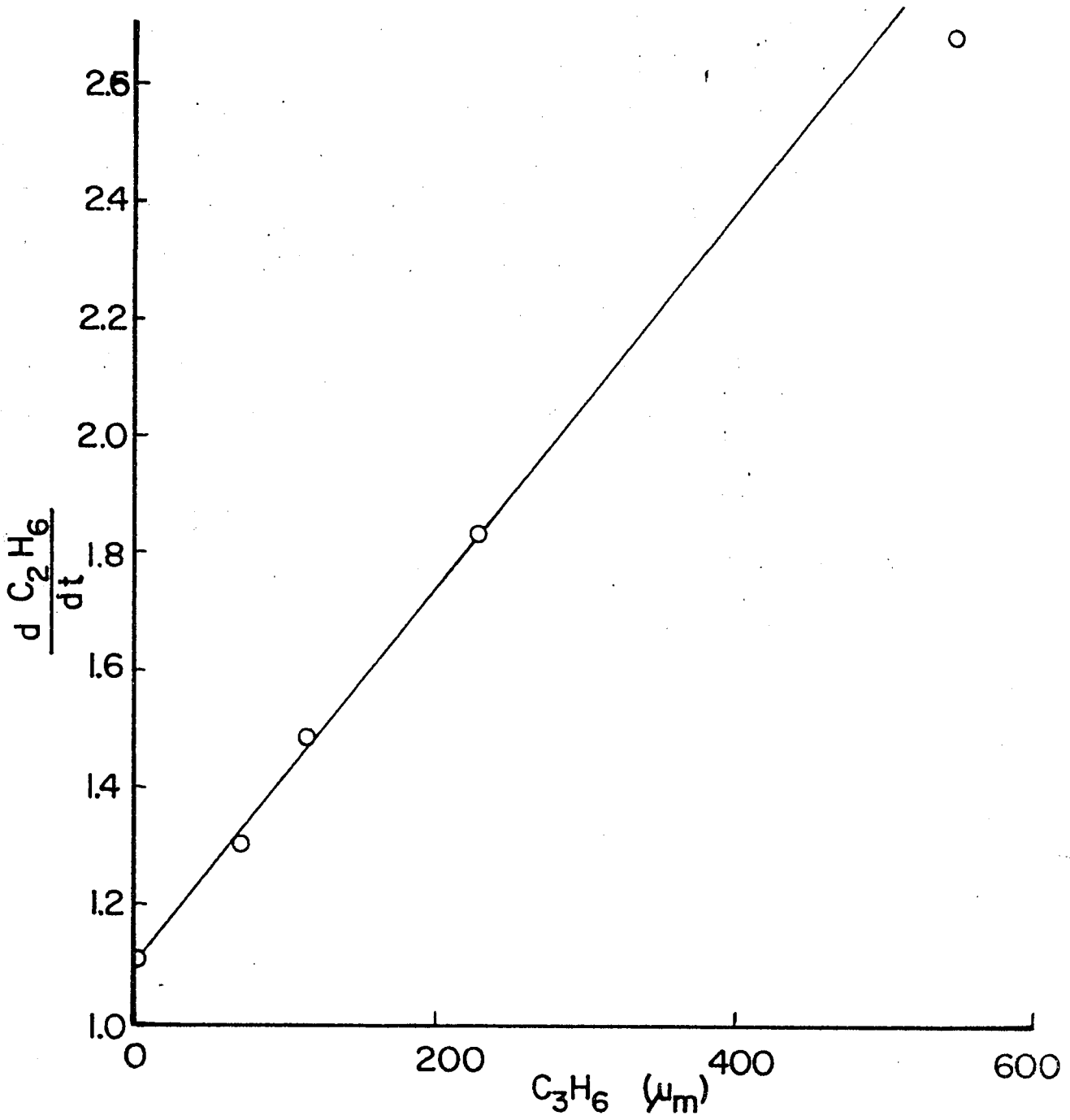

Figure 30: Pyrolysis of C_2H_5I; plot of the rate of ethane production against propylene **concentration.**

$$C_2H_5I + C_3H_6 \longrightarrow C_2H_6 + C_3H_5I$$

C_3H_5I then decomposes[119] to produce extra iodine in the system.

This type of bimolecular reaction is not unreasonable. Klemn and Bernstein[120] studied the kinetics of the reaction of methyl iodide with toluene at about 350°C and found that methane was the sole end product of the methyl iodide carbon, so that CH_4 production could be used as a measure of the extent of the reaction. Iodine production came from the benzyl iodide formed.

Thus the reaction of ethyl iodide with propylene could be interpreted by the following reaction scheme

$$C_2H_5I \longrightarrow HI + C_2H_4 \quad \ldots\ldots\ldots \quad (1)$$

$$HI + C_2H_5I \longrightarrow C_2H_6 + I_2 \quad \ldots\ldots\ldots \quad (2)$$

$$C_2H_5I + C_3H_6 \longrightarrow C_3H_5I + C_2H_6 \quad \ldots\ldots\ldots \quad (3)$$

$$2C_3H_5I \longrightarrow I_2 + (C_3H_5)_2 \quad \ldots\ldots\ldots \quad (4)$$

The stationary state treatment of the steps (1), (2) and (3) gives

$$d\frac{C_2H_6}{dt} = k_1(C_2H_5I) + k_3(C_2H_5I)(C_3H_6)$$

$$\text{or } \left(\frac{1}{C_3H_6}\right)\left(\frac{dC_2H_6}{dt}\right) = \frac{k_1}{(C_3H_6)}(C_2H_5I) + k_3(C_2H_5I)$$

$$= (C_2H_5I)\left\{k_3 + \frac{k_1}{(C_3H_6)}\right\}$$

Thus a plot of $\frac{dC_2H_6}{dt} \times \left(\frac{1}{C_3H_6}\right)_t$ against $(C_2H_5I)_t$ should give

a straight line passing through the origin. This plot is shown in figure 31 where the predicted behavior is seen to be obeyed. The ethane production is assumed above to be linear with time and for the rate of ethane production, C_2H_6/time has been taken. However, this assumption is true only for the initial stages of the reaction.

From expressions (1), (2) and (3)

$$- d \frac{(C_2H_5I)}{dt} = 2k_1(C_2H_5I) + k_3(C_2H_5I)(C_3H_6)$$

and $$- d \frac{(C_3H_6)}{dt} = k_3(C_2H_5I)(C_3H_6)$$

Let $x = (C_2H_5I)$, $y = (C_3H_6)$

then $$- \frac{dx}{dt} = 2k_1x + k_3xy \qquad \text{.....} \quad \text{(i)}$$

and $$- \frac{dy}{dt} = k_3xy \qquad \text{.....} \quad \text{(ii)}$$

or dividing (i) by (ii)

$$\frac{dx}{dy} = \frac{2k_1}{k_3} y^{-1} + 1$$

or $$\int_{x}^{x_o} dx = \frac{2k_1}{k_3} \int_{y}^{y_o} \frac{dy}{y} + \int_{y}^{y_o} dy$$

or $$x_o - x = \frac{2k_1}{k_3} \ln \frac{y_o}{y} + y_o - y \qquad \text{.....} \quad \text{(iii)}$$

$$x_o - x = (C_2H_6) + (C_2H_4)$$

$$Y_o - y = (C_3H_6)_o - (C_3H_6) = (C_2H_6) - (C_2H_4)$$

. . (iii) becomes

$$(C_2H_6)+(C_2H_4) = \frac{2k_1}{k_3} \ln \frac{(C_3H_6)_o}{(C_3H_6)_o - (C_2H_6)+(C_2H_4)} + (C_2H_6) - (C_2H_4)$$

$$(C_2H_4) = \frac{2k_1}{k_3} \ln \frac{(C_3H_6)_o}{(C_3H_6)_o - (C_2H_6) + (C_2H_4)}$$

i.e., the plot (C_2H_4) against $\ln \frac{(C_3H_6)_o}{(C_3H_6)_o - (C_2H_6)+(C_2H_4)}$ should give a straight line, the slope of which will be $\frac{k_1}{k_3}$.

Figure 32 shows such a plot where the behavior is seen to be well obeyed. The calculated value of k_3 is 9.2×10^{-7} mm.$^{-1}$ Sec.$^{-1}$

With regard to the transition state in the reaction of C_3H_6 and C_2H_5I, addition to the double bond does not seem probable since this would yield s-pentyl iodide which, as a secondary iodide, would be expected to pyrolyse to produce pentene-1, pentene-2 and pentane rather than ethane. The reaction of HI and C_3H_6

$$2HI + C_3H_6 \longrightarrow C_3H_8 + I_2$$

can be understood in terms of normal addition to C=C, followed by rapid HI + i-C_3H_7I reaction to yield the products. An analogous scheme for the reaction between C_3H_6 and C_2H_5I is impossible and some new type of transition state seems to be formed.

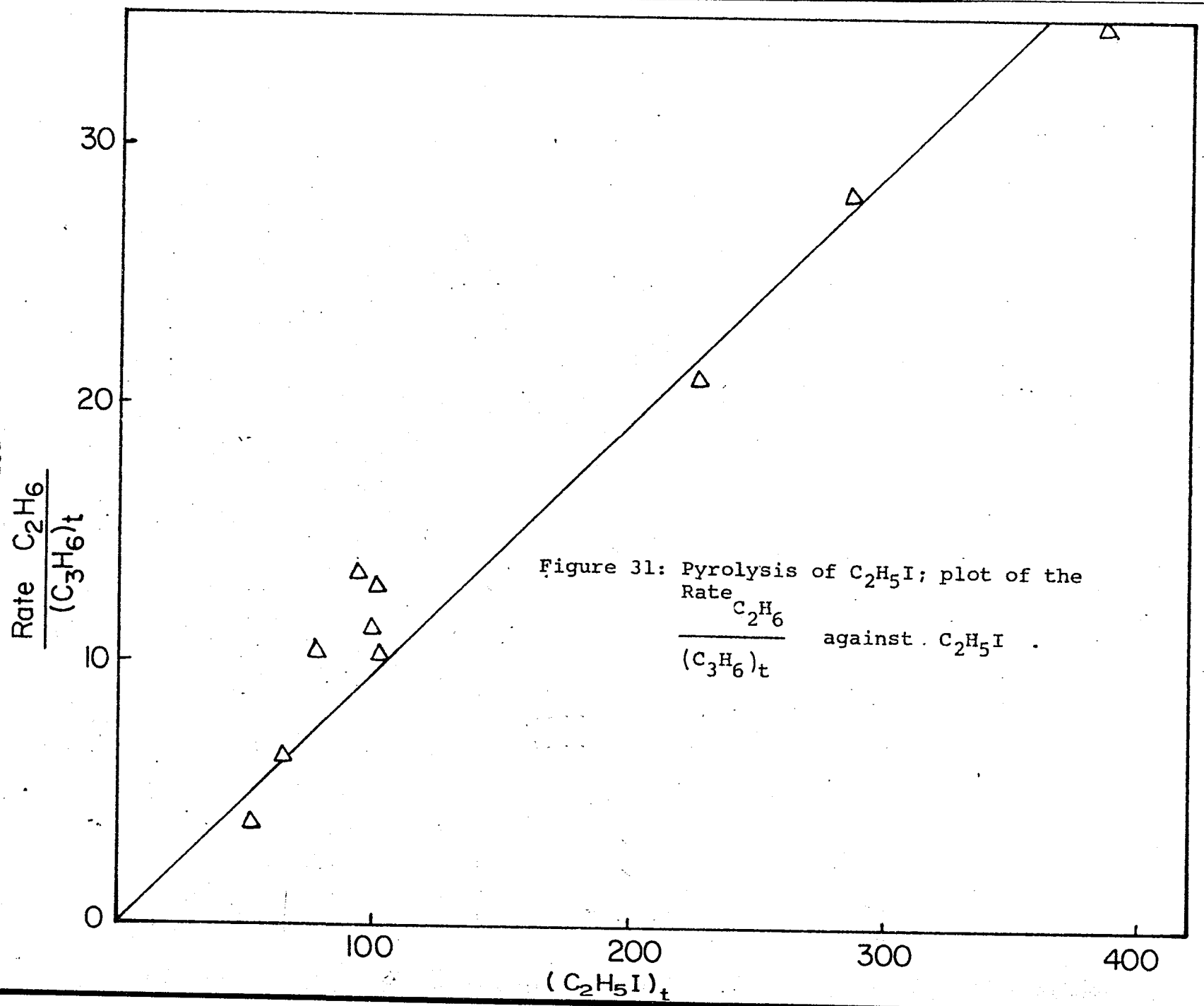

Figure 31: Pyrolysis of C_2H_5I; plot of the $\frac{\text{Rate}_{C_2H_6}}{(C_3H_6)_t}$ against C_2H_5I .

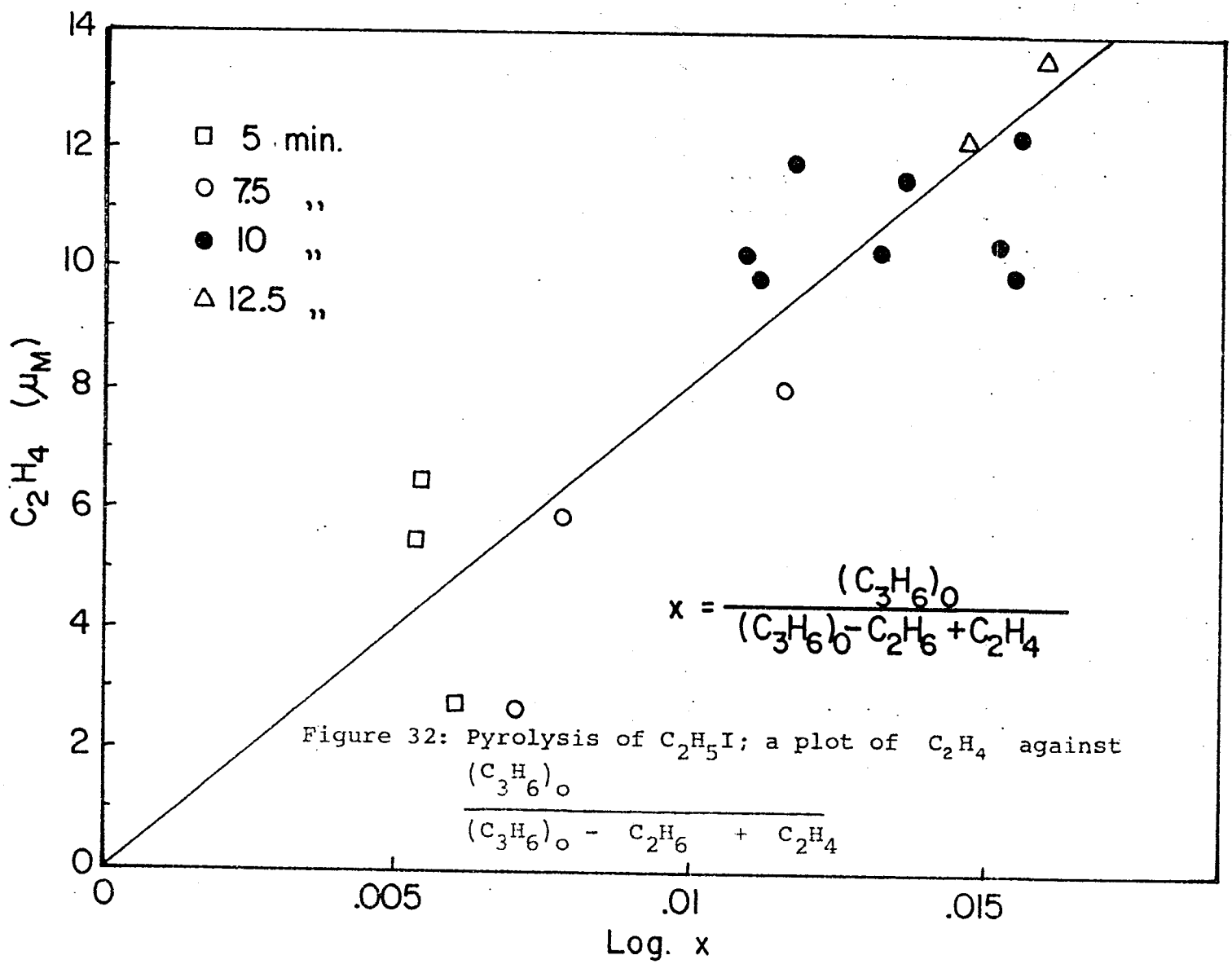

Figure 32: Pyrolysis of C_2H_5I; a plot of C_2H_4 against $\frac{(C_3H_6)_o}{(C_3H_6)_o - C_2H_6 + C_2H_4}$

NOTE

Cyclohexene inhibition study of C_2H_5I

Cyclohexene has been found to be a suitable inhibitor in alkyl chloride and alkyl bromide pyrolyses. A few ethyl iodide pyrolyses were done in the presence of cyclohexene. The results were quite unexpected. The ethane production increased enormously, the ethylene production decreased to zero and iodine production was largely reduced. When the cyclohexene concentration was much less than that of ethyl iodide, some iodine production was observed (c.f. run No. 154). Where C_6H_{10} was much greater than C_2H_5I a new and sharp peak appeared on the chromatogram, whose retention time was about 40 seconds. The retention time of ethane and ethylene were 2 and 3.5 minutes respectively.

Table 6.6.

Temperature 347.5°C

Run Number 150 $[RI]_o$ = 51.3 mm. Cyclohexene = 0		Run Number 151 $[RI]_o$ = 53.7 mm. Cyclohexene = 40.7mm.		Run Number 152 $[RI]_o$ = 36.3 mm. Cyclohexene = 27.8mm.	
Time (min.)	Pressure (mm.)	Time (min.)	Pressure (mm.)	Time (min.)	Pressure (mm.)
		0	94.0	0	64.1
0	51.3	0.5	96.7	0.5	72.0
5	53.0	0.75	97.7	1	76.2
10	54.3	1	99.0	1.30	78.8
		1.5	102.0	2	82.1
		2	104.6	3	89.4
		3	110.7	4	96.4
		4	116.6	5	103.0
		5	122.5		
		6	127.4		
		7	131.0		
		8	134.1		
		9	136.4		
		10	137.7		
I_2 = 12 micromoles		I_2 = 0.8 micromoles		I_2 = 4.5 micromoles	

Run Number 153 $[RI]_o$ = 58.9 mm. Cyclohexene = 47.0 mm.		Run Number 154 $[RI]_o$ = 57.9 mm. Cyclohexene = 5 mm.		Run Number 155 $[RI]_o$ = 69.0 mm. Cyclohexene = 0	
Time (min.)	Pressure (mm.)	Time (min.)	Pressure (mm.)	Time (min.)	Pressure (mm.)
		0.25	62.9		
0	105.9	0.5	67.9	0	69.0
0.5	115.9	1	74.5	0.5	69.5
2	126.8	1.5	76.4	1	69.6
4	145.7	2.5	76.8	2	69.9
5	152.3	4	77.4	4	70.6
7	159.6	6	77.8	6	71.4
10	168.8	8	78.5	8	72.0
		10	79.1	10	72.7
I_2 = 1.8 micromoles		I_2 = 51 micromoles		I_2 = 17 micromoles	

The chromatographic results together with the pressure change and the iodine production are summarised in table 6.7.

Table 6.7:

Temperature 347.5°C

Run No.	$[RI]_o$ (mm.)	Time (min.)	Cyclohexene (mm.)	$\triangle P$ (mm.)	I_2 (mm.)	C_2H_4 (mm.)	C_2H_6 (mm.)	New peak
150	51.3	10	0	3.0	2.8	2.7	2.8	No
151	53.7	10	40.3	43.7	0.2	0	17.6	Yes
152	36.3	5	27.8	38.9	1.05	0	19.0	Yes
153	58.9	10	47.0	62.9	0.45	0	19.5	Yes
154	57.9	10	5.0	16.2	11.9	2.8	12.9	No
155	69.0	10	0	3.7	4.0	3.9	3.9	No

The complete disappearance of ethylene in runs 151, 152 and 153 suggests that almost all of the iodide has reacted very rapidly with the cyclohexene. This is also supported by the observed sharp rise of pressure in the case of a low concentration of cyclohexene. In the cases of higher concentrations of added cyclohexene, the initial reaction seems to be very fast and the initial ethyl iodide concentration is unlikely to be observed correctly. (The fast reaction having taken place while the vaporisation is still incomplete).

The stoicheiometry of the new reaction could be guessed from run No. 154. The presence of iodine and ethylene in the products suggests that the pyrolysis of the iodide is occuring together with the fast cyclohexene reaction. These results approximately fit a stoicheiometry based on

$$2C_2H_5I + C_6H_{10} \longrightarrow 2C_2H_6 + I_2 + C_6H_8$$

together with

$$2C_2H_5I \longrightarrow C_2H_6 + C_2H_4 + I_2$$

The disappearance of iodine in the runs with more cyclohexene may be due to addition of iodine to cyclohexene or more probably to cyclohexadiene when the reaction mixture is frozen out in liquid N_2.

This system appears to merit further study. As with the propylene effect, it is difficult to visualise the transition state of the reaction

alkyl iodide + Olefin $\longrightarrow$ alkane + products.

SECTION - 7

A GENERAL DISCUSSION OF THE MECHANISM OF ALKYL IODIDE PYROLYSES.

Unlike alkyl chlorides or bromides, sufficient studies of alkyl iodides were not made in the past to present a general picture of the nature of their pyrolyses. However, previous workers observed that many iodide pyrolyses have several features in common with their chloro and bromo analogues.

The present investigation of the pyrolyses of different iodides renders the picture of simple alkyl iodide decomposition nearly complete and it is possible to talk about the nature of their decomposition in more general terms. In spite of some unusual features of these systems, alkyl iodides do pyrolyse similarly to alkyl chlorides or bromides and the rate relationship

$$k_{\text{tertiary C-I}} > k_{\text{secondary C-I}} > k_{\text{primary C-I}}$$

is observed to be obeyed for all the halides. Tables of relative rates have given in section 2.3.

On the basis of the then available data on iodide pyrolyses and the re-interpreted mechanism of the reactions between alkyl iodides and hydrogen iodide[80,81] Benson[92] predicted two general rate determining processes in the decompositions of alkyl iodides:

$$RI \longrightarrow HI + \text{Olefin} \quad \ldots\ldots\ldots \text{(A)}$$

and

$$I + RI \longrightarrow I + HI + \text{Olefin} \quad \ldots\ldots\ldots \text{(B)}$$

According to this author, unimolecular first order processes are governed by (A) while mechanism (B) is responsible

for the autocatalytic behavior where kinetics are first order in iodide and one half order in iodine. Both (A) and (B) are followed by a rapid reaction

$$RI + HI \longrightarrow RH + I_2$$

Benson maintained the view that C_2H_5I, $i\text{-}C_3H_7I$ and $t\text{-}C_4H_9I$ pyrolyse through (A) and the rate determining step (B) seems to govern the pyrolyses of $n\text{-}C_3H_7I$, $i\text{-}C_4H_9I$ and $n\text{-}C_4H_9I$.

Holmes and Maccoll[25] have observed that $i\text{-}C_3H_7I$ and $s\text{-}C_4H_9I$ pyrolyse autocatalytically in the lower range of their pyrolytic temperatures and at higher temperatures both of them decompose unimolecularly. Also, in the present investigation, pyrolysis of $t\text{-}C_4H_9I$ has been seen to proceed via an autocatalytic and a unimolecular process simultaneously; here the autocatalytic process is much slower than the unimolecular climination.

The mechanism of the autocatalytic process had not been positively identified before the present work was undertaken. The abstraction of H and I from alkyl iodides can in some cases be almost isoenergetic. On the basis of the bond dissociation energies[94] and $E(HI + C_3H_6I) = 14$ K.Cals[86] it has been shown in section 5 that the two processes (B) and (C)

$$I + RI \longrightarrow C_3H_6I + HI \quad \ldots\ldots\ldots \text{(B)}$$

and

$$I + RI \longrightarrow R + I_2 \quad \ldots\ldots\ldots \text{(C)}$$

have activation energies equal to 38 and 34.9 K.Cals respectively. For this calculation it has been assumed that the back reaction

of (B) has zero activation energy. Both the processes have been identified in the present investigation. The process (B) takes place in the case of n-C_3H_7I and the process (C) governs the autocatalytic step in the t-C_4H_9I pyrolysis. The autocatalysis of type (C) has been also observed in the case of reactions of other alkyl iodides with hydrogen iodide[79,80,81]. It may well be that with RI and HI the process (C) can become wholly rate determining since alkyl radicals will react rapidly with HI.

Benson's[92] view that the lowering of the activation energies of iodide pyrolysis by about 7 K.Cals $mole^{-1}$ for every α-Me group substitution has not been found by other workers. The author supported this postulation from his pyrolytic activation energy of 42.9 for i-C_3H_7I and estimated activation energy of 36.4 for t-C_4H_9I from the study of the reverse reaction. Both these values are doubtful because Benson did not take into consideration the heterogeneous nature of the reactions involved. The activation energy of 47.9 K.Cals $mole^{-1}$ for i-C_3H_7I as determined by Holmes and Maccoll[25] and that of 38.0 K.Cals $mole^{-1}$ for t-C_4H_7I as obtained in the present investigation cast doubt on the above generalisation.

The results of the present investigation together with the previous data on alkyl iodide pyrolyses bear out the assertion that the environment of the C-I bond to be broken is the major factor determining the nature of the pyrolysis. In general, it can be safely suggested that all those alkyl iodides in which the Iodine atom has a β - methyl group pyrolyse unimolecularly with the elimination of HI. The

autocatalytic rate determining step (B) above seems to be typical of primary iodides (other than ethyl) or iodides where the Iodine atom has no methyl group β to it. The autocatalytic nature of the i-butyl iodide pyrolysis (which is a primary iodide) supports the latter assertion.

On the basis of the above argument n-pentyl iodide would pyrolyse autocatalytically by step (B) while 2-iodopentane would pyrolyse by the unimolecular elimination of hydrogen iodide. 3-iodopentane may pyrolyse by either of the processes (B) or (C).

The pyrolysis of t-C_4H_9I seems to be odd in the sense that the reaction between it and HI is not very fast.

Surface effects:

Surface effects are more prominent in alkyl iodide pyrolyses than with the other halides. The general trend, however, is the same. Surface decomposition is found to be least in ethyl iodide and other primary iodides. In the cases of i-propyl iodide or s-butyl iodide some heterogeneity is observed on a clean glass surface. t-butyl iodide is extremely surface sensitive.

CLAIMS TO ORIGINAL RESEARCH

1. An attempt has been made to find Arrhenius parameters for the pyrolysis of t-butyl iodide by the use of various reaction vessel surfaces.

   It has been shown that the partially heterogeneous elimination of HI is accompanied by a homogeneous iodine catalysed reaction.

2. The pyrolysis of n-propyl iodide has been re-investigated with a view to determine the mechanism of the reaction. Arrhenius parameters agree well with those of previous workers and by studying the induction period and the effect of added ethyl iodide a mechanism was proposed.

3. A brief investigation of n-butyl iodide pyrolysis suggests that the compound pyrolyses in a similar manner to n-propyl iodide.

4. The pyrolysis of ethyl iodide has been re-investigated. Arrhenius parameters agree well with those of other workers.

   The effect of added C_3H_6 has been used to show that the rate determining step is unimolecular elimination of HI.

REFERENCES

1. Paneth F. and Hofeditz W.; Ber., 62B, 1335 (1929)
2. Rice F.O. and Johnston W.O.; J.A.C.S., 56, 214 (1934)
3. Rice F.O.; Trans. Far. Soc., 30, 152 (1934)
4. Daniels F. and Vernon E.L.; J.A.C.S., 54, 2563 (1932)
5. Daniels F.; "Chemical Kinetics" Ithaca (1938)
6. Lossing F.P. and Tickner A.W.; J. Chem. Phys., 20, 907 (1952)
7. Maccoll A.; J. Chem. Soc., 965 (1955)
8. Rice F.O. and Herzfeld K.F.; J.A.C.S., 56, 284 (1934)
9. Goldfinger P., Letort M. and Niclaus M.; "Contribution a l'Etude de la Structure Moleculaire", Victor Henry Commemorative volume, Descer (1948)
10. Barton D.H.R. and Howlett K.E.; J. Chem. Soc., 155 (1949)
11. Ashmore P.G.; "Catalysis and Inhibition of Chemical Reactions" Chapter 11, Butterworths (1963)
12. Burgess C.H. and Chapman D.L.; J. Chem. Soc., 89, 1399 (1906)
13. Griffiths C. and Norrish R.G.W.; Proc. Roy. Soc., A130, 591 (1931)
14. Rice F.O. and Polly O.L.; J. Chem. Phys., 6, 273 (1938)
15. Hinshelwood C.N.; "The Kinetics of a Chemical Change" Oxford, p. 92 (1940)
16. Maccoll A. and Thomas P.J.; J. Chem. Soc., 5033 (1957)
17. Green J.H.S., Harden G.D., Maccoll A. and Thomas P.J.; J. Chem. Phys., 21, 178 (1953)
18. Stubbs F.J. and Hinshelwood C.N.; Far. Soc. Disc., 10, 129 (1951)
19. Wall L.A. and Moore W.J.; J. Phys. Coll. Chem., 55, 961 (1951)
20. Rice F.O. and Varnerin R.E.; J.A.C.S., 76, 324 (1954)

21. Good P.T.; Ph.D. Thesis, London (1956)

22. Blades A.T. and Murphy G.W.; J.A.C.S., 74, 6219 (1952)

23. Wojciechowski B.W. and Laidler K.J.; Can. J. Chem., 38, 1027 (1960)

24. Thomas P.J.; J. Chem. Soc., 1192 (1959)

25. Holmes J.L. and Maccoll A.; J. Chem. Soc., 5919 (1963)

26. Genaux T., Kern F. and Walters W.D.; J.A.C.S., 75, 6196 (1953)

27. Frey H.M.; Annual Reports, Chem. Soc., LVII, (1960)
Frey H.M.; Pyrolytic symposium, Ottawa (1964)

28. Emovon E.V. and Maccoll A.; J. Chem. Soc., 227 (1964)

29. Brearly D., Kistiakowsky G.B. and Stauffer C.H.; J.A.C.S., 58, 43 (1936)

30. Barton D.H.R.; J. Chem. Soc., 2174 (1949)

31. Blades A.T.; Can. J. Chem., 36, 1043 (1958)

32. Harden G.D.; Ph.D. Thesis, London (1954)

33. Barton D.H.R., Head A.J. and Williams R.J.; J. Chem. Soc., 453 (1953)

34. Ingold C.K.; "Structure and Mechanism in Organic Chemistry", G.Bell and Sons Ltd., (1953)

35. Green J.H.S. and Maccoll A.; J. Chem. Soc., 2449 (1955)

36. Glasstone S., Laidler K.J. and Eyring H.; "Theory of Rate Processes", McGraw Hill (1941)

37. Maccoll A. and Thomas P.J.; Nature, 176, 392 (1955)

38. Irsa A.P.; J. Chem. Phys., 26, 18 (1957)

39. Farmer J.B. and Lossing F.P.; Can. J. Chem., 33, 86 (1957)

40. Streitswieser A.; Chem. Review, 56, 571 (1956)

41. Maccoll A.; "Theoritical Organic Chemistry" Butterworths, (1958)

42. Maccoll A.; "Transition State symposium" J. Chem. Soc., (1962)

43. Ingold C.K.; Proc. Chem. Soc., 279 (1957)

44. Benson S.W. and Bose A.N.; J. Chem. Phys., 39, 3463 (1963)

45. Swinbourne E.S.; Aust. J. Chem., 11, 314 (1958)

46. Swinbourne E.S. and Maccoll A.; J. Chem. Soc., 149 (1964)

47. Swinbourne E.S. and Maccoll A.; Aust. J. Chem., 17, 1217 (1964)

48. Maccoll A. and Thomas P.J.; J. Chem. Soc., 2445 (1955)

49. Barton D.H.R. and Onyon P.F.; Trans. Far. Soc., 45 725 (1949)

50. Daniels F. and Veltnam P.L.; J. Chem. Phys., 7, 756 (1939)

51. Agius P.J. and Maccoll A.; J. Chem. Soc., 973 (1955)

52. Holbrook K.A. and Rooney J.J.; J. Chem. Soc., 247 (1965)

53. Broatch W.N., McEwan A.C. and Tipper C.F.H.; Trans. Far. Soc., 50, 576 (1954)

54. Horner E.C.A. and Style D.W.G.; ibid, 50, 1197 (1954)

55. Baldwin R.R. and Simmons R.F.; ibid, 5, 680 (1955)

56. Holbrook K.A.; Proc. Chem. Soc., 418 (1964)

57. Holmes J.L. and Kuo S.M.; C.I.C. Conference, Montreal (1965)

58. Semenov N.N.; "Some Problems in Chemical Kinetics and Reactivity", Princeton University Press (1959)

59. Sehon A.H. and Szwarc M.; Proc. Roy. Soc., 209A, 110 (1951)

60. Barton D.H.R. and Howlett K.E.; J. Chem. Soc., 165 (1949)

61. Barton D.H.R. and Head A.J.; Trans. Far. Soc., 46, 114 (1950)

62. Bhattacharya R.; Private Communication (1964)

63. Capon N.; Ph.D. Thesis, London (1964)

64. Tsang Wing.; J. Chem. Phys., 41, 2487 (1964)

65. Goldberg A.E. and Daniels F.; J.A.C.S., 79, 1314 (1957)

66. Barton D.H.R., Head A.J., and Williams R.J.; J. Chem. Soc., 2039 (1951)

67. Maccoll A. and Thomas P.J.; J. Chem. Soc., 979 (1955)

68. Semenov N.N., Sergeev G.B. and Kapralova G.A.; Dokl. Akad. Nauk, S.S.S.R., 105, 301 (1955)

69. Hartman M., Reydtmann H. and Rick G.; Z. Phys. Chem., Frankfurt, 28, 71 (1961)

70. Maccoll A. and Stone R.H.; J. Chem. Soc., 2756 (1961)

71. Sergeev G.B.; Dokl. Akad. Nauk, S.S.S.R., 106, 299 (1956)

72. Kale M.N. and Maccoll A.; J. Chem. Soc., 5020 (1957)

73. Howlett K.E.; J. Chem. Soc., 4487 (1952)

74. Harden G. and Maccoll A.; J. Chem. Soc., 2454 (1955)

75. Wong S.C.; Ph.D. Thesis, London (1958)

76. Roberts B.; Ph.D. Thesis, London (1961)

77. Tsang Wing; J. Chem. Phys., 40, 1498 (1964)

78. Kistiakonsky G.B.; J.A.C.S., 59, 165 (1937)

79. Ogg R.A. (Jr.); J.A.C.S., 56, 526 (1934)

80. Benson S.W. and O'Neal E.; J. Chem. Phys., 34, 514 (1961)

81. Sullivan J.H.; J. Phys. Chem., 65, 722 (1961)

82. Butler E.T. and Polanyi M.; Trans. Far. Soc., 39, 19 (1943)

83. Jones J.L. and Ogg R.A.; J.A.C.S., 59, 1931 (1937)

84. Jones J.L. and Ogg R.A.; J.A.C.S., 59, 1934 (1937)

85. Jones J.L. and Ogg R.A.; J.A.C.S., 59, 1939 (1937)

86. Ogg R.A. and Polanyi M.; Trans. Far. Soc., 31, 482 (1934)

87. Benson S.W. and Bose A.N.; J. Chem. Phys., 37, 2935 (1962)

88. Benson S.W. and Bose A.N.; J. Chem. Phys., 37, 1081 (1962)

89. Teranishi H. and Benson S.W.; J. Chem. Phys., 40, 2946 (1964)

90. Bose A.N. and Benson S.W.; J. Chem. Phys., 38, 878 (1963)

91. Holmes J.L.; Ph.D. Thesis, London (1957)

92. Benson S.W.; J. Chem. Phys., 38, 1945 (1963)

93. Trotman-Dickenson A.F.; "Gas Kinetics" Butterworths (1955)

94. Benson S.W.; "Foundation of Chemical Kinetics" McGraw Hill, (1959)

95. Lee R.A.; Ph.D. Thesis, London (1959)

96. Holmes J.L. and Choudhary G.; Pyrolytic Symposium, Ottawa, (1964)

97. Jones J.L.; J.A.C.S., 60, 1877 (1938)

98. Purnell J.H. and Quinn C.P.; J. Chem. Soc., 4128 (1961)

99. Andsley A. and Goss F.R.; J. Chem. Soc., 497 (1942)

100. Handbook of Physics and Chemistry, 45th. Ed. (1964-65)

101. Timmermans J. and Delcourt; J. Chem. Phys., 31, 85 (1934)

102. Vogel A.I.; J. Chem. Soc., 636 (1943)

103. Dillon T. and Young G.; J.A.C.S., 51, 2389 (1929)

104. Kharasch M.S. and Mayo F.R.; J.A.C.S., 55, 2468 (1933)

105. Jones J.L. and Ogg R.A.; J.A.C.S., 59, 1943 (1937)

106. Butler E.T., Mandel E. and Polanyi M.; Trans. Far. Soc., 41, 298 (1945)

107. Stimson R.A. and Ross V.R.; J. Chem. Soc., 1602 (1962)

108. Kistiakowsky G.B.; J.A.C.S., 50, 2315 (1928)

109. Bodenstein M.; Z. Phys. Chem., 29, 295 (1899)

110. Holmes J.L.; Personal Communication

111. Glass V.S. and Hinshelwood C.N.; J. Chem. Soc., 1817 (1929)

112. Schumacher H.J.; "Chemiche Gas Reactionen" Leipzig (1938)

113. Schumacher H.J.; Z. Angew Chem., 53, 501 (1940)

114. Lossing F.P., Ingold K.U. and Henderson I.H.S.; unpublished.

115. Aronstein; Rec. Trav. Chim., 1, 134 (1882)

116. Kahan Z.; J. Chem. Soc., 93, 132 (1908)

117. Lessig E.T.; Phys. Chem., 36, 2325 (1932)

118. Szwarc M.; Chem. Reviews 47, 75 (1950)

119. Shaw A.; Ph.D. Thesis, Manchester (1948)

120. Klemm F. and Bernstein R.B.; J.A.C.S., 82, 5987 (1960)